UNIVERSITY OF MIAMI
NOV 3 0 1965
LIBRARY

industrial mathematics

1951

UNIVERSITY OF MIAMI
NOV 3 0 1965
LIBRARY

industrial mathematics

1951

EDITORIAL STAFF

A. E. Roach, Editor-in-Chief
R. V. Churchill
R. O. Darling
A. W. Jacobson
L. G. Johnson
E. D. McCarthy

VOLUME 2

A publication of the

INDUSTRIAL MATHEMATICS SOCIETY
5135 CASS AVENUE, DETROIT 2, MICHIGAN

THE MEDIAN RANKS OF SAMPLE VALUES IN THEIR POPULATION WITH AN APPLICATION TO CERTAIN FATIGUE STUDIES

LEONARD G. JOHNSON
Research Laboratories Division, General Motors Corporation
Detroit, Michigan

Introduction

Ball bearing fatigue data consist of a list of the number of hours endured by the individual bearings of a group of a certain size. We may be given, for example, the number of hours that each of ten identical bearings endured under a fixed load. From this sample of ten bearings we would like to determine the general distribution of the fatigue life of such bearings. In other words, we would like to determine the nature of the population, given the sample. By the population we mean the large general group of similar bearings of which the sample is only a small portion. Thus, the population may consist of all the bearings of the same type as those of the sample which were produced during a certain month, or in a certain plant, or by a special process.

The usual method of estimating populations from samples is to put the data into a frequency table and then to construct a histogram, or frequency polygon, which is finally smoothed into a frequency curve. Such a procedure, however, is not reliable for small samples, since the results vary too much with a change in the size of the class interval, and generally, false peaks cannot be distinguished from true ones. With the small samples which arise in fatigue life studies it has been found to be much more fruitful to order the data according to life and to construct a cumulative plot, or ogive curve. In other words, the estimation of the integral of the frequency function is easier than the direct estimation of the frequency function itself.

In order to make a cumulative plot, it becomes necessary to decide what rank is to be assigned to each particular failure in a group. The first failure in a group of ten tested will have a definite percentage of the population failing before it, if the entire population were tested. If we knew exactly the percentage of the population below the first failure in ten, then that percentage would be the true rank of the first failure in ten. However, since we do not know the true rank, the best that we can do is to estimate what it is. We use an estimate such that in the long run the positive and negative errors of the estimate cancel each other. That is, half of the time we would give the first failure in ten a rank that is too high, and the other half of the time we would give it a rank that is too low. A rank with this property is called a "median" rank.

It is the purpose of the present mathematical discussion to determine the median ranks to be assigned respectively to the first, second, third, etc., up to the tenth failure in a sample of ten failures, and, likewise, for all the failures in a sample of any finite size.

Deriving the Median Ranks

Assume the following situation is given:

A sample of n observations in numerical order: $_{O}x_1$, $_{O}x_2$, $_{O}x_3$, ... , $_{O}x_n$.

Probability density function of population: f(x) (unknown)

Cumulative distribution function of population: F(x) (unknown)

We define,

True rank of ${}_oX_1 = {}_nZ_1 = F({}_oX_1)$ (unknown)

True rank of ${}_oX_2 = {}_nZ_2 = F({}_oX_2)$ (unknown)

True rank of ${}_oX_3 = {}_nZ_3 = F({}_oX_3)$ (unknown)

. . .

. . .

. . .

In general, True rank of ${}_oX_j = {}_nZ_j = F({}_oX_j)$ (unknown)

Since the true rank of an observation is unknown, the best that we can do is to estimate what that true rank is. Consider next the set of all possible samples of size n from the same population. The table below is a partial list of these samples:

Sample 1: ${}_oX_1^{(1)}, {}_oX_2^{(1)}, {}_oX_3^{(1)}, \ldots\ldots, {}_oX_n^{(1)}$

Sample 2: ${}_oX_1^{(2)}, {}_oX_2^{(2)}, {}_oX_3^{(2)}, \ldots\ldots, {}_oX_n^{(2)}$

Sample 3: ${}_oX_1^{(3)}, {}_oX_2^{(3)}, {}_oX_3^{(3)}, \ldots\ldots, {}_oX_n^{(3)}$

. . . .

. . . .

Sample r: ${}_oX_1^{(r)}, {}_oX_2^{(r)}, {}_oX_3^{(r)}, \ldots\ldots, {}_oX_n^{(r)}$

The true ranks of the $j^{\underline{th}}$ observations in these samples of size n may be listed as follows:

$$F({}_oX_j^{(1)}) = {}_nZ_j^{(1)}$$

$$F({}_oX_j^{(2)}) = {}_nZ_j^{(2)}$$

$$F({}_oX_j^{(3)}) = {}_nZ_j^{(3)}$$

. .

. .

. .

$$F({}_oX_j^{(r)}) = {}_nZ_j^{(r)}$$

We shall show that these ranks are distributed according to the probability density function

$$g({}_nZ_j) = \frac{n!}{(j-1)!\ (n-j)!}\ {}_nZ_j^{\,j-1}\ (1-{}_nZ_j)^{n-j}$$

This follows from the multinomial theorem, as demonstrated below:

Divide the entire population into the following three regions:

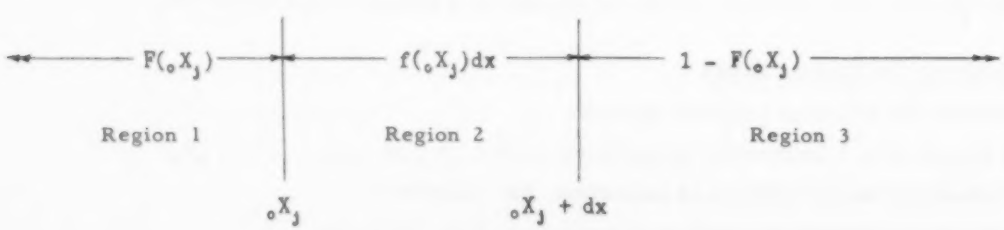

The expressions $F({}_oX_j)$, $f({}_oX_j)\,dx$, and $1 - F({}_oX_j)$ represent the probabilities that a single observation would fall into regions 1, 2, and 3, respectively.

Therefore, it follows that the probability of exactly (j-1) values falling into region 1, and exactly one value falling into region 2, and exactly (n-j) values falling into region 3 is given by the expression

$$\frac{n!}{(j-1)!\ 1!\ (n-j)!}\ [F({}_oX_j)]^{j-1} \cdot f({}_oX_j)dx \cdot [1 - F({}_oX_j)]^{n-j}$$

(This is an application of the multinomial theorem on joint probabilities.)

Now put $F({}_oX_j) = {}_nZ_j$. Then, $f({}_oX_j)dx = d_nZ_j$.

Hence, the above probability becomes

$$\frac{n!}{(j-1)!\ (n-j)!}\ {}_nZ_j^{j-1}\ (1 - {}_nZ_j)^{n-j} d_nZ_j$$

Therefore, the probability density function of ${}_nZ_j$ is

$$g({}_nZ_j) = \frac{n!}{(j-1)!\ (n-j)!}\ {}_nZ_j^{j-1}(1 - {}_nZ_j)^{n-j} \qquad (A)$$

By definition, the mean value of ${}_nZ_j$ is

$$\int_0^1 {}_nZ_j \cdot g({}_nZ_j)d_nZ_j \quad = \quad \int_0^1 {}_nZ_j \cdot \frac{n!}{(j-1)!\ (n-j)!}\ {}_nZ_j^{j-1}(1 - {}_nZ_j)^{n-j} d_nZ_j$$

This integral can be reduced to a Beta function, and its value turns out to be $j/(n+1)$. This is the mean rank of the $j^{\underline{th}}$ observation in n. We could use this as an estimate of the true rank of the $j^{\underline{th}}$ observation in n, but in certain applications the median value of ${}_nZ_j$ has been found to be more useful an an estimate. Let us now proceed to find the median value of ${}_nZ_j$, i.e., the median rank of the j^{th} value in n.

By integration of equation (A), we find that the cumulative distribution function of ${}_nZ_j$ is

$$G({}_nZ_j) = 1 - (1-{}_nZ_j)^n - n\,{}_nZ_j(1-{}_nZ_j)^{n-1} - \frac{n^{(2)}}{2!}\,{}_nZ_j^2(1-{}_nZ_j)^{n-2} - \cdots - \frac{n^{(j-1)}}{(j-1)!}\,{}_nZ_j^{j-1}(1-{}_nZ_j)^{n-j+1} \qquad (B)$$

(Note: $n^{(2)} = n(n-1)$ $\quad n^{(3)} = n(n-1)(n-2)$, etc.,.. $n^{(j-1)} = n(n-1)(n-2)\cdots\cdots(n-j+2)$.)

The median value of ${}_nZ_j$ is found by putting $G({}_nZ_j) = \frac{1}{2}$ in equation (B) and then solving for ${}_nZ_j$, i.e., by solving the following equation for ${}_nZ_j$:

$$1 - (1-{}_nZ_j)^n - n\,{}_nZ_j(1-{}_nZ_j)^{n-1} - \frac{n^{(2)}}{2!}\,{}_nZ_j^2(1-{}_nZ_j)^{n-2} - \cdots - \frac{n^{(j-1)}}{(j-1)!}\,{}_nZ_j^{j-1}(1-{}_nZ_j)^{n-j+1} = \tfrac{1}{2} \qquad (C)$$

Such an equation contains exactly one real root between 0 and 1, and Table 1 consists of such roots for n and j up to 20. The table is constructed by solving equation (C) exactly for j = 1 and for j = n, for each value of n up to 20. The intermediate values in each column are then filled in by forming an arithmetic progression. When this is done, we find that in every case $.495 \le G({}_nZ_j) \le .505$, which is good enough for practical purposes.

For n>20 the following convenient formula may be used:

$\lambda_n(j) = \dfrac{j - (1-\ln 2) - (2\ln 2 - 1)\left(\frac{j-1}{n-1}\right)}{n}$, where $\lambda_n(j)$ denotes the median rank of the j^{th} value in n.

An Application

Eighteen identical ball bearings were placed in test machines and subjected to a fixed radial load. The following table lists the number of hours the individual bearings endured at 2000 rpm:

TABLE A

Failure No.	Endurance in Hours
1	183
2	355
3	538
4	618
5	697
6	834
7	862
8	887
9	1056
10	1147
11	1351
12	1506
13	1578
14	1607
15	1683
16	1710
17	2020
18	2410

As a result of testing thousands of bearings, it has been found that the fatigue life follows a Weibull distribution, whose probability density function is

$$f(x) = \alpha\beta x^{\beta-1} exp(-\alpha x^{\beta}) \quad (\alpha \text{ and } \beta \text{ are positive constants.})$$

Therefore, the cumulative distribution function of the life is

$$F(X) = 1 - exp(-\alpha x^{\beta}), \text{ where } F(x) \text{ is the fraction failed within the first x hours.}$$

Let S(x) = the fraction surviving the first x hours

$$\text{Then, } S(x) = exp(-\alpha x^{\beta})$$

$$\therefore \frac{1}{S(x)} = exp(\alpha x^{\beta})$$

$$\ln \frac{1}{S(x)} = \alpha x^{\beta}$$

$$\ln \ln \frac{1}{S(x)} = \ln \alpha + \beta \ln x$$

Hence, if we plot Log $\frac{1}{S(x)}$ vs. x on logarithmic paper, we should get a straight line, if the distribution is a Weibull distribution.

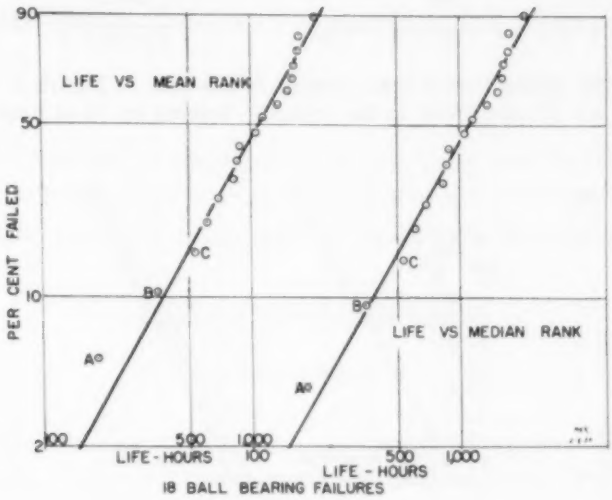

Figure 1.

Figure 1 shows a plot of the data in Table A. It is plotted on some special probability paper on which a Weibull distribution becomes a straight line of slope β. The vertical scale represents Log Log $\frac{1}{S(x)}$ = Log Log $\frac{1}{1 - F(x)}$, but is graduated in terms of values of F(x), the fraction failed within the first x hours, while the horizontal is an ordinary logarithmic scale, representing Log x.

In the left half of the figure, each individual bearing life is given its mean rank, while in the right half of the figure, it is given its median rank. The same straight line is drawn in both cases, and it represents the maximum likelihood estimate of the Weibull population from which the sample is drawn. Determining the maximum likelihood estimate from a set of data as shown in Table A is an arduous task, and it would be desirable to have a quick graphical method of determining the best position of the straight line representing the Weibull population.

To draw the line very near the lower extreme values when mean ranks are used would lead to a slope which is too small, because of the high probability of lower extreme values falling considerably to the left in such a case. On the other hand, it has been found that if median ranks are used in the plotting, then the danger of underestimating the slope is eliminated because, in that case, a point is just as liable to fall to the right as to the left of the maximum likelihood line. In other words, we can very quickly arrive at an estimate of the population parameters by drawing a line by sight which takes the general direction of the array of points and which splits the array 50 - 50. For this reason median ranks are preferred to mean ranks.

Additional Remarks

Equation (B) can also be used to determine tolerance limits for the j^{th} value in n. If we were seeking the rank below which we can expect 30% of all j^{th} observations in n, we would solve the following equation for ${}_nZ_j$:

$$1 - (1-{}_nZ_j)^n - n\,{}_nZ_j(1-{}_nZ_j)^{n-1} - \frac{n^{(2)}}{2!}\,{}_nZ_j^2(1-{}_nZ_j)^{n-2} - \cdots - \frac{n^{(j-1)}}{(j-1)!}\,{}_nZ_j^{j-1}(1-{}_nZ_j)^{n-j+1} = \frac{3}{10} \quad \text{(D)}$$

Similarly, if we were seeking the rank below which we can expect 70% of all j^{th} observations in n, we would solve the following equation for ${}_nZ_j$:

$$1-(1-{}_nZ_j)^n - n\,{}_nZ_j(1-{}_nZ_j)^{n-1} - \frac{n^{(2)}}{2!}{}_nZ_j^2(1-{}_nZ_j)^{n-2} - \cdots - \frac{n^{(j-1)}}{(j-1)!}{}_nZ_j^{j-1}(1-{}_nZ_j)^{n-j+1} = \tfrac{7}{10} \quad (E)$$

Figure 2 illustrates the application of this process to the data in Figure 1. Solutions of equations (D) and (E) for n = 18 are found in the columns headed by 18 in Tables 2 and 3 respectively.

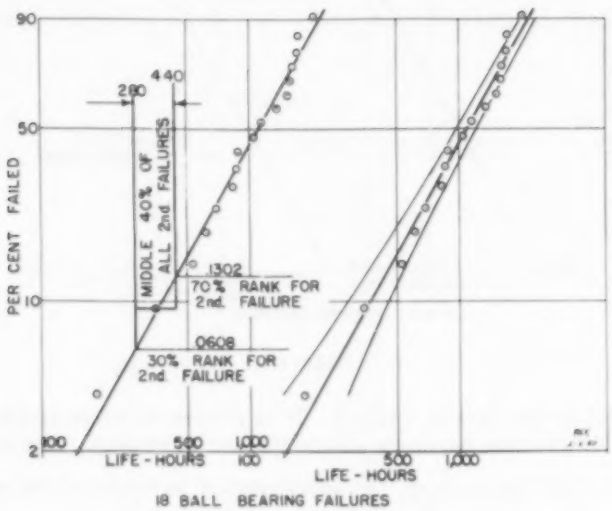

Figure 2.

Referring to Tables 2 and 3 for n = 18 and j = 2, we see that they tell us that between the ranks .0608 and .1302 we can expect the middle 40% of all second failures in eighteen. On the straight line in Figure 2, 280 hours corresponds to the rank .0608 and 440 hours corresponds to the rank .1302. Hence, the middle 40% of all second failures in eighteen will lie between 280 hours and 440 hours, if such samples of eighteen come from the population represented by the straight line. The same type of limits can be determined for the first failure, the third failure, the fourth failure, etc., up to the eighteenth failure in the sample of eighteen. When this is done, we obtain a middle 40% band as shown in the right half of Figure 2.

A complete list of solutions of equation (D) for n and j up to 20 is given in Table 2. For n>20, the following formula may be used to find the 30% rank of the j^{th} value in n:

$$M = \frac{j}{n+1}$$

$${}_{.3}R_n(j) = M - \left(.645 - \frac{.125}{5^{\alpha_3}}\right)\sqrt{\frac{M(1-M)}{n+2}}\,; \quad j \le \frac{n+1}{2}\,; \quad \alpha_3 = \frac{2(1-2M)}{n+3}\sqrt{\frac{n+2}{M(1-M)}}$$

The above formula applies only to the lower half of a sample. For the upper half of the sample, use the following formula:

$${}_{.3}R_n(n+1-j) = 1-M - \left[1.01 - .49\left(\frac{9}{7}\right)^{\alpha_3}\right]\sqrt{\frac{M(1-M)}{n+2}} \qquad j \le \frac{n+1}{2}$$

(M and α_3 are the same as above.)

Likewise, a complete list of solutions of equation (E) for n and j up to 20 is given in Table 3. For n>20, the following formulas may be used for the 70% rank of the j^{th} value in n:

For the lower half of a sample: $$.7R_n(j) = 1 - .3R_n(n+1-j) = M + [1.01 - .49(\frac{9}{7})^{\alpha_3}] \sqrt{\frac{M(1-M)}{n+2}}$$

For the upper half of a sample: $$.7R_n(n+1-j) = 1 - .3R_n(j) = 1 - M + (.645 - \frac{.125}{5^{\alpha_3}}) \sqrt{\frac{M(1-M)}{n+2}}$$

(In all these formulas, $j \leq \frac{n+1}{2}$, and M and α_3 are the same as previously defined.)

TABLE 1 — MEDIAN RANKS

Sample Size = n

j \ n	1	2	3	4	5	6	7	8	9	10
1	.5000	.2929	.2063	.1591	.1294	.1091	.0943	.0830	.0741	.0670
2		.7071	.5000	.3864	.3147	.2655	.2295	.2021	.1806	.1632
3			.7937	.6136	.5000	.4218	.3648	.3213	.2871	.2594
4				.8409	.6853	.5782	.5000	.4404	.3935	.3557
5					.8706	.7345	.6352	.5596	.5000	.4519
6						.8909	.7705	.6787	.6065	.5481
7							.9057	.7979	.7129	.6443
8								.9170	.8194	.7406
9									.9259	.8368
10										.9330

Sample Size = n

j \ n	11	12	13	14	15	16	17	18	19	20
1	.0611	.0561	.0519	.0483	.0452	.0424	.0400	.0378	.0358	.0341
2	.1489	.1368	.1266	.1178	.1101	.1034	.0975	.0922	.0874	.0831
3	.2366	.2175	.2013	.1873	.1751	.1644	.1550	.1465	.1390	.1322
4	.3244	.2982	.2760	.2568	.2401	.2254	.2125	.2009	.1905	.1812
5	.4122	.3789	.3506	.3263	.3051	.2865	.2700	.2553	.2421	.2302
6	.5000	.4596	.4253	.3958	.3700	.3475	.3275	.3097	.2937	.2793
7	.5878	.5404	.5000	.4653	.4350	.4085	.3850	.3641	.3453	.3283
8	.6756	.6211	.5747	.5347	.5000	.4695	.4425	.4184	.3968	.3774
9	.7634	.7018	.6494	.6042	.5650	.5305	.5000	.4728	.4484	.4264
10	.8511	.7825	.7240	.6737	.6300	.5915	.5575	.5272	.5000	.4755
11	.9389	.8632	.7987	.7432	.6949	.6525	.6150	.5816	.5516	.5245
12		.9439	.8734	.8127	.7599	.7135	.6725	.6359	.6032	.5736
13			.9481	.8822	.8249	.7746	.7300	.6903	.6547	.6226
14				.9517	.8899	.8356	.7875	.7447	.7063	.6717
15					.9548	.8966	.8450	.7991	.7579	.7207
16						.9576	.9025	.8535	.8095	.7698
17							.9600	.9078	.8610	.8188
18								.9622	.9126	.8678
19									.9642	.9169
20										.9659

TABLE 2 — 30% RANKS

Sample Size = n

j	1	2	3	4	5	6	7	8	9	10
1	.3000	.1633	.1121	.0853	.0689	.0577	.0497	.0436	.0389	.0350
2		.5477	.3633	.2724	.2180	.1818	.1559	.1365	.1214	.1093
3			.6694	.4916	.3898	.3233	.2763	.2413	.2142	.1926
4				.7401	.5780	.4761	.4053	.3533	.3128	.2802
5					.7860	.6396	.5414	.4701	.4157	.3726
6						.8182	.6857	.5925	.5225	.4675
7							.8400	.7214	.6335	.5655
8								.8603	.7499	.6670
9									.8748	.7731
10										.8866

Sample Size = n

j	11	12	13	14	15	16	17	18	19	20
1	.0319	.0293	.0271	.0252	.0235	.0220	.0208	.0196	.0186	.0177
2	.0994	.0911	.0841	.0781	.0729	.0684	.0644	.0608	.0576	.0547
3	.1749	.1600	.1480	.1370	.1280	.1200	.1130	.1066	.1010	.0959
4	.2555	.2336	.2154	.1987	.1854	.1737	.1635	.1543	.1462	.1389
5	.3392	.3097	.2848	.2626	.2447	.2292	.2156	.2035	.1928	.1834
6	.4249	.3878	.3560	.3284	.3056	.2861	.2689	.2540	.2405	.2291
7	.5125	.4677	.4289	.3957	.3679	.3442	.3234	.3050	.2891	.2757
8	.6021	.5494	.5035	.4645	.4316	.4035	.3789	.3572	.3385	.3229
9	.6949	.6329	.5798	.5348	.4967	.4640	.4354	.4100	.3886	.3706
10	.7923	.7186	.6581	.6066	.5632	.5257	.4929	.4642	.4394	.4188
11	.8963	.8086	.7388	.6804	.6311	.5886	.5514	.5182	.4909	.4675
12		.9045	.8225	.7564	.7006	.6527	.6109	.5748	.5431	.5167
13			.9115	.8345	.7717	.7183	.6716	.6307	.5960	.5664
14				.9176	.8450	.7853	.7335	.6888	.6497	.6166
15					.9229	.8543	.7973	.7473	.7043	.6674
16						.9275	.8624	.8080	.7600	.7191
17							.9316	.8698	.8177	.7720
18								9353	.8764	.8264
19									.9386	.8824
20										.9416

TABLE 3 — 70% RANKS

Sample Size = n

j	1	2	3	4	5	6	7	8	9	10
1	.7000	.4523	.3306	.2599	.2140	.1818	.1600	.1397	.1252	.1134
2		.8367	.6367	.5084	.4220	.3604	.3143	.2786	.2501	.2269
3			.8879	.7276	.6102	.5239	.4586	.4075	.3665	.3330
4				.9147	.7820	.6767	.5947	.5299	.4775	.4345
5					.9311	.8182	.7237	.6467	.5843	.5325
6						.9423	.8441	.7587	.6872	.6274
7							.9503	.8635	.7858	.7198
8								.9564	.8786	.8074
9									.9611	.8907
10										.9650

Sample Size = n

j	11	12	13	14	15	16	17	18	19	20
1	.1037	.0955	.0885	.0824	.0771	.0725	.0684	.0647	.0614	.0584
2	.2077	.1914	.1775	.1655	.1550	.1457	.1376	.1302	.1236	.1176
3	.3051	.2814	.2612	.2436	.2283	.2147	.2027	.1920	.1823	.1736
4	.3979	.3671	.3419	.3196	.2994	.2817	.2665	.2527	.2400	.2280
5	.4875	.4506	.4202	.3934	.3689	.3473	.3284	.3112	.2957	.2809
6	.5751	.5323	.4965	.4652	.4368	.4114	.3891	.3693	.3503	.3326
7	.6608	.6122	.5711	.5355	.5033	.4743	.4486	.4252	.4040	.3834
8	.7445	.6903	.6440	.6043	.5684	.5360	.5071	.4818	.4569	.4336
9	.8251	.7664	.7152	.6716	.6321	.5965	.5646	.5358	.5091	.4833
10	.9006	.8400	.7846	.7374	.6944	.6558	.6211	.5900	.5606	.5325
11	.9681	.9089	.8520	.8013	.7553	.7139	.6766	.6428	.6114	.5812
12		.9707	.9159	.8630	.8146	.7708	.7311	.6950	.6615	.6294
13			.9729	.9219	.8720	.8263	.7844	.7460	.7109	.6771
14				.9748	.9271	.8800	.8365	.7965	.7595	.7243
15					.9765	.9316	.8870	.8457	.8072	.7709
16						.9780	.9356	.8934	.8538	.8166
17							.9792	.9392	.8990	.8611
18								.9804	.9424	.9041
19									.9814	.9453
20										.9823

APPLICATIONS OF ELEMENTARY MATHEMATICS TO PROBLEMS IN MAGNETISM

S. R. WILLIAMS
Professor of Physics, Emeritus, Amherst College, Amherst, Massachusetts

Magnetic Field at a Given Point O Due to a Small Magnet. — Some magneticians are beginning to feel that the concept of isolated magnetic poles is obsolete. They insist that magnetic problems should be solved in terms of moving electric charges which produce the so-called magnetic poles. Until such time as we can express fundamental problems connected with magnets in terms of the magnetic moment of a spinning electron, however, we will do well not to throw this useful concept of magnetic poles into the discard.

Coulomb discovered certain laws about the way magnetic poles react on one another and expressed them in a single formula with considerable precision. In any medium this familiar formula is

$$F = \frac{m_1 m_2}{\mu r^2}$$

The usefulness of the concept of isolated magnetic poles may be seen in their application to the problem of finding numerical values for the magnetic field strengths which surround a magnetic dipole. Everyone is familiar with the experiment of scattering iron filings about a magnet as shown in Fig. 1. Wherever we see the filings lining up in definite rows, we think of them as representing the paths along which the forces due to the poles act. These lines of force indicate that we are in the presence of a magnetic field. The magnetic field intensity at any point in such a field is, by definition, measured by the force in dynes which that field exerts upon a unit magnetic pole placed at the point in the field where we wish to know its value. In the following paragraphs we will see how far we can go in solving this problem by simple mathematical procedure.

A magnet, N - S, Fig. 2, has a magnetic field surrounding it something like the one shown in Fig. 1. What will be the strength of the magnetic field of this magnet at a point O when r is the radius vector connecting O with the center C of the magnet? θ is the angle which the axis of the magnet makes with the radius vector r and ℓ is the distance between the two poles of the magnet. In Fig. 2 one may picture the point O as located at the origin of a system of rectangular co-ordinates and the magnet, N - S, swinging anywhere about this point, but with its axis parallel to the Y-axis. When this is done θ is the angle both between the radius vector r and the axis of the dipole and between the radius vector r and the axis of Y.

At O is placed a unit magnetic pole (positive), because the force on it due to the magnet, N - S, will be the field intensity of the magnet at the point O, and the direction in which it tends to move will be the direction of the field. This last point is also a matter of definition.

It will be assumed that this experiment will be carried out in a vacuum, so that the field intensity at a distance r from a single magnetic pole will be by definition:

$$H = \frac{m}{r^2}$$

This follows from Coulomb's law for the forces between magnetic poles in a vacuum.

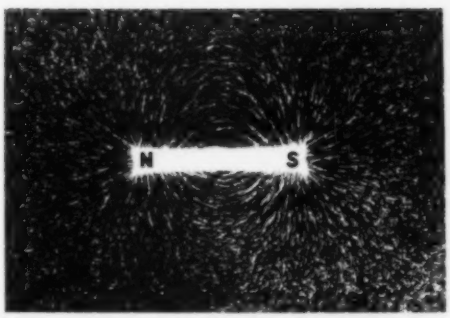

Fig. 1. The Field of Force About a Dipole.

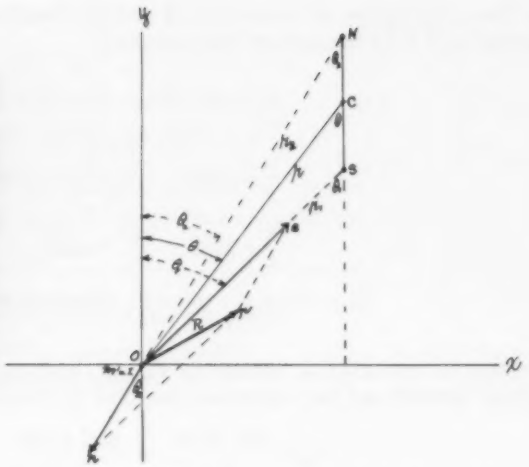

Fig. 2. The Field Strength of a Magnet, N - S, at a Point O.

In this problem the dipole is treated as though it had two independent isolated magnetic poles. It is to be noted that the N-pole can act individually on the unit positive magnetic pole placed at O. The same thing holds for the S-pole. The field intensity of the N-pole at O is $H_N = m/r_2^2$ and that of the S-pole is $H_S = m/r_1^2$.

The total force on the unit magnetic pole at O will then be these two forces indicated above and represented in magnitude and direction by the two vectors, On and Os, in Fig. 2. As a matter of convenience it will be found best to resolve these forces into their components along the axes of X and Y. When these are found, compound them into their resultant, which will be found to be $Or = R = \sqrt{X^2 + Y^2}$, the actual force acting on the unit magnetic pole at O, or the field intensity of the dipole, N - S, at the point O, which will be the answer to our problem.

For each pole, N and S, there will be two components, one along the X-axis and the other along the Y-axis, or there will be two components along each axis. Thus, taking the Y-axis first there will be the two components along it and the total force acting in that direction will be

$$F_X = m\frac{\sin\theta_1}{r_1^2} - m\frac{\sin\theta_2}{r_2^2}$$

while for the Y-axis

$$F_Y = m\frac{\cos\theta_1}{r_1^2} - m\frac{\cos\theta_2}{r_2^2}$$

It will now be recalled that in the original statement of the problem the only terms given were θ, r and ℓ. In these equations for F_X and F_Y there are other values given, all of which are unknown. These are θ_1, θ_2, r_1, and r_2 and equivalents for these must be found in terms of the known quantities given. Let us write out all of these relations which we can find and then use what we need of them.

Digression: $$r_1^2 = r^2 + \frac{\ell^2}{4} - r\ell\cos\theta = r^2 - r\ell\cos\theta$$

$$r_2^2 = r^2 + \frac{\ell^2}{4} + r\ell\cos\theta = r^2 + r\ell\cos\theta$$

when the assumption is made that ℓ is very small with respect to the value of r. This assumption will hold throughout this solution.

$$r_2 + r_1 = 2r. \quad r_2 - r_1 = \ell\cos\theta. \quad r_1 r_2 = r^2.$$

$$\frac{y}{r} = \cos\theta. \quad \frac{y - \frac{\ell}{2}}{r_1} = \cos\theta_1. \quad \frac{y + \frac{\ell}{2}}{r_2} = \cos\theta_2$$

$$\frac{x}{r} = \sin\theta. \quad \frac{x}{r_1} = \sin\theta_1. \quad \frac{x}{r_2} = \sin\theta_2$$

$$\sin\theta_1 - \sin\theta_2 = \frac{\ell \sin\theta\cos\theta}{r}. \quad \cos\theta_2 - \cos\theta_1 = \frac{\ell\sin^2\theta}{r}.$$

Returning to the original equations for F_x and F_y, the foregoing values will be substituted wherever needed and the equations can then be transformed as follows:

$$F_x = \frac{mr_2^2 \sin\theta_1}{r_1^2 r_2^2} - \frac{mr_1^2 \sin\theta_2}{r_2^2 r_1^2}$$

$$= \frac{m}{r^4}(r_2^2 \sin\theta_1 - r_1^2 \sin\theta_2)$$

$$= \frac{m}{r^4}\left[(r^2 + r\ell\cos\theta)\ \sin\theta_1 - (r^2 - r\ell\cos\theta)\ \sin\theta_2\right]$$

$$= \frac{m}{r^4}\left[r^2(\sin\theta_1 - \sin\theta_2) + r\ell\cos\theta\ (\sin\theta_1 + \sin\theta_2)\right]$$

$$= \frac{m}{r^4}\left[r^2\frac{(\ell\sin\theta\cos\theta)}{r} + 2r\ell\sin\theta\cos\theta\right]$$

$$= \frac{m\ell}{r^3}\left[\sin\theta\cos\theta + 2\sin\theta\cos\theta\right]$$

$$= \frac{M}{r^3}\left[3\sin\theta\cos\theta\right]$$

where $M = m\ell$, the magnetic moment of the dipole. Similarly,

$$F_y = \frac{m\, r_2^2 \cos\theta_1}{r_1^2 r_2^2} - \frac{m\, r_1^2 \cos\theta_2}{r_2^2 r_1^2}$$

$$= \frac{m}{r^4}(r_2^2 \cos\theta_1 - r_1^2 \cos\theta_2)$$

$$= \frac{m}{r^4}\left[(r^2 + r\ell\cos\theta)\cos\theta_1 - (r^2 - r\ell\cos\theta)\cos\theta_2\right]$$

$$= \frac{m}{r^4}\left[r^2(\cos\theta_1 - \cos\theta_2) + r\ell\cos\theta\ (\cos\theta_1 + \cos\theta_2)\right]$$

$$= \frac{m}{r^4}\left[r^2\left(-\frac{\ell}{r}\sin^2\theta\right) + 2r\ell\cos^2\theta\right]$$

$$= \frac{m\ell}{r^3}\left[-\sin^2\theta + 2\cos^2\theta\right]$$

$$= \frac{M}{r^3}\left[\cos^2\theta - 1 + 2\cos^2\theta\right]$$

$$= \frac{M}{r^3}\left[3\cos^2\theta - 1\right]$$

As indicated above the total force at O due to the dipole will be

$$F_t = R = Or = \sqrt{F_x^2 + F_y^2}$$

$$F_t = \sqrt{\frac{M^2}{r^2}\left[(3\sin\theta\cos\theta)^2 + (3\cos^2\theta - 1)^2\right]}$$

$$= \sqrt{\frac{M^2}{r^6}(9\sin^2\theta\cos^2\theta + 9\cos^4\theta - 6\cos^2\theta + 1)}$$

$$= \sqrt{\frac{M^2}{r^6}\left[9\cos^2\theta(\sin^2\theta + \cos^2\theta) - 6\cos^2\theta + 1\right]}$$

$$= \sqrt{\frac{M^2}{r^6}(9\cos^2\theta - 6\cos^2\theta + 1)}$$

$$= \frac{M}{r^3}\sqrt{3\cos^2\theta + 1}$$

To arrive at this quite simple result we had to make the assumption that ℓ was small with respect to r. This is often what we have to do with mathematics in order to get any result at all - make some simplifying assumption. If we had not done it in this case, we would have had equations beyond our powers to handle with elementary mathematics.

Since $m\ell = M$, the magnetic moment of the dipole, appears in all of these problems, we could have started with it in the beginning and thereby have simplified the calculations greatly.

In the meantime, interpretation of the final results is in order, because mathematics has no practical value or significance unless it can be interpreted. When $\theta = 90^0$, $\cos 90^0 = O$ and, therefore, the final result becomes

$$F_t = \frac{M\sqrt{1}}{r^3} = \frac{M}{r^3}$$

This holds for the condition that the magnet stands broadside to the point O. O lies on a line which is at right angles to the axis of the magnet erected at the center of the magnet. This is known as the B tangent position used by Gauss in his method for finding the value of the earth's magnet field. On the other hand, if θ is O^0, $\cos\theta = 1$ and

$$F_t = \frac{M}{r^3}\sqrt{3 + 1} = \frac{2M}{r^3}$$

In this case, the point O lies on a line which is a continuation of the axis of the magnet. It is the A tangent position of Gauss. If the distance r is the same for both cases, the force at O in the latter position will be twice that in the former position.

Mathematics Applied to a Medium Filled with Magnetic Dipoles

Having found the expression for the magnetic field around a single magnet, or dipole, it is quite conceivable that by a process of integration it would be possible to find at any point within a medium filled with dipoles - and all turned in the same direction - the resultant force of all such dipoles. One may set up such an equation, but its solution is too complex for our purposes in dealing with simple mathematics as a tool.

By the use of a little imagination, however, the problem can be solved quite readily. The following solution also illustrates what has already been mentioned, that engineering and physics are rich in pictures, and all that is needed is to find the right picture which can be expressed in simple mathematics.

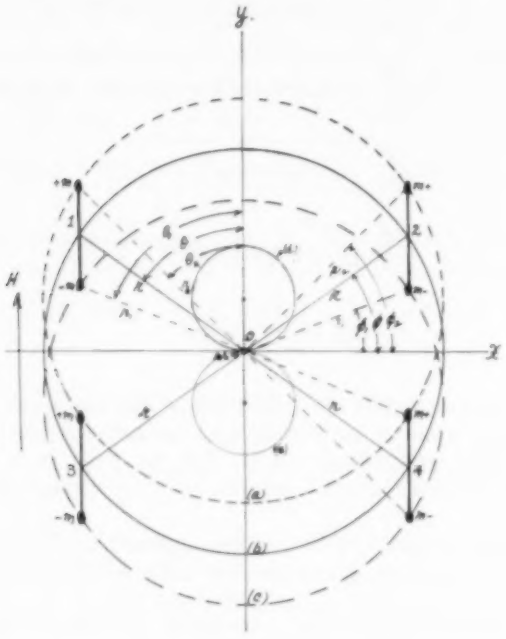

Fig. 3. Resultant Magnetic Field Due to Paired Dipoles

In Fig. 3 is shown by a solid line circle the cross-section of a very large sphere (b) of radius r, filled with magnetic dipoles turned in helter-skelter fashion. This group of dipoles has a magnetic field H applied to it in the direction shown. This turns all of the dipoles into the same direction as the applied field H. In this state the medium is said to be magnetically saturated. For simplicity's sake only four dipoles, Nos. 1, 2, 3, and 4 will be indicated, but they will show that when the sphere is magnetized to saturation, the positive or north-seeking poles will all lie in the sphere (a) whose cross-section is represented by the circle drawn in short dashes, while all the negative or south-seeking poles will be located in the sphere (c) represented by the circle drawn in long dashes.

We now raise the question: What is the force at O, the center of the original sphere, when the field H is withdrawn but all dipoles still remain in the position of magnetic saturation and each one exerts a field at O given by the equation

$$F = \frac{M}{r^3} \sqrt{3\cos^2\theta + 1}$$

If one had a mass m, say near the middle of the earth where the distance to the center was one mile, the effective gravitational force acting upon the mass m would be due only to that part of the earth which lies within the sphere of the one mile radius. While all the rest of the earth would be acting upon the mass m, there would still be a neutralization of all of these forces, and only the pull of the sphere of one mile radius would be effective in attracting the mass m. A similar situation exists between the unit magnetic pole at the center of the original sphere and the attractions which the positive and negative poles in the other two spheres

exert upon it. The unit magnetic pole at the center of the original sphere is off the center of the other two spheres by a distance which is equal to half the length of the dipoles. Call this distance $\ell/2$. Consequently only the positive poles in the upper small sphere (d) will have any effect on the unit magnetic pole, $m' = 1$, and the same will be true for the negative poles found in the small sphere (e) below the center. The result of these forces on the unit pole is that the positive poles in the upper sphere push $m' = +1$ downward toward the bottom of the page, and equally so the negative poles in the lower small sphere attract $m' = +1$ downward toward the bottom of the page, and we see that the resultant force at O is in a direction opposite to that which H originally imposed on the point O. This is why we call this a demagnetizing force. The radii of the two small spheres will both be equal to $\ell/2$, hence the volume of each one of the small spheres will be

$$V = \frac{4\pi}{3}\left(\frac{\ell}{2}\right)^3 = \frac{\pi\ell^3}{6}$$

Multiply this volume by the number of magnetic poles per unit volume (= n) to find the number of positive, as well as negative, poles in the upper and lower small spheres respectively. The total number then will be

$$N = \frac{\pi n \ell^3}{6}$$

Now apply Coulomb's law to the forces between the poles in each of the small spheres and the unit pole, $m' = +1$.

$$F_+ = \frac{-N \times 1}{\left(\frac{\ell}{2}\right)^2} = \frac{-nm\pi\ell^3}{\frac{6\ell^2}{4}} = -\frac{2\pi nm\ell}{3}$$

$$F_- = \frac{-N \times 1}{\left(\frac{\ell}{2}\right)^2} = \frac{-nm\pi\ell^3}{\frac{6\ell^2}{4}} = \frac{-2\pi nm\ell}{3}$$

Where $m_1 = m_2 = m$, the pole strengths of the dipoles imbedded in the medium.

The total force at O, therefore, will be

$$F_t = (-F_+) + (-F_-) = -2F$$

$$= \frac{-4\pi nm\ell}{3} = \frac{-4}{3}\pi n M$$

where M is the magnetic moment of each dipole being considered. Inasmuch as n is the number of dipoles per unit volume, then nM is the magnetic moment per unit volume of the medium containing all of these dipoles. By definition, the magnetic moment per unit volume is the same as the intensity of magnetization (and here it is measured within the medium. Since $nM = I$,

$$F_t = \frac{-4\pi I}{3}$$

This equation gives the value of the force which all the dipoles in the medium contained in the large sphere of radius r exert upon a unit magnetic pole at the center of the sphere. The results are familiar equations.

Critical Angle, $\theta_c = 2\theta$. In making the drawing shown in Fig. 3, it was interesting to see how, as magnets 1 and 2, moved symmetrically around the circle, i.e., in a plane from $\theta = 90^0$ to $\theta = 0^0$, there was a definite line at which, as the centers of the magnets moved over these lines at A and C, or E and F, Figs. 4 and 5, a magnetometer needle at O reversed its direction of pointing. This was observed by simply placing at O a magnetometer needle and sliding the magnets 1 and 2 symmetrically around on the circle but still keeping their constant direction of pointing. See Figs. 3 and 4. Thus if the two magnets were in the sector between lines OA and OC, Figs. 4 and 5, the magnetometer needle would point toward B. The same thing happened when the magnets were between the lines OD and OF. On the other hand, if the magnets passed over into the sectors between the lines OA and OD, or between OC and OF, the magnetometer needle would point toward E. There seemed to be very definite boundary lines between the four sectors indicated in Figs. 4 and 5.

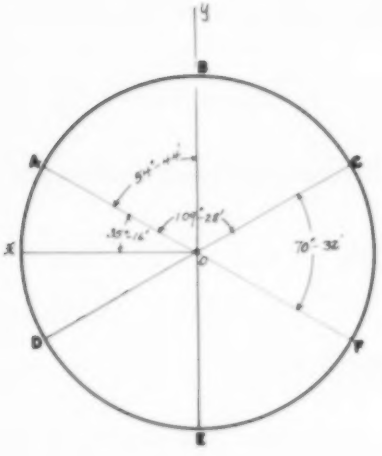

Fig. 4. In the solid cones, ABCO and DEFO, the dipoles contained therein augment H in the Y direction. All dipoles in the sphere outside of these two cones oppose H in the Y direction.

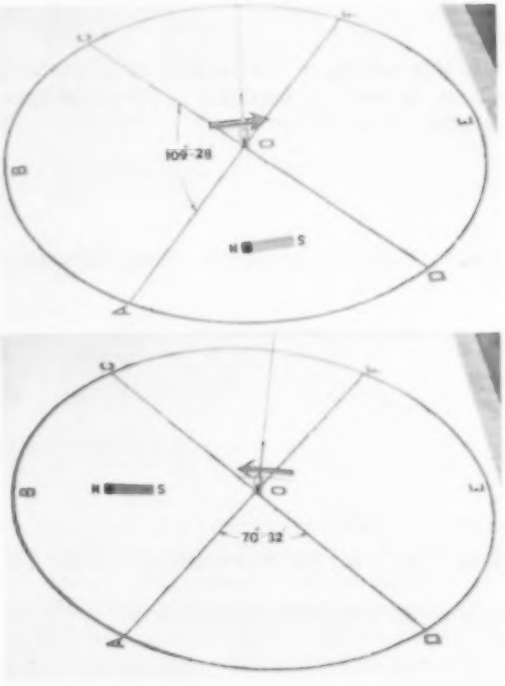

Fig. 5. In a sphere filled with uniformly distributed dipoles, the contribution of any given dipole to the resultant field at O depends upon its position in the sphere.

In Fig. 5 only one movable dipole is indicated in order that the field surrounding it may the more readily be imagined, showing how it operates on the magnetometer at O. In dealing with symmetrically placed dipoles the components of the magnetic forces between them and parallel to the line joining their centers annul each other.

From the experience in finding the magnetic field about a single magnet, it seemed quite possible to find what the combined fields of two dipoles would be. Thus the study has advanced to a consideration of two or paired dipoles. Magnets 1 and 2, Fig. 3, were taken first and the question raised: What will be thd field intensity of two such dipoles at a common point O, and how does the angle 102 between them affect that result? The preliminary experiment, outlined above, indicated that there was a certain critical angle, $2\theta = \angle 102 = \theta_c$ where the effect of the paired dipoles would be equal to zero.

Here is a splendid opportunity to show how simple mathematics may be used in telling us a great deal about the question which we have just raised. It is only going another step in the same procedure which was used in finding the magnetic field surrounding a single magnet. Furthermore, the drawing in Fig. 3 was at first simply by chance, yet as we advanced in studying this problem it didn't seem so out of place when one thought of iron atoms being laid up in cubic form. Here we are dealing with an octet of dipoles placed at the corners of a parallelepiped which is our unit to give zero field at the center of the parallelepiped. A brief study of Fig. 3 shows that it is merely a doubling of the problem shown in Fig. 2. Instead of dealing with the two poles of a single dipole, here we are handling the four poles of two dipoles and the procedure becomes exactly the same as that previously considered.

Mathematical Determination of the Critical Angle

Case I. Inasmuch as there will be 4 poles for the pair of magnets which will operate upon the unit magnetic pole, $m' = +1$, at the center of the circle, there will be four components to add along the X-axis and four along the Y-axis.

We start by writing the forces which the poles of the two equal and paired magnets exert on $m' = +1$. This is done by the use of Coulomb's law for magnetic poles. For convenience in starting, write down in a tabular form the forces due to all four poles participating in the study, remembering that we assume that all four poles are equal and may be represented by the letter m. Care must be used in writing down these individual forces that the proper signs are attached to them so that they will be in harmony with the signs usually assigned to the various quadrants used in geometry.

TABLE

Force	X Component	Y Component
$F_1 = m/r_1^2$	$- m\sin\theta_1/r_1^2$	$+ m\cos\theta_1/r_1^2$
$F_2 = m/r_2^2$	$+ m\sin\theta_2/r_2^2$	$- m\cos\theta_2/r_2^2$
$F_3 = m/r_2^2$	$- m\sin\theta_2/r_2^2$	$- m\cos\theta_2/r_2^2$
$F_4 = m/r_1^2$	$+ m\sin\theta_1/r_1^2$	$+ m\cos\theta_1/r_1^2$

It will be observed that when proper signs are given to the force components the total force along the X-axis will be $F_X = O$, while along the Y-axis

$$F_y = (F_1 + F_4) - (F_2 + F_3) = \left(\frac{2m\cos\theta_1}{r_1^2}\right) - \left(\frac{2m\cos\theta_2}{r_2^2}\right)$$

When this is evaluated we shall have the total resultant force acting upon $m' = +1$ at O, due to the dipoles, 1 and 2. This can be carried out in exactly the same way as the earlier equations were carried out. Again we shall have the same unknowns as we did earlier; these need not be rewritten here. Putting the unknown values of θ_1, θ_2, r_1, and r_2 in terms of the known values of θ, r and ℓ, and substituting these quantities in the equation for F_y we get the following form:

$$F_y = \frac{2mr_2^2\cos\theta_1 - 2mr_1^2\cos\theta_2}{r_1^2\, r_2^2}$$

$$F_y = \frac{2m}{r^4}\left[r^2\left(\frac{2a}{r}\right)(-\sin^2\theta) + 4\arccos^2\theta\right]$$

$$= \frac{4m\ell}{r^3}\left[(-\sin^2\theta) + 2\cos^2\theta\right]$$

$$= \frac{4M}{r^3}\left[2\cos^2\theta - \sin^2\theta\right]$$

An interpretation of this equation shows that the only condition under which $F_y = O$ is when the quantity within the squared bracket becomes equal to zero, or

$$2\cos^2\theta = \sin^2\theta = 1 - \cos^2\theta$$

whence,

$$3\cos^2\theta = 1$$

$$\cos\theta = \sqrt{\frac{1}{3}} = 0.57735$$

$$\theta = 54^0 - 44' = 54.733+ \text{ degrees}$$

$$\theta_c = 2\theta = 109.466+ \text{ degrees}$$

Case II. Paired Dipoles 2 and 4, Fig. 3. Of equal interest is it to see what effect the paired dipoles 2 and 4 will have on $m' = 1$ at O. Again we may write expressions for the forces which the four poles exert on $m' = 1$ and tabulate the components as we did for the magnets 1 and 2.

TABLE

Forces	X-Components	Y-Components
$F_1 = m/r_1^2$	$- m \cos\phi_1/r_1^2$	$- m \sin\phi_1/r_1^2$
$F_2 = m/r_2^2$	$+ m \cos\phi_2/r_2^2$	$+ m \sin\phi_2/r_2^2$
$F_3 = m/r_2^2$	$- m \cos\phi_2/r_2^2$	$+ m \sin\phi_2/r_2^2$
$F_4 = m/r_1^2$	$+ m \cos\phi_1/r_1^2$	$- m \sin\phi_1/r_1^2$

Again,

$$F_x = O$$

while,

$$F_y = \frac{2m \sin\phi_2}{r_2^2} - \frac{2m \sin\phi_1}{r_1^2}$$

$$= \frac{2m}{r^4}\left[r_1^2 \sin\phi_2 - r_2^2 \sin\phi_1\right]$$

As in Case I, one must substitute for the values of the unknown factors their equivalents in terms of the known terms. See above for these values. In terms of the known,

$$F_y = \frac{2m}{r^4}\left[(r^2 + 2r\ell \sin\phi)(\sin\phi_2) - (r^2 - 2r\ell \sin 0)(\sin\phi_1)\right]$$

$$= \frac{2m}{r^4}\left[r^2(\sin\phi_2 - \sin\phi_1) + 2\ell r \sin\phi\,(\sin\phi_2 + \sin\phi_2)\right]$$

$$= \frac{2m}{r^4}\left[r^2(\sin\phi_2 - \sin\phi_1) + 4\ell r \sin^2\phi\right]$$

$$= \frac{2m}{r^4}\left[2\ell r(\sin^2\phi - 1) + 4\ell r \sin^2\phi\right]$$

$$= \frac{4m\ell}{r^3}\left[\sin^2\phi - 1 + 2\sin^2\phi\right]$$

$$= \frac{4M}{r^3}\left[3\sin^2\phi - 1\right]$$

Interpreting this equation, it may be seen that $F_y = O$ only when the quantity in the squared brackets is equal to zero, or

$$3\sin^2\phi = 1$$

$$\sin^2\phi = \frac{1}{3}$$

$$\sin\phi = \sqrt{\frac{1}{3}} = 0.57735$$

$$\phi = 35^0 - 16' = 35.266 \text{ degrees}$$

The results obtained in Case I and in Case II may be thought of as parts of a common picture in any plane drawn through the sphere and including the Y-axis. In a simple drawing like Fig. 4 it may be seen how the angle found in Case I and that in Case II are related to each other. It will be seen that they are supplements, one of the other. That these angles are correct, as found mathematically, is demonstrated in Fig. 6 for Case I and in Fig. 7 for Case II.

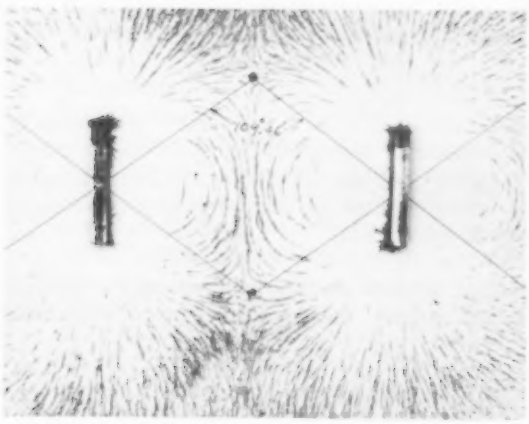

Fig. 6. Neutral points to two similar magnets when broadside to each other.

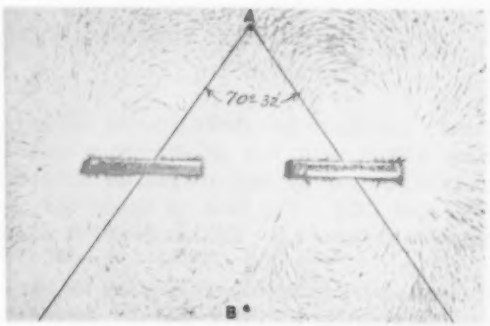

Fig. 7. Around a line containing the axes of the two magnets is a circle of zero, or neutral, points. The plane of this circle is normal to the plane of the paper and intersects the latter of the points A and B.

Four dipoles laid at the points A, B, C, and D in Fig. 4, or at points 1, 2, 3, and 4 in Fig. 3 would produce a zero field at O. Furthermore, if we consider ABCDEF as the periphery of a large sphere inclosing uniformly distributed dipoles throughout its volume, it may be seen that all dipoles lying in the two solid cones, ABCO and DEFO, within the sphere, give a resultant field at O which is directed in the same direction as the applied field H, while all dipoles lying in the band which encircles the sphere, represented in cross-section by the triangles, AOD and COF, give a resultant field at O which is opposed to H. Here we see why the conical poles of an electromagnet are the most efficient when ground to an angle of 109.46^0.

It is beyond the limits of this paper to go into a discussion of how a magnet shaped like the one shown in Fig. 7 would behave. Would it have a greater magnetic moment per unit volume than any other shaped magnet?

By simple processes of integration, it may be shown that the volume of the two solid cones, ABCO and DEFO form 0.42262 part of the total sphere and that the belt around the sphere, represented by AOD and COF, form the remaining, or the 0.57738 part of the sphere. This

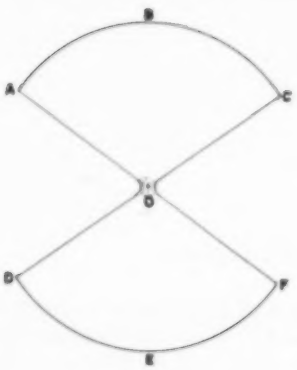

Fig. 8. Cross-sectional View of "El Diablo" magnet

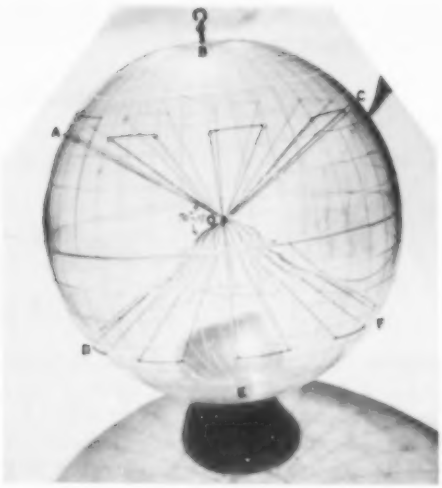

Fig. 9. A hollow plastic sphere through which strings have been pulled to outline the solid cones, ABCO and DEFO.

means that there are more dipoles helping to oppose the field H at O than there are co-operating with it. Fig. 9 is an attempt to show in 3-dimensional space the two solid cones, ABCO and DEFO, and the belt around the sphere represented in cross-section by the two triangles, AOD and COF. For lack of space the physical interpretation of the mathematical results must be reserved for another paper in some physical periodical.

By some very simple mathematics we have arrived at definite results which could be verified experimentally, and have thereby demonstrated that simple mathematics can be a valuable tool in science.

HIGH-EFFICIENCY CANTILEVER SPRINGS

DOUGLAS G. ANDERSON
McIntosh Stamping Corporation
Detroit, Michigan

Introduction

Springs made by a stamping process from flat sheet material are usually rectangular in cross-section, although they are frequently bent or curved in profile. When material cost is high and the volume of production large, it would often be economical to make the increased investment required for tools to make a more efficient form of spring. So far as the author knows, however, there has been no practical method for selecting and specifying such springs.

Nomenclature

The following nomenclature is used:

- A Area of cross-section normal to stress.
- c Maximum value of y for a given cross-section.
- C Ratio of width to thickness (for Part II of the section shown in Figure 1).
- E Modulus of elasticity.
- e Efficiency.
- e_G Gross efficiency.
- $f(k)$ Function of k appearing in the expression for Z.
- $F(k)$ Function of k appearing in the expression for Q.
- I Moment of inertia of cross-section.
- k Ratio of depth of forming to thickness (for section shown in Figure 1).
- L Length as measured along neutral surface from point of application of load.
- M Moment.
- P Load.
- Q A certain function of the proportions of a spring.
- R Radius of curvature of neutral surface.
- S Stress. (When not under an integral sign, S is the maximum stress acting in the region considered).
- S_a Highest stress allowable for the application.
- t Thickness of sheet material.
- U Energy of deformation of an elastic body.
- V Volume.
- V_G Gross volume of untrimmed blank.
- W Width of section.
- W_B Width of blank required to produce a section of width W and depth $(k + 1)t$.
- w_k Ratio of $(W_B - W)$ to t, a function of k.
- y Distance from neutral axis of cross-section.
- Z Section modulus, I/c.
- Δ Deflection at the point of application of load.
- δ Deflection of edge of section with respect to neutral axis, due to distortion of the section (see Figure 5).

Efficiency

The essential function of a spring is to deflect under load and so to store energy. The energy stored in an elastic body of uniform cross-section, when it is uniformly and fully stressed, is

$$U = \frac{1}{2} P\Delta = \frac{1}{2}(S_a A)\left(\frac{S_a}{E} L\right) = \frac{1}{2} \frac{S_a^2}{E} AL = \frac{S_a^2 V}{2E}.$$

If the stress is not uniform throughout the body, the energy stored will be less. The strength of the material is then not fully utilized. With respect to energy storage, the efficiency of the body is

$$e = \frac{\int_V S^2 dV}{S_a^2 V}$$

which holds for a body of any shape.

For economical tooling and handling costs, usually a spring will be blanked from a strip just wide enough for one trimmed blank. The volume of a length of this strip just long enough for one trimmed blank is then the amount of material actually used to make the spring (neglecting the value of the scrap). This volume is called the "gross volume," and the gross efficiency is defined as

$$e_g = \frac{\int_V S^2 dV}{S_a^2 V_G} .$$

Choice of Section

The form of cross-section to be used should be symmetrical about an axis at right angles to the neutral axis to avoid deflection normal to the direction of application of the load. It should concentrate as much of the metal as possible as far from the neutral axis as possible to maximize $\int_a S^2 dA$. It should be readily formable from material of uniform thickness. These considerations lead to the form shown in Figure 1. Its properties, and in particular its section modulus, are functions of t,k, and C. The theoretically preferable sharp corners and vertical walls are modified for ease of forming in dies without close clearances.

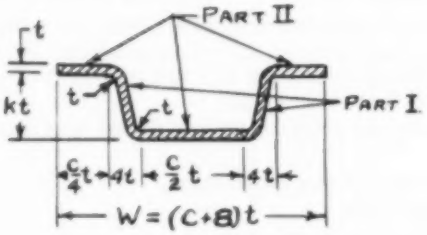

Figure 1.

Load and Deflection

The problem is to choose t and to vary k or C or both along the length of the spring in such a way as to obtain high efficiency with the load and deflection required. The first step is to obtain a relation involving the deflection.

Neglecting shear stress, the energy equation for a beam with a single concentrated load is

$$2U = P\Delta = \int \frac{S^2 dV}{E} = \frac{1}{E} \int_L \int_A S^2 dA dL \qquad (1)$$

Assuming, as is usual in elementary beam theory, that the stress at any point of a section taken normal to the neutral surface is proportional to its distance from the neutral axis of the section, we may write

$$P\Delta = \frac{1}{E}\int_L \frac{S^2}{c^2}\left[\int_A y^2 dA\right] dL \tag{2}$$

where S is the greatest stress within the area A. But the integral within brackets is, by definition, the moment of inertia of the section. Substituting in Eq (2) and dividing by P, we have the deflection formula

$$\Delta = \frac{1}{PE}\int_L \frac{S^2 I}{c^2} dL \tag{3}$$

Eq (3) can easily be derived from the deflection formulae of the curvature method, Van den Broek's elastic energy method, or the theorem of Castigliano. It is unusual in that I appears in the numerator of the integrand. This simplifies the evaluation of the integral in many cases where I is a function of L.

At any cross-section of a cantilever we have

$$M = PL = S\frac{I}{c} = SZ \tag{4}$$

For the highest efficiency, S should obviously be independent of L, that is, the spring should be a beam of constant strength. Then $dL = \frac{S}{P} dZ$ and Eq (3) may be written

$$\Delta = \frac{S^3}{P^2 E}\int_L \frac{Z}{c} dZ \tag{5}$$

for a cantilever beam of constant strength.

Returning to the consideration of the section shown in Figure 1, we now wish to find its section modulus. It is convenient to consider parts I and II separately. By definition, $I = I_I = I_{II}$. But also, $c_I = c_{II} = c$, and therefore

$$Z = \frac{I}{c} = \frac{I_I}{c} + \frac{I_{II}}{c} = Z_I + Z_{II} \tag{6}$$

Expression Z_I and Z_{II} as functions t, k, and C, we have

$$Z = t^3\left[f_I(k) + C\, f_{II}(k)\right] \tag{7}$$

The function f_i is not readily expressible in terms of k directly, but Table I gives values for both f_I and f_{II} for values of k from 0 to 10. From Eqs (4) and (7), we can write

$$\frac{PL}{St^3} = f_I(k) + C\, f_{II}(k) \tag{8}$$

This equation has been plotted for several values of C in Figure 2.

It is impractical to extend the constant-stress condition to the region where k is less than 1. A smooth variation in depth of section is obtained by making k proportional to L from k = 0 to k = 1.

Although in some cases it might be advantageous to vary C with L, particularly in the region where k is small, we will confine our attention to springs of uniform width, where C is constant. Then each curve of Figure 2 represents a member of our family of springs.

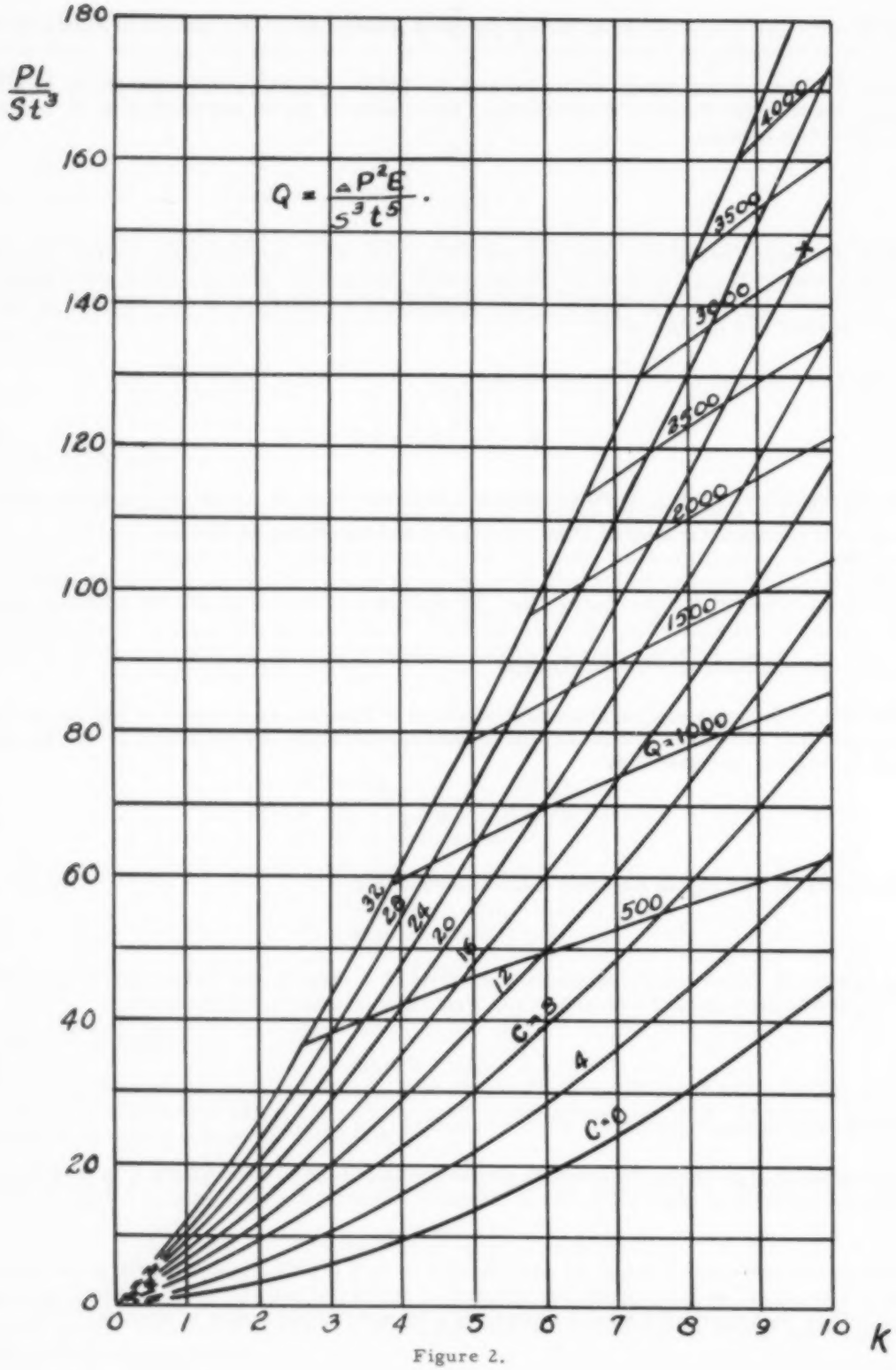
PL/St³
Q = ΔP²E / S³t⁵ .
180
160
140
120
100
80
60
40
20
0
0 1 2 3 4 5 6 7 8 9 10 K
4000
3500
3000
2500
2000
1500
Q=1000
500
32
28
24
20
16
12
C=8
4
C=0

Figure 2.

Substituting Eq (7) directly in Eq (5) and expanding we have, since $c = \frac{1}{2}(k+1)t$,

$$\Delta = \frac{S^3 t^5}{P^2 E} \int_L \frac{2}{(k+1)} \left[f_I(k) + C f_{II}(k)\right] \cdot d\left[f_I(k) + C f_{II}(k)\right]$$

$$= \frac{2 S^3 t^5}{P^2 E} \left\{ \int_L \frac{f_I(k)\, df_I(k)}{k+1} + C \left[\int_L \frac{f_I(k) df_{II}(k)}{k+1} + \int_L \frac{f_{II}(k) df_I(k)}{k+1} \right] + C^2 \int_L \frac{f_{II}(k) df_{II}(k)}{k+1} \right\}$$

Since the integrals are functions of k alone, we can write

$$\frac{\Delta P^2 E}{S^3 t^5} = F_0(k) + C F_1(k) + C^2 F_2(k) = Q(c,k) \qquad (9)$$

Note that Q is a quadratic in C. Our interest in it stems from the condition imposed upon it by the deflection. However, it has a more general significance than the method of derivation might lead one to suspect. It might be called a "shape factor"; by the choice of suitable parameters in place of C and k it is definable for any class of homogeneous elastic bodies. For a cantilever of uniform rectangular section, $\frac{\Delta P^2 E}{S^3 t^5} = \frac{1}{54}(\frac{W}{t})^2$. For a constant-strength cantilever of constant thickness, $\frac{\Delta P^2 E}{S^3 t^5} = \frac{1}{36}(\frac{W}{t})^2$.

Values of F_0, F_1, and F_2 are given in Table I. The values for k = 1 are the coefficients of a quadratic in C which, for values of C from 4 to 32, closely approximates the exact solution for a beam in which k is proportional to L from k = 0 to k = 1. The values of the F's for higher values of k were obtained by numerical integration.

Table I also gives values of w_k, a function of k needed for determining the width of the flat blank from which the spring is to be formed. At any section, the width of blank is

$$W_B = W + w_k t \qquad (10)$$

TABLE I

k	0	1	2	3	4	5	6	7	8	9	10
$f_i(k)$	1.33	1.56	3.29	6.02	9.55	13.83	18.84	24.55	30.75	37.70	45.8
$f_{ii}(k)$	.167	.333	.722	1.167	1.634	2.091	2.595	3.083	3.574	4.067	4.560
$F_0(k)$	0	.75	4.2	11.2	23.4	41.5	66.6	99.6	139.9	189.9	246.3
$F_1(k)$	0	.58	2.06	4.66	8.45	13.38	19.43	26.56	34.60	43.73	53.48
$F_2(k)$	0	.054	.212	.449	.737	1.061	1.411	1.780	2.164	2.560	2.965
W_k	0	.1	.7	1.8	3.3	5.0	6.8	8.7	10.7	12.7	14.7

Eq (10) was plotted against k, for values of C from 4 to 32, and the lines of constant Q were transferred to Figure 2.

Use of the Chart

Suppose that the spring is required to have the following characteristics:

P = 100 lbs. $\quad \Delta$ = .25 in. $\quad$ S = 100,000 lbs./sq. in.

E = 30,000,000 lbs./sq. in. $\quad$ W= .96 in.

Assuming t = .030, solve for Q.

$$Q = \frac{\Delta P^2 E}{S^3 t^5} = \frac{.25 \times 10^4 \times 3 \times 10^7}{10^{15} \times 3^5 \times 10^{-10}} = 3085.$$

From Figure 1, we have

$$C = \frac{W}{t} - 8 \tag{11}$$

Solving for C, $C = \frac{.96}{.030} - 8 = 32 - 8 = 24.$

At the point (Q = 3085, C = 24) of Figure 2, we read that k = 9.6 approx., and $\frac{PL}{St^3} = 148.$

Solving for L, $L = \frac{148\ St^3}{P} = \frac{148 \times 10^5 \times 3^3 \times 10^{-6}}{10^2} = 4.02.$

From Figure 3 we read, at k = 9.6, $w_k = 13.9$.

Solving for W_B, $W_B = W + w_k t = .96 + 13.9 \times .03 = 1.38.$

Intermediate values of k and W_B are easily determined. For any desired value of L, compute $\frac{PL}{St^3}$. With this value, and C = 24, find k from Figure 2, then w_k from Figure 3, and compute W_B. These data, arranged in tabular form, will be used by the draftsman and the diemaker.

Efficiency and Distortion

In the above example, t was chosen arbitrarily. A larger value would yield smaller values for C and k. Returning to our expression for gross efficiency, and substituting in terms of our new functions, we have

$$e_g = \frac{\int_V S^2 dv}{S_a^2 V_g} = \frac{P\ E}{S^2 L W_B t} = \frac{Q}{\left(\frac{PL}{St^3}\right)(c + 8 + w_k)} \tag{12}$$

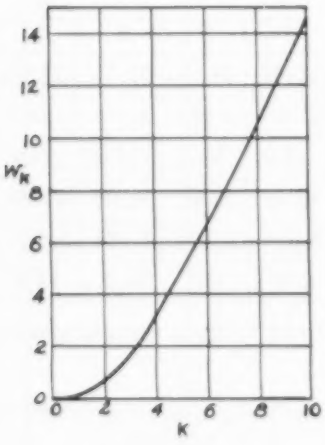

Figure 3

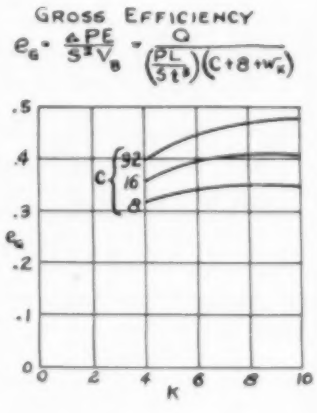

Figure 4

Figure 4, which is a graph of Eq (12), shows that there is an optimum value of k for each value of C. but it also indicates that large values of C are desirable. This judgment must be modified by consideration of distortion and possible buckling.

Curvature of the spring due to its own deflection causes a distortion of each cross-section, of the type shown in Figure 5. The value of δ is given approximately by

$$\delta = \frac{2}{k+1} \cdot \frac{S^2 t}{E^2} \left\{ 3\left(\frac{C}{4}\right)^4 + \sqrt{\left(\frac{k}{4}\right)^2 + 1} \left[685 + 64\left(\frac{C}{4}\right) + 36\left(\frac{C}{4}\right)^2 + 24\left(\frac{C}{4}\right)^3 \right] \right\} \qquad (13)$$

This formula is based on the assumption that the neutral surface is initially plane, and that δ/t is so small compared to k that the resulting change in stress distribution may be neglected. It does not apply when k is less than 1. In general, this distortion is most serious when k 1. Figure 6 shows δ/t as a function of C when k = 1 and S/E = .0033, as in our example above. Obviously it would be inadvisable to use a value of C much greater than 24.

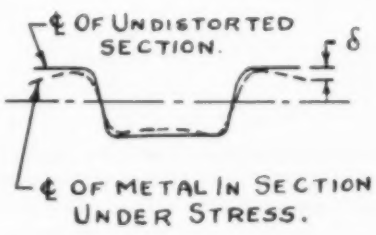

Figure 5

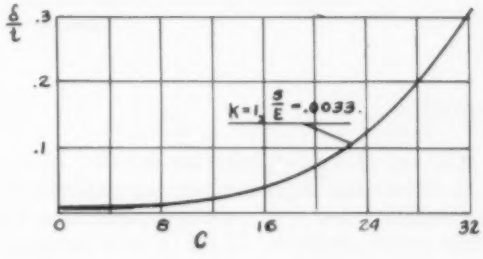

Figure 6

If the neutral surface of the spring has appreciable curvature in the stressed condition, the limitation on C is more severe. Let R be the radius of curvature of the profile view of the neutral surface in the stressed condition, positive when the center of curvature is on the compression side of the spring. Then the factors outside the curved brackets on the right-hand side of Eq (13) are replaced by $\frac{St^3}{ER}$.

It is favorable to stability for the curvature to be negative, so that I increases with the distortion, and for the free edges of the spring to be on the tension side, to reduce any tendency to buckle by column action.

Comparison with Conventional Springs

Where design conditions allow the use of this ribbed spring, its advantages are truly remarkable. Table II compares the spring of our example with the triangular and uniform-section flat springs which meet the same design requirements. The material saved is from 50 to 75 percent. The stability with respect to variation in stock thickness is often a prime consideration. An advantage not shown by the table is the greatly increased accuracy of profile made possible by the large depth of section, compared to stock thickness. The author has also had occasion to use aluminum for a spring of this type, in an application where endurance limit was not a factor, but where resistance to weathering was very important. Replacement of the steel spring previously used, which was stressed to 100,000 psi, by an aluminum spring stressed to 40,000 psi working in the same space, was possible only because of the additional degree of freedom allowed by ribbing the spring. The savings due to elimination of heat-treatment and plating costs, and the higher efficiency of the shape, made the new spring less expensive than the one it replaced.

TABLE II

Type of Spring	Length	Gross Volume	%change in rate / %change in stock thickness	
			Stress	Deflection
Ribbed	4.02	.166	1+	1+
Uniform Rectangular Section	4.29	.337	2	3
Triangular Flat	3.06	.675	2	3

AN APPLICATION OF LIEBMAN'S ITERATION METHOD TO VISCOUS FLOW

LEONARD S. LUSTICK
Research Laboratories Division, General Motors Corporation
Detroit, Michigan

Introduction

The solution of many problems arising in applied mathematics entails solving a particular partial differential equation with its associated boundary conditions. The nature of the differential equation and its boundary conditions makes it often impossible to attain an analytical solution to the problem. The Liebman Iteration Method is a numerical method of attaining the solution at a discreet number of points.

It might be well to reflect a moment on the sifnificance of a differential equation and how such an impersonal sign language as mathematics can represent and predict the behavior of an actual physical situation.

The differential equation itself is only a mathematical statement which is consistent with basic physical laws, such as the familiar F = Ma, the conservation of matter and energy, etc. Certain assumptions are made in writing the differential equation. How well the equation represents the physical situation is dependent on the accuracy of the assumptions, which is in turn dependent on the observer's knowledge or feeling of the physical situation.

The partial differential equation by itself has an infinite number of solutions. However, the solution we are interested in is determined uniquely by the singular boundary conditions. This last statement is not obvious, and would require a considerable amount of mathematical maturity to prove. Since this maturity is not at the disposal of this writer, a bit of mathematical philosophy will be substituted for it. This philosophy is known as Hadamar's principle and, in effect, states that if a governing partial differential equation arises out of a reasonable physical situation, and it is satisfied everywhere in a particular domain, including the boundaries, the solution thus obtained is unique.

Statement of Problem

In the problem concerned with in this paper, it is desired to determine the outlet pressure of a pump necessary to support a load W on a stationary cylindrical shaft and to determine also the pressure distribution under the shaft. The geometry of the problem is shown schematically in Figure 1.

Since the solution obtained by Liebman's method applies only to a specific geometry, it will be necessary to assign dimensions to the pertinent parameters of the problem. These parameters will have the following values:

Diameter of inlet hole, d = 1/4''
Length of shaft, l = 1-3/4''
Diameter of shaft, D = 1-1/2''

Applications for this type of problem might arise where it is necessary to avoid the initial boundary lubrication conditions upon starting and before the shaft has accelerated to speed.

It might also be used in problems where the relative motion between the shaft and bearing is negligible and no hydrodynamic oil film can be sustained, such as in the wrist pin of an automobile.

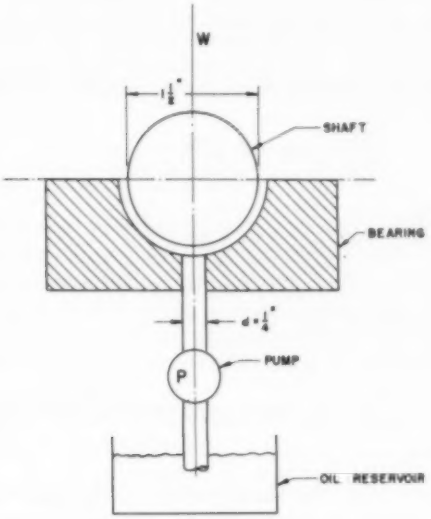

SCHEMATIC GEOMETRY OF PROBLEM

Figure 1

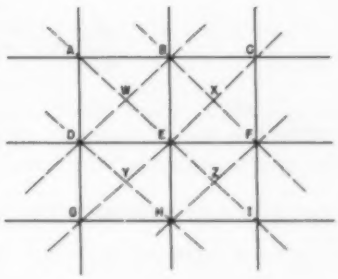

CRITERION TO DETERMINE IF ADVANCE TO FINER NET IS NECESSARY – $\frac{W+X+Y+Z}{4} \cdot E$

Figure 2

Basic Equations and Assumptions Used in Deriving the Governing Differential Equation

The basic physical laws used in deriving the governing differential equation for the above problem are the familiar F = MA and the conservation of mass. The utilization of these laws in the light of rational assumptions results in the governing equation, $\frac{\delta^2 P}{\delta x^2} + \frac{\delta^2 P}{\delta y^2} = o$, which is recognized as LaPlace's equation with pressure as the dependent variable.

The assumptions used in obtaining this equation are listed below:

(1) The acceleration of the oil is zero.
(2) The effect of curvature is neglected.
(3) Steady-state conditions exist.
(4) The oil is an incompressible fluid.

Reduction of the Governing Equation to Non-Dimensional Form

Having once determined the governing equation, it is advisable for purposes of the iteration method to reduce it to a non-dimensional form. In our particular case this can be done quite easily by multiplying the equation, $\frac{\delta^2 P}{\delta x^2} + \frac{\delta^2 P}{\delta y^2} = o$ by $\frac{1}{P_o}$. The equation is now reduced to $\frac{\delta^2 U}{\delta x^2} + \frac{\delta^2 U}{\delta y^2} = o$, where U equals the non-dimensional parameter $\frac{P}{P_o}$.

Reduction of Governing Equation to a Difference Equation

With the equation in non-dimensional form, the next step is to reduce it to a difference equation by means of finite difference theory. This difference equation can be realized in the following way. Suppose for purposes of illustration we visualize the domain of our problem divided into a square mesh as shown in Figure. 2. U_0 is the value of the function at one arbitrarily chosen discreet point, O, in the mesh.

U_1, U_2, U_3, U_4 are values of the function at the four surrounding points. Then it follows that

$$\left(\frac{\delta U}{\delta x}\right)_n \approx \frac{U_0 - U_1}{a}; \qquad \left(\frac{\delta U}{\delta x}\right)_2 \approx \frac{U_2 - U_0}{a}$$

$$\frac{\delta^2 U}{\delta x^2} \approx \frac{\left(\frac{\delta U}{\delta x}\right)_2 - \left(\frac{\delta U}{\delta x}\right)_n}{a} \approx \frac{U_2 - 2U_0 + U_1}{a}$$

In like manner,

$$\frac{\delta^2 U}{\delta y^2} \approx \frac{U_4 - 2U_0 + U_3}{a^2}$$

Hence, the governing differential equation, $\frac{\delta^2 U}{\delta x^2} + \frac{\delta^2 U}{\delta y^2} = o$, can be written for arbitrary point 0 as the difference equation, $U_1 + U_2 + U_3 + U_4 - 4w_0 = 0$.

At points adjacent to the boundary it often happens that the surrounding points are not equally spaced around it, as shown in Figure 3. In the event of this condition, the difference equation at this type point is

$$U_1 + \frac{U_2}{\lambda_2} + U_3 + U_4 - \left(2 + \frac{1}{\lambda_2}\right).$$

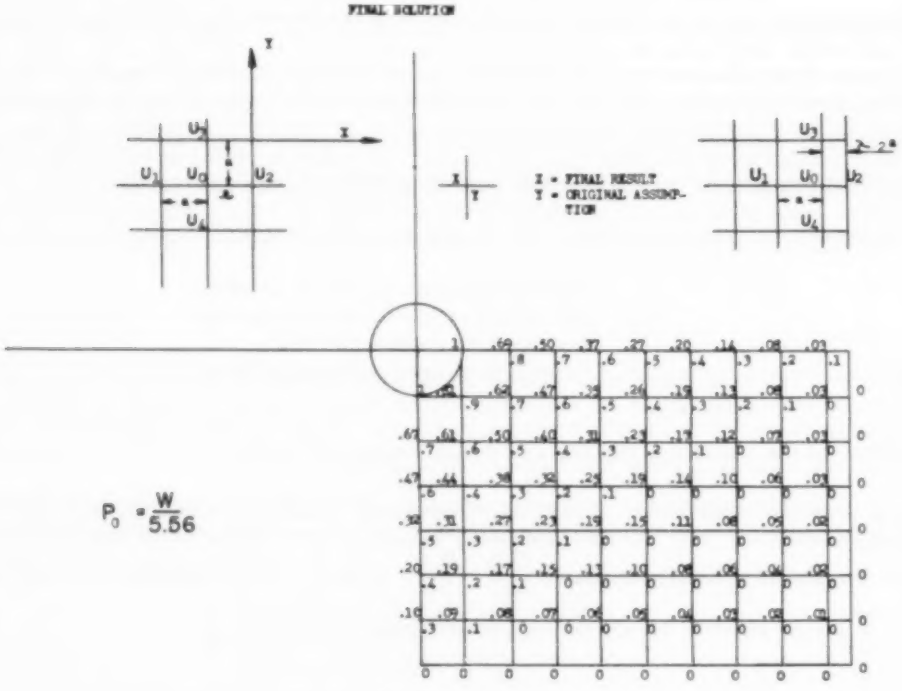

Figure 3

The problem of iteration is at once obvious and is seen to consist of simultaneously satisfying the difference equation at a large number of specified discreet points in the domain.

The final result of the iteration procedure is shown in Figure 3.

The value of P_0 (the inlet pump pressure) was obtained by numerical integration, taking cognizance of the fact that the bearing is cylindrical and adding only the vertical components of the pressure. These, of course, must be equal to W.

Summary of Iteration Method

(1) Derive from basic physical laws the governing partial differential equation.
(2) Non-dimensionalize the above equation.
(3) Transform the equation in (2) into a difference equation.
(4) Establish the mesh and make original assumption as to the value of the function at the nodal points. This original assumption can save considerable time if accurate.
(5) Proceed by an orderly method to simultaneously satisfy the difference equation at the nodal points.
(6) q Check to see if an advance to a finer net is required. Referring to Figure 2, the procedure is as follows:
   (a) W is calculated as average of A, B, D and E. X, Y and Z are calculated in like manner.
   (b) E is then calculated as the average of W, X, Y and Z.
   (c) The above value of E should check closely with the previously determined value. If this condition is not met, it is an indication to advance to a finer net using the previous approximation and linear interpolation to determine the original assumption the finer net.

In closing, it should be pointed out that no attempt at originality has been made aside from the specific geometry of the problem which is similar to a problem solved in a graduate course at Syracuse University.

The purpose of this paper has been to illustrate the steps in using the Iteration Method in solving a boundary value problem.

PERFORMANCE OF CENTRIFUGAL PUMPS FROM AFFINITY LAWS AT NON-CORRESPONDING OPERATING POINTS

ARVID E. ROACH and HOWARD H. KEHRL
Research Laboratories Division, General Motors Corporation
Detroit, Michigan

Introduction

This paper is concerned with the problem of governing a variable-speed centrifugal pump drive. The problem is: In what manner shall the speed of the pump be varied in order that its head-capacity curve may intersect the head-capacity curve of the receiver system at any specified point on the latter curve? The solution proposed in the paper is illustrative of a method of handling such problems by means of the principle of dynamic similitude, which method may be useful where not enough is known about the physical situation to enable one to solve the differential equations for the system.

Nomenclature

The following nomenclature is used:

Symbol		Dimensions
Q	Capacity, or quantity of fluid passing through the pump, cubic feet per second	L^3T^{-1}
H	Head developed by pump, or energy transferred from pump to fluid, foot-pounds per slug	L^2T^{-2}
N	Speed of pump impeller, revolutions per second	T^{-1}
D	Diameter of pump impeller or other characteristic linear dimension, feet	L
ρ	Density of fluid flowing, slugs per cubic foot	ML^{-3}
μ	Viscosity of fluid flowing, slugs per foot-second	$ML^{-1}T^{-1}$
r	Ratio of any linear dimensions of pump	Dimensionless

Subscripts:

1	Initial conditions
2	Final conditions
m	Model pump
p	Prototype pump

Affinity Laws for Centrifugal Pumps

The plot of the variation in head developed by a centrifugal pump with variation in capacity at constant impeller speed is called the characteristic curve (Fig. 1) of the pump. This curve is obtained experimentally, usually at a single impeller speed. The variation of head and capacity at other speeds retains the general form of Fig. 1 and may readily be computed by means of the affinity laws for centrifugal pumps.

The affinity laws were first found experimentally but may be derived by dimensional analysis. From experimental and theoretical considerations, it may be shown that the capacity of a

pump is a function of the conditions of operation, the size and proportions of the pump, and the properties of the pumped fluid, that is,

$$Q = f(H, N, D, \rho, \mu, r', r'', \ldots r^n) \tag{1}$$

where $r', r'', \ldots r^n$ are such ratios of linear dimensions of the pump as may be needed to describe its geometry.

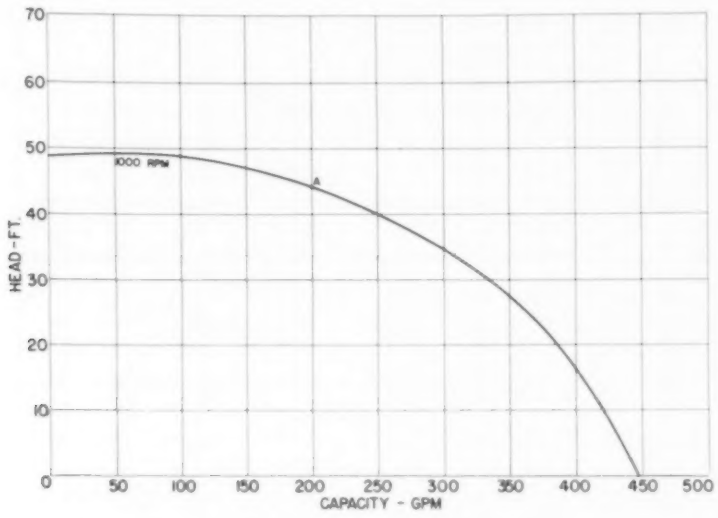

Figure 1

By the π theorem, Eq (1) may be rewritten in the form

$$\pi_1 = F(\pi_2, \pi_3, \ldots \pi_{n-3}) \tag{2}$$

where $\pi_1, \pi_2, \ldots \pi_{n-3}$ are the n - 3 possible independent dimensionless ratios which may be formed from the variables of Eq (1).

Solving for the dimensionless π's, we obtain

$$\pi_1 = Q\,N^{-1}\,D^{-3},\ \pi_2 = H\,N^{-2}\,D^{-2},\ \pi_3 = \rho\,N\,D^2\,\mu^{-1},\ \pi_4 = r', \text{ etc.}$$

Eq (2) becomes

$$Q = N\,D^3 \cdot F(H\,N^{-2}\,D^{-2}, \rho\,N\,D^2\,\mu^{-1}, r', r'', \ldots r^n) \tag{2a}$$

where the form of the function F is unknown.

Let the subscripts p and m designate a prototype pump and a model pump respectively. Then

$$\frac{Q_p}{Q_m} = \frac{N_p\,D_p^3 \cdot F(H_p\,N_p^{-2}\,D_p^{-2},\ \rho\,N_p\,D_p^2\,\mu^{-1}, r_p', r_p'', \ldots, r_p^n)}{N_m\,D_m^3 \cdot F(H_m\,N_m^{-2}\,D_m^{-2},\ \rho\,N_m\,D_m^2\,\mu^{-1}, r_m', r_m'', \ldots, r_m^n)} \tag{3}$$

Eq (3) provides a basis for comparing pumps, that is, for predicting the performance of a prototype pump from the known performance of a model pump whenever the separate arguments of the unknown function F are equal, that is, whenever $(\pi_2)_p = (\pi_2)_m$, $(\pi_3)_p = (\pi_3)_m$, etc.

The parameter $\pi_3 = \rho N D^2 \mu^{-1}$ is Reynolds' number. Unless different fluids are used in the prototype and the model, it will in general be impossible to make $(\pi_3)_p = (\pi_3)_m$, while keeping $(\pi_2)_p = (\pi_2)_m$, etc. However, π_3 affects primarily the fluid friction of the pump and, as shown by Fig. 2, large changes in Reynolds' number have relatively little influence on the hydraulic resistance to flow so long as the flow is fully turbulent. The influence of Reynolds' number on the operation of centrifugal pumps may therefore be assumed negligible, an assumption which is justified in practice by the virtual independence of the hydraulic efficiency of centrifugal pumps upon Reynolds' number.

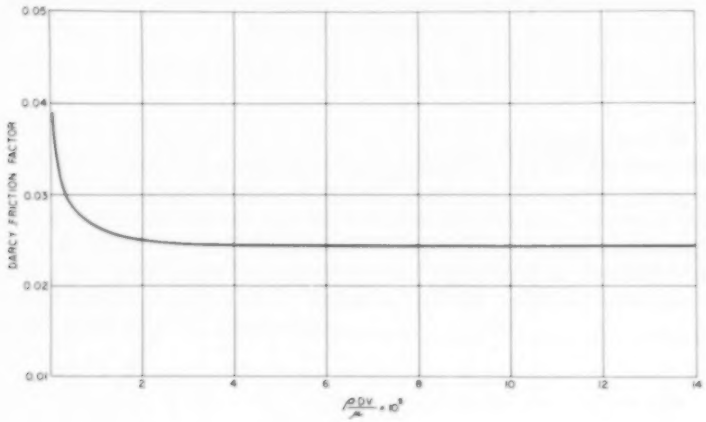

Figure 2

The conditions $(\pi_4)_p = (\pi_4)_m$, etc., may be fulfilled simply by making the model a geometric image of the prototype, a condition which is easily satisfied on a macroscopic scale.

The affinity laws thus reduce to the statement that

$$\frac{Q_p}{Q_m} = \frac{N_p\ D_p^3}{N_m\ D_m^3} \quad \text{when} \quad \frac{H_p}{H_m} = \frac{N_p^2\ D_p^2}{N_m^2\ D_m^2}, \tag{4}$$

and vice versa. These laws may be used to investigate the effect of changes in scale of geometrically similar pumps or of changes in speed for a given pump.

A simple problem will serve to illustrate some of the properties of these laws. Let it be required to determine the characteristic curves for the pump of Fig. 1 at several other speeds of operation. Take as the basis for computation the point A having the coordinates $H_A = 44$, $Q_A = 200$, and $N_A = 1000$. At speed $N_B = 1200$, we have

$$Q_B = Q_A \frac{N_B}{N_A} \left(\frac{D_B}{D_A}\right)^3 = 200 \times 1.2 = 240$$

and

$$H_B = H_A \left(\frac{N_B}{N_A}\right)^2 \left(\frac{D_B}{D_A}\right)^2 = 44 \times 1.44 = 63.4$$

We may tabulate these results with others computed in this manner for different speeds:

N	H	Q
800	28.2	160
900	35.6	180
1000	44.0	200
1100	53.4	220
1200	63.4	240

Points computed in this manner are called corresponding points and are characterized by the property that π_1 = constant, π_2 = constant, etc. Similar groups of corresponding points may be computed for other operating points from the given curve, and in this way a family of characteristic curves may be plotted, as in Fig. 3. Note that all corresponding points lie on square parabolas, such as O-A-B, a fact which is evident from inspection of Eq (4) when $D_p = D_m$. Curves computed in this manner have been shown to correspond very closely to experimentally determined characteristic curves. The principal restriction is that one is compelled always to deal with corresponding points.

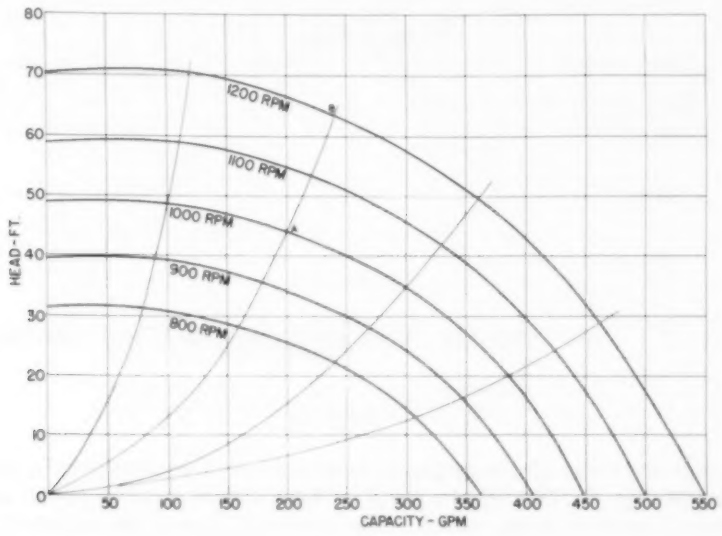

Figure 3

Performance at Non-Corresponding Operating Points

Problems arise in which it is desired to compute operating data which does not lie on the parabolic locus of corresponding points. For example, consider a pump delivering fluid to a discharge system composed of an arrangement of distribution pipes. The characteristics of the pump and discharge system may be such as is represented in Fig. 4. The pump will operate at point A where its characteristic curve intersects the system curve. Suppose that the pump is driven by means of a variable-speed motor and that it is desired to determine the speed at which it must run in order that its characteristic curve will intersect the system curve at some other point C not lying on the locus of corresponding points passing through point A. The affinity laws, as stated, offer no means of proceeding from point A to point C, for these points are non-corresponding. In practice, such a problem is usually solved graphically by sketching a family of pump characteristic curves at different speeds and by picking off the speed of the characteristic curve passing through point C.

An ingenious short cut, suggested by Mr. John G. Wright (Mechanical Engineering Department, College of Engineering, Wayne University), makes use of the fact that at some point on the characteristic curve there is a point D which is in correspondence with the point C. This point may be determined graphically by plotting the parabolic locus of corresponding points passing through point C. Having determined the coordinates of point D in this manner, the remaining coordinates of point C may be found from the affinity laws.

A graphical solution is of limited usefulness in specifying what kind of governor is needed to regulate the pump speed so as to satisfy changing system requirements. What is needed for

this purpose is an analytical relation between the speed change ΔN required for a given capacity change ΔQ and head change ΔH.

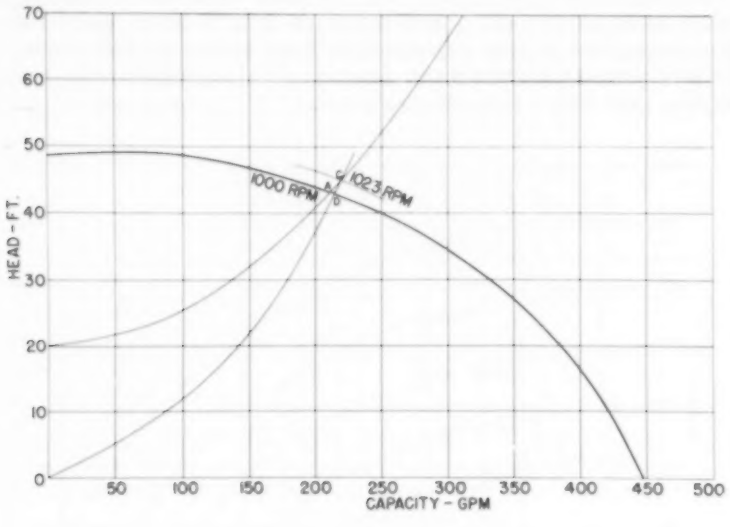

Figure 4

The complete characteristic of a centrifugal pump may be represented by a surface in H-Q-N space, as shown in Fig. 5. The system curve is independent of pump speed and may likewise be represented as a surface in this space. The operating line of the combined pump and discharge system will be determined by the intersection of these surfaces.

The known data of the problem are, for the pump, H_1, Q_1, N_1 and $\left[\frac{\partial Q}{\partial H}\right]_1$. These data are not sufficient to characterize completely the characteristic surface. However, if some other derivative, say $\left[\frac{\partial Q}{\partial N}\right]_1$, were known sufficient data would be available to characterize a plane tangent to the characteristic surface at the point H_1, Q_1, N_1. The intersection of this plane with the system surface would represent, for small changes ΔQ and ΔH, the operating line of the pump-system combination.

The derivative $\left[\frac{\partial Q}{\partial N}\right]_1$ may be obtained by differentiating Eq (2a) which may be rewritten for convenience in the form

$$QN^{-1}D^{-3} = f\,(HN^{-2}D^{-2}, \text{ and other } \pi\text{'s}) \qquad (5)$$

where all the π's are considered to be constant, except $QN^{-1}D^{-3}$ and $HN^{-2}D^{-2}$ which are permitted to undergo small changes. The difficulty which arises in differentiating a function whose form is unknown has been ably treated by Mr. M. D. Hersey in a paper ("A Relation Connecting the Derivatives of Physical Quantities") published in the Scientific Papers of the Bureau of Standards, Vol. 15, 1919-20. This paper, which depends upon and is a corollary to Buckingham's π-theorem, has apparently been neglected by later investigators in this field and, in our opinion, merits further consideration.

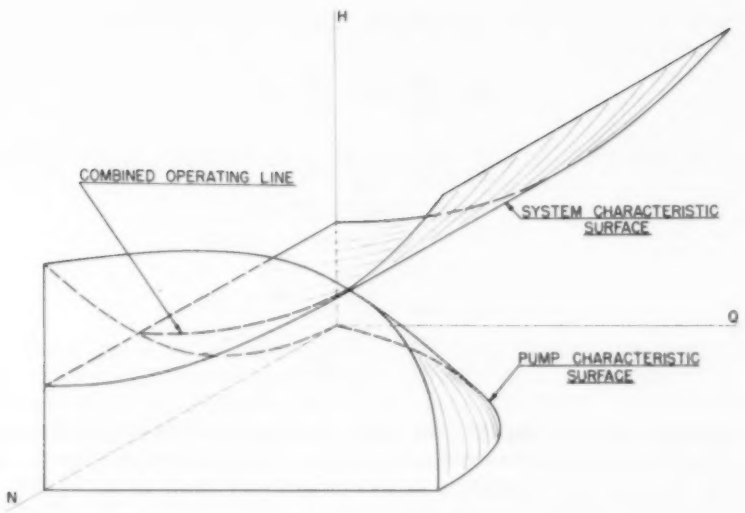

Figure 5

Following Hersey's method in differentiating Eq (5), we have

$$\frac{\partial(QN^{-1}D^{-3})}{\partial N} = \frac{df}{d(HN^{-2}D^{-2})} \cdot \frac{\partial(HN^{-2}D^{-2})}{\partial N}$$

$$= \frac{df}{d(HN^{-2}D^{-2})} \cdot \frac{-2(HN^{-2}D^{-2})}{N} \tag{6}$$

But also

$$\frac{\partial(QN^{-1}D^{-3})}{\partial N} = \frac{\partial Q}{\partial N} \frac{(QN^{-1}D^{-3})}{Q} - \frac{(QN^{-1}D^{-3})}{N} \tag{7}$$

From Eqs (6) and (7), we have

$$(HN^{-2}D^{-2}) \frac{df}{d(HN^{-2}D^{-2})} = \frac{-N(QN^{-1}D^{-3})}{2} \left(\frac{1}{Q} \frac{\partial Q}{\partial N} - \frac{1}{N}\right) \tag{8}$$

Similarly, we may write

$$(HN^{-2}D^{-2}) \frac{df}{d(HN^{-2}D^{-2})} = H(QN^{-1}D^{-3}) \left(\frac{1}{Q} \frac{\partial Q}{\partial H}\right) \tag{9}$$

From Eqs (8) and (9), we have

$$\frac{\partial Q}{\partial N} = \frac{Q}{N} - 2 \frac{H}{N} \frac{\partial Q}{\partial H} \tag{10}$$

which is the desired derivative.

Since $Q = f(H, N)$, then

$$dQ = \frac{\delta Q}{\delta H}\, dH + \frac{\delta Q}{\delta N}\, dN$$

and

$$dN = \frac{dQ - \frac{\delta Q}{\delta H}\, dH}{\frac{\delta Q}{\delta N}}$$

or

$$dN = \frac{dQ - \frac{\delta Q}{\delta H}\, dH}{\frac{Q}{N} - 2\frac{H}{N}\frac{\delta Q}{\delta H}} \qquad (11)$$

To illustrate the application of Eq (11), we may consider the following problem: A pump supplies fluid to a system having the combined characteristics shown in Fig. 4. It is required to change the pump speed so as to supply a larger quantity of fluid to the system. At the initial condition, the pump and system curves intersect at $Q = 212.4$ gpm, $H = 43.2$ ft, and $N = 1000$ rpm; at this point the measured value of $\delta Q/\delta H = 13.65$. At the final condition, the system curve and new pump curve are to intersect at $Q = 220$ gpm, $H = 45.0$ ft. The new speed for the pump will be

$$N = 1000 + \frac{7.6 + (13.65 \times 1.8)}{\frac{212.4}{1000} + \frac{2 \times 43.2 \times 13.65}{1000}} = 1000 + 23.2 = 1023.2 \text{ rpm.}$$

A graphical solution using Wright's method gives $Q = 215$ gpm and $H = 43$ ft for the point on the original pump curve corresponding to the final point $Q = 220$ gpm and $H = 45$ ft. From the affinity laws, $N = 1023$ rpm.

Such excellent agreement will be obtained only when the change in operating point is fairly small. As the change becomes larger, Eq (11) will yield results which are increasingly in error.

ANALYTICAL DERIVATION OF GEAR TOOTH "X" FACTOR

DOUGLAS HUGHSON
Modern Engineering Service
Berkley, Michigan

The tooth form factor plays an important part in most gear tooth bending stress formulae in use today. This form factor was originated by Wilfred Lewis and presented in a paper read before the Engineers Club of Philadelphia, on October 15, 1892. For standard gears, the factor y which is equal to 2X/3p has been tabulated in many machine design texts. These tables are of little use in the design of special gears which have become widespread today.

For years it has been common practice in automotive gear work to lay out the gear tooth ten or twenty times size and to scale the X Factor. The accuracy of this time-consuming method is of course limited by the accuracy of the draftsman.

The analytical method discussed here, although theoretically correct only for gears hobbed with a sharp corner tool, may be applied even when the hob corners are rounded slightly. The factor becomes more conservative as the radius of the hob tooth corner increases.

For symbols and equations, refer to Figure 1.

When the tooth center line coincides with the y axis, and the gear center falls on the origin, the equation of the fillet becomes

$$x = R \sin \alpha - b \sin \alpha - R \alpha \cos \alpha + K \cos \alpha \tag{1}$$

$$y = R \cos \alpha - b \cos \alpha + R \alpha \sin \alpha - K \sin \alpha \tag{2}$$

where R is the pitch radius of gear, K is $\frac{t}{2} + b \tan \Phi_M$, b is the tooth dedendum, t is the tooth thickness at R, and Φ_M is the pressure angle at R.

Selecting any point x, y, on the tooth fillet, we have

$$X_v = \frac{x^2}{A-y} \tag{3}$$

where A is the greatest distance from the center of the gear to a point on the tooth center line through which the tooth force acts.

The tooth X factor is defined at the minimum value of X_v:

$$\frac{dX_v}{d\alpha} = \frac{2(A-y)\, x \frac{dx}{d\alpha} + x^2 \frac{dy}{d\alpha}}{(A-y)^2} = 0$$

or

$$2(A-y) \frac{dx}{d\alpha} + x \frac{dy}{d\alpha} = 0 \tag{4}$$

From (1),

$$\frac{dx}{d\alpha} = R \alpha \sin \alpha - K \sin \alpha - b \cos \alpha = y - R \cos \alpha \tag{5}$$

From (2),

$$\frac{dy}{d\alpha} = R \alpha \cos \alpha - K \cos \alpha + b \sin \alpha = -x + R \sin \alpha \tag{6}$$

Then substituting (5) and (6) in (4), we have

$$2(A-y)\,(y-R\cos\alpha) - x(x-R\sin\alpha) = 0$$

or

$$2Ay-2AR\cos\alpha - 2y^2 + 2Ry\cos\alpha - x^2 + xR\sin\alpha = 0$$

When X_V is a minimum, referring to the point on the fillet as $x_1\ y_1$ and the corresponding point at which the hob pitch line is tangent to the gear pitch circle as $x_2\ y_2$, we have

$$2Ay_1 - 2Ay_2 - 2y_1^{\,2} + 2y_1\,y_2 - x_1^{\,2} + x_1\,x_2 = 0$$

or

$$2(A-y_1)\,(y_1 - y_2) - x_1\,(x_1 - x_2) = M = 0 \tag{7}$$

where

$$y_1 = R_r\cos\alpha + (R\alpha - K)\sin\alpha \tag{8}$$

$$x_1 = R_r\sin\alpha - (R\alpha - K)\cos\alpha \tag{9}$$

$$y_2 = R\cos\alpha \tag{10}$$

$$x_2 = R\sin\alpha \tag{11}$$

$$A = \frac{r_b}{\cos(\Phi_o - \beta_o)} \tag{12}$$

and r_b is the base radius of gear, Φ_o is the pressure angle at outside radius, β_o is the angle subtended at center of gear by one-half outside tooth thickness, and R_r is the root radius of gear.

Equation (7) may be solved by substituting various trial values of α in (8), and (9), (10) and (11) and by substituting values of x_1, y_1, x_2 and y_2 obtained together with 'A' back into (7) until a value of α which gives a solution for (7) is obtained.

By substituting the values of x_1 and y_1 corresponding to this value of α in (3), the Gear Tooth X Factor is given by:

$$X = \frac{x_1^{\,2}}{A-y_1} \tag{13}$$

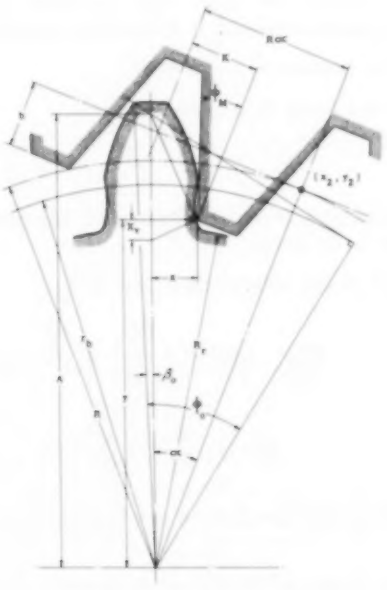

Figure 1

From the foregoing we see that the solution in part consists of a set of equations, namely (7), (8), (9), (10), (11) and (12), that must be solved by trial. This theoretically exact although cumbersome solution is presented in the hope that someone may discover a suitable substitution to simplify these equations and arrive at an analytical approximate solution of sufficient accuracy for stress analysis.

In Figure 1 a badly undercut tooth has been purposely chosen to show that the formulae apply to hobbed involute teeth whether undercut or not

A sample calculation is detailed below to show the steps to be followed in the solution of the problem.

Mention should be made that Mr. Leonard G. Johnson of the Research Laboratories Division of General Motors Corporation has arrived at similar results from a somewhat different approach. His results were given in a talk before the Michigan Section of the Mathematical Association of America on March 25, 1950, at Ann Arbor, Michigan.

Sample Calculation

$N = 17$	$\Phi_M = 20^0$	$t_o = .084260$
$P = 8$	$2R = 2.125000$	$A = 1.161698$
$b = .144625$	$2r_b = 1.996847$	$K = .150814$
$t = .196350$	$2R_o = 2.375000$	$R_r = .917875$

o	x_1	y_1	x_2	y_2	M
20^0 .349066	.107135	.937788	.363396	.998423	.000301
19.90^0 .347321	.107242	.937343	.3161653	.999056	.000408
19.9576^0 .348326	.107180	.937599	.362657	.998692	.000000

$$X = \frac{.107180^2}{.224099} = .051261$$

$$y = \frac{2 \times .051261}{3 \times .392699} = .087023$$

Addendum

Subsequent to the presentation of the paper, it was brought to the author's attention that, in addition to the paper by Mr. Leonard G. Johnson referred to above, there is a third paper on this subject. This is Mr. M. Maletz' paper on "Analytical Determination of the Form Factor in the Beam Formula for a Tooth," presented before the American Gear Manufacturers Association in May, 1941. The papers by Mr. Johnson and by the author deal with the special case of a rack-shaped and sharply cornered tool; Mr. Maletz' paper deals with disk-type as well as rack-type tools, having sharp or round or chamfered tips.

SURFACE STRESS AND STRAIN OF SPIRAL INVOLUTE GEARS

VICTOR E. FRANCIS
National Broach and Machine Company
Detroit, Michigan

VICTOR E. FRANCIS

The Industrial Mathematics Society lost one of its most active members when Victor E. Francis died of a heart attack in July, 1951, at the age of 29 years. A graduate of the College of the City of New York, Mr. Francis was an employee of the National Broach and Machine Company and was well-known as a contributor of articles on scientific gear engineering to "Machinery" and "Product Engineering." His last paper, which was presented before the Industrial Mathematics Society on May 24, 1951, appears on the following pages.

The design of spiral or crossed-axes gears has always been a difficult problem for several reasons.

The first part of the design problem is to obtain the proper helix angles of the gears. There are an infinite number of usable helix angles for any set, given the center distance and the desired ratio. Each gear may have a helix angle of zero to ninety degrees, theoretically. However, the range of these halix angles may be cut down by certain practical design considerations, such as pitch or pitch diameter size. For instance, a speedometer drive gear must have a hole big enough to fit over the transmission output shaft, which limits the gear pitch diameter to a minimum value and in turn limits its helix angle.

The second part of this problem is to find the load-carrying capacity of the gears selected. Since the load-carrying capacity is a function of the allowable maximum stress induced by the load, it will be the object of this paper to show how both the maximum surface compressive stress and the deformation at the point of contact may be found on a spiral gear set for any given load. This particular analysis is applied to involute helicoids only and cannot be applied to enveloping worm gear sets or to Gleason-type hypoid gears.

It should be noted that the theoretical instantaneous surface contact which occurs between crossed-axes gears is that of a point. In parallel-axes gears this theoretical contact is a straight line running the full face width of the gears. Because of this point contact, the load-carrying capacity of spiral gears as compared to parallel-axes gears is very low. Thus a comparatively small load produced a relatively high compressive stress at the point of contact. This point of contact deforms under load to a small ellipse of contact, and the two contacting gear teeth actually come closer together due to this flattening. On most gear sets with higher crossed axes angles the total deformation of the teeth that occurs is due solely to this surface flattening. The tooth bending that takes place is usually negligible due to the low tooth load. Likewise the bending stress occurring at the root of the gear teeth is small enough to be ignored. Any failure that will occur will be at the points of contact only, such as failure of the surface and not bending failure.

Quite a few years ago, gear design experts suggested using the Hertz equations of contacting surfaces for determining the stresses and strains for parallel-axes gears. The work done by

Almen, Buckingham, McFarland, and Straub and the present A. G. M. A. work are all based on the Hertz formulas. This method of attack will be continued here on crossed-axes gears.[1]

The validity of the Hertz equations requires several assumptions, which must also hold true when the equations are applied to spiral gears. These assumptions are:

(1) The materials in contact must be homogeneous.
(2) Contact must take place under static conditions.
(3) The subsurface stresses in both bodies must decrease to zero before reaching the outside diameter of a gear or the opposite tooth flank surface or either face.
(4) The proportional or elastic limit of the materials must not be exceeded.

The first condition of homogeneity and the fourth condition of limiting stress are easily met, because most metals are sufficiently uniform to be considered homogeneous (excepting perhaps some cast materials) and because we do not desire to go beyond the elastic limit as that is considered to be failure. For the third condition, it is only when the contact occurs near the outside diameter of a gear that the subsurface stresses do not become zero before reaching the outside diameter; otherwise most gear face widths and tooth thicknesses are sufficiently large to fulfill the requirement. However, for the second assumption it is impossible for running gears to be in static contact. Until someone develops other than an empirical answer we will have to use velocity correction factors, which at the present time are almost universally used on parallel-axes gears. Such are the PV or PVT maximum limits or the Barth type factors.

Maximum and Minimum Radii of Curvature of Involute Helicoids

It is a known fact that all involute helicoids can be generated by a series of straight lines that are all tangent to a helix on a base cylinder, as shown in Figs. 1 and 2. Hence it can be said that an involute helicoid is a surface composed of a series of straight lines called generatrices. For any given gear helix angle and normal pressure angle, these generatrices have

Figure 1. "Involute Helicoid". Straight Generatrices in Helicoidal Surface and Involute Profile of its Transverse Section. Courtesy of National Broach & Machine Co.

[1] A first step in this direction was an approximation published by Prof. E. Buckingham on pg. 534 of Ref. 1. For details see our footnote 2.

a given angle to the gear axis. This angle is the base helix angle, which is the angle of the helix on the base diameter. The multiple relationships between the helix angle ψ, the normal pressure angle ϕ_n, and the base helix angle ψ_b can be found in Dr. W. F. Vogel's "Involutometry and Trigonometry," page 266 of Reference 8.

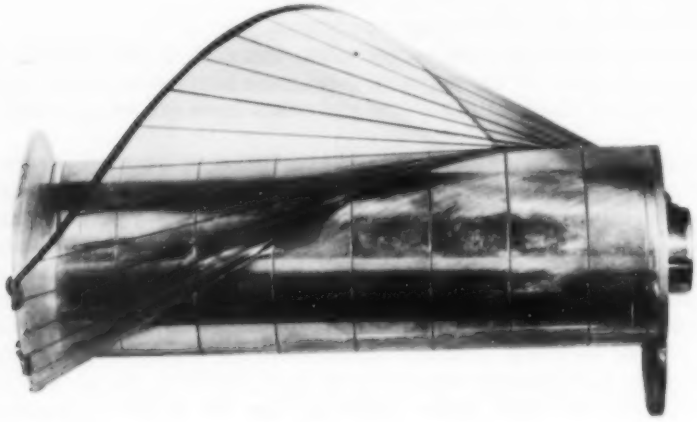

Figure 2. Tangency of Straight Generatrices to Base Helix of Surface. Courtesy of National Broach & Machine Co.

To use the Hertz equations, it is necessary to find both the minimum and maximum radius of curvature of each of the surfaces in contact and also the angle between the planes which contain the principal curvatures of both surfaces.

We have already seen that the maximum radii of curvature of both members are infinite. Their arcs are contacting straight-line generatrices of the two involute helicoids.

When two crossed-axes involute gears are in mesh their contacting generatrices, the straight lines, will intersect at some angle H, since the generatrices coincide only for parallel-axes gears. Therefore it will be necessary to find the angle H.

The minimum radius of curvature is required next. We know from the theory of continuous surfaces that the minimum radius of curvature of a surface at a given or selected point Q lies in a plane which is at right angles to the plane containing the maximum radius of curvature of the surface at that point.

Therefore we have a series of straight lines which compose the surface of the helicoid and another series of lines at right angles to this surface which will be the normals of the surface. These latter lines will be tangent to the base cylinder, and the angle they produce with the axis of the cylinder is the base lead angle, or 90^0 minus the base helix angle. The length of such a normal measured from the point of tangency on the base cylinder to the point Q on the surface is the minimum radius of curvature at the given or selected point Q.

From Figure 3, it can be seen that the minimum radius of curvature of the surface is ρ_q at any point Q of the involute helicoid whose transverse pressure angle is ϕ_q.

$$\rho_q = \frac{R_b \tan \phi_q}{\cos \psi_b} \qquad (1)$$

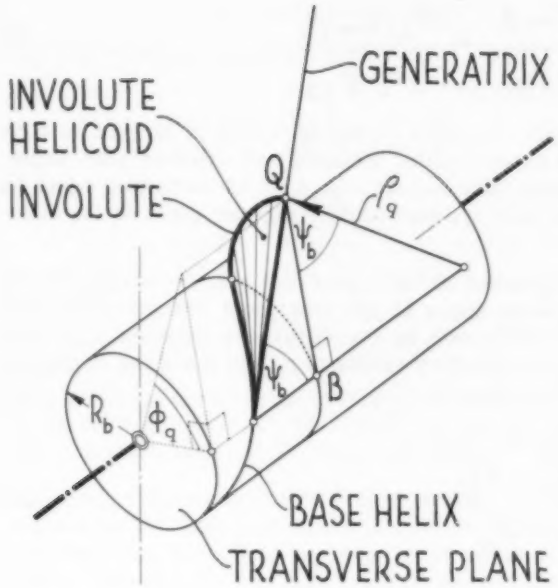

Figure 3. Principal Radii of Curvature of Involute Helicoid. The maximum radius of curvature of an involute helicoid (namely, that of any of its straight generatrices) is infinite in magnitude. The minimum radius of curvature of this surface at the freely selected point Q is labelled ρ_q. By contrast, BQ is the radius of curvature of the involute at Q but not a "principal" radius of curvature of the helicoid. Note that the normal pressure attacks in the direction of ρ_q, if Q is the contact point of a helical involute tooth.

Radii of Curvature of Varying Contact Elements of Meshing Spiral Gear Tooth Surfaces

For meshing gear teeth it is necessary to find ϕ_q values of such surface elements which are instantaneously in contact.

The values ρ_{q_1} and ρ_{q_2} of two contacting spiral gears may be considered as the radii of two steel cylinders, crossing each other at an angle H and pressed against each other with a force F_n equal to the "normal" tooth load. If angle H is established according to the equations of the next section, then the contact of the "substitute steel cylinders" is equivalent to the point contact of the spiral teeth for all calculations of stress and strain.[2]

It can be seen from any involute spur gear set that the total theoretical length of the path of contact is constant for any given operating pressure angle. Therefore, the sum of the radii of curvature of the gears at any point of contact is equal to this theoretical length of the path of contact. This will also hold true for crossed-axes gears. The sum of the two ρ_q values of contacting surface elements will remain constant for any spiral gear set. Then as the ρ_q of one gear decreases, the ρ_q of the mating gear must increase. Therefore, it is necessary only to find the sum, and then it will be possible to find the stress or strain at any point on either gear profile. The equation for this sum is obtained by finding the two special ρ_q values at the pitch point, which we will label ρ_1 and ρ_2. If, by the same token, we label the known transverse main pressure angles at the pitch point ϕ_1 and ϕ_2, then we obtain from Eq (1)

[2] This concept of "Substitute Rolls" has been introduced on pg. 534 of Ref. 1. But the approximate character of this solution leads to errors of both the "Roll Size" and the "Angle H" between the rolls. The error of the resulting tooth load is always on the safe side.

$$\rho_1 + \rho_2 = \frac{R_{b1} \tan \phi_1}{\cos \psi_{b1}} + \frac{R_{b2} \tan \phi_2}{\cos \psi_{b2}} \tag{2}$$

This $(\rho_1 + \rho_2)$ can be considered as the length of a piece of string which is tangent to both base cylinders when they are placed at their proper center distance and crossed axis angle. The string must also be tangent to both normal base helices. $(\rho_1 + \rho_2)$ is therefore equal to the distance from the tangency point on one base cylinder to the tangency point on the other base cylinder.

The greatest ρ_q values occur at the outer diameter of each gear and will be designated by ρ_{out}. By the same token, the smallest ρ_q values occur at the innermost contact radius and will be labelled ρ_{in}. They can be easily determined by the difference between ρ_{out} and $(\rho_1 + \rho_2)$. These special values ρ_{in} and ρ_{out} are limiting values of ρ_q and mark the beginning and end of gear contact. They may be found as follows:

$$\rho_{out\,1} = \frac{\sqrt{R_{o1}^2 - R_{b1}^2}}{\cos \psi_{b1}} \tag{3}$$

$$\rho_{in\,1} = (\rho_1 + \rho_2) - \rho_{out\,1} \tag{4}$$

$$\rho_{out\,2} = \frac{\sqrt{R_{o2}^2 - R_{b2}^2}}{\cos \psi_{b2}} \tag{5}$$

$$\rho_{in\,2} = (\rho_1 + \rho_2) - \rho_{out\,2} \tag{6}$$

In these equations R_o is the outside radius of the gear and R_b is the radius of the base cylinder.

After finding the limiting ρ_{out} and ρ_{in} values, the stresses and deflections at the limiting contact positions can be computed. Then we can arbitrarily select as many additional values of ρ_q between these limiting values as we desire to compute the stress or deformation.

Angle H Between Contacting Generatrices of Meshing Spiral Gear Teeth

This angle H is constant, i.e. independent of the contact position of the gears in any gear set. Its equations, derived for three types of gear sets, are:

Σ = Angle of gear crossed axes (shaft angle)
ϕ_n = Normal pressure angle
ϕ = Transverse pressure angle
ψ = Helix angle
} at the pitch cylinder

Ψ_b = Base helix angle

All other angles are parameters.

Then for $\Sigma = 90^\circ = \Psi_1 + \Psi_2$ (Right-angle drive)

$\tan \beta = \tan \Psi_{b1} \sin \Phi_1$

$\tan H = \tan (\beta + \Phi_2) \sin \Psi_{b2}$

For $\Sigma = \Psi_1 - \Psi_2$, where $\Psi_1 > \Psi_2$ (Spiral set having opposite hands)

$\tan \alpha = \tan \Psi_{b1} \cos \Phi_1$

$\tan \beta = \tan \Psi_{b1} \sin \Phi_1 \cos \alpha \ / \sin (\alpha - \Sigma)$

$\tan H = \tan (\beta - \Phi_2) \sin \Psi_{b2}$

For $\Sigma = \Psi_1$ (a helical and spur gear meshing together), where $\Psi_2 = 0$.

$\tan H = \sin \Psi_{b1} \tan \Phi_1$

For the most common occurrence, 90° drive sets, the chart (Fig. 7) shows the angle H for any helix angle for 14-1/2°, 20° and 25° normal pressure angle gears. The use of this chart saves the computation of the above equations.

The important aspect of this chart is that it is possible to get a generatrix intersecting angle as low as 28°, which is equivalent to having two "substitute cylinders" crossed at 28°. It is obvious that their load-carrying capacity is much greater than that of the "substitute cylinders" placed at 90°, as advocated in the approximate solution of Reference 1.

Details of Derivation of Angle H

The derivation of the equations for a right-angle drive gear set is shown in Fig. 4. A is the true length of the generatrix of gear 1, whose projection in the transverse plane is inclined at

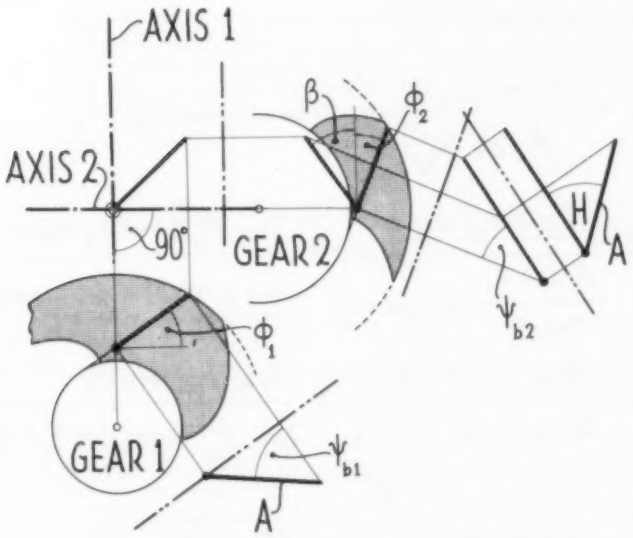

Figure 4. Illustrating the Derivation for a Right-Angle Drive. The involute helicoids of two meshing teeth contact each other in only one point of their helicoidal surfaces. The illustration shows the establishment of the angle H between the contacting generatrices of the two helicoids.

the transverse operating pressure angle ϕ_1. The angle ψ_{b1} is the base helix angle of this gear. The angles ϕ_2 and ψ_{b2} are the corresponding angles on the mate. Then from Fig. 4 of the preceding page

$$\tan\beta = \frac{A\sin\psi_{b1}\sin\phi_1}{A\cos\psi_{b1}} = \tan\psi_{b1}\sin\phi_1 \tag{7}$$

$$\tan H = \frac{\frac{A\cos\psi_{b1}}{\cos\beta}\sin(\beta+\phi_2)}{\frac{A\cos\psi_{b1}}{\cos\beta}\frac{\cos(\beta+\phi_2)}{\sin\psi_{b2}}}$$

$$\tan H = \tan(\beta+\phi_2)\sin\psi_{b2} \tag{8}$$

or eliminating the parameter β,

$$\tan H = \frac{(\tan\psi_{b1}\sin\phi_1 + \tan\phi_2)\sin\psi_{b2}}{1-\tan\psi_{b1}\sin\phi_1\tan\phi_2} \tag{8a}$$

The derivation of the angle H for the gear set with crossed axis angle equal to the difference of the gear helix angles is shown in Fig. 5.

$$\tan\alpha = \frac{A\sin\psi_{b1}\cos\phi_1}{A\cos\psi_{b1}} = \tan\psi_{b1}\cos\phi_1 \tag{9}$$

$$\tan\beta = \frac{A\sin\psi_{b1}\sin\phi_1}{\frac{A\cos\psi_{b1}}{\cos\alpha}\sin(\alpha-\Sigma)} = \frac{\tan\psi_{b1}\sin\phi_1\cos\alpha}{\sin\alpha\cos\Sigma-\cos\alpha\sin\Sigma} \tag{10a}$$

$$\tan\beta = \frac{\tan\psi_{b1}\sin\phi_1}{\tan\alpha\cos\Sigma-\sin\Sigma} = \frac{\tan\psi_{b1}\sin\phi_1}{\tan\psi_{b1}\cos\phi_1\cos\Sigma-\sin\Sigma}$$

$$\tan\beta = \frac{\sin\phi_1}{\cos\phi_1\cos\Sigma-\sin\Sigma/\tan\psi_{b1}}$$

$$\tan H = \frac{\frac{A\cos\psi_{b1}}{\cos\alpha}\frac{\sin(\alpha-\Sigma)}{\cos\beta}\sin(\beta-\phi_2)}{\frac{A\cos\psi_{b1}}{\cos\alpha}\frac{\cos(\alpha-\Sigma)}{\cos\psi_{b2}}}$$

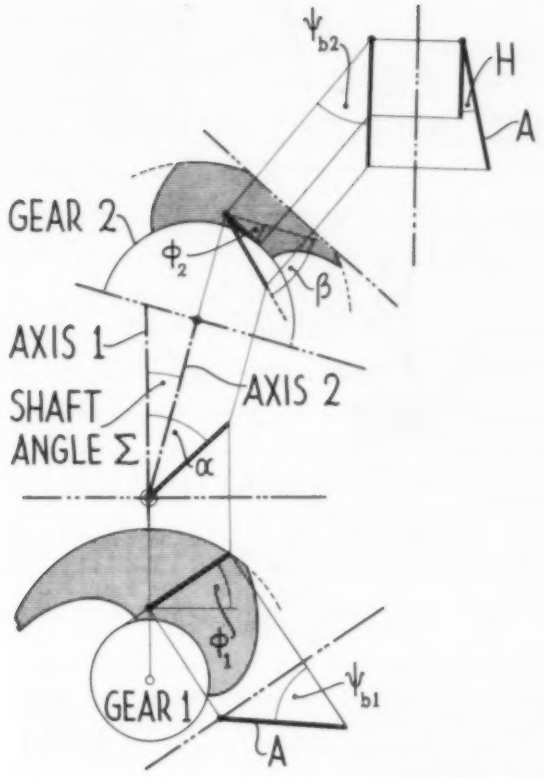

Figure 5. Gear Axes Crossing at Any Angle. The establishment of angle H is shown for the case when the angle Σ between the gear axes is the difference of the helix angles ψ_1 and ψ_2 at the pitch cylinders of the gears.

$$\tan H = \frac{\tan(\alpha - \Sigma)\sin(\beta - \phi_2)\cos\psi_{b2}}{\cos\beta}$$

$$\tan H = \tan(\beta - \phi_2)\sin\psi_{b2} \tag{11}$$

The derivation of the angle H for a spur gear mating with a helical gear is shown in Fig. 6.

$$\tan\alpha = \frac{A\sin\psi_{b1}\cos\phi_1}{A\cos\psi_{b1}} = \tan\psi_{b1}\cos\phi_1$$

$$\tan H = \frac{A\sin\psi_{b1}\sin\phi_1/\cos\phi_n}{\frac{A\cos\psi_{b1}}{\cos\alpha}\cos(\Sigma - \alpha)} = \frac{\tan\psi_{b1}\sin\phi_1}{\cos\phi_n(\cos\Sigma + \sin\Sigma\tan\alpha)}$$

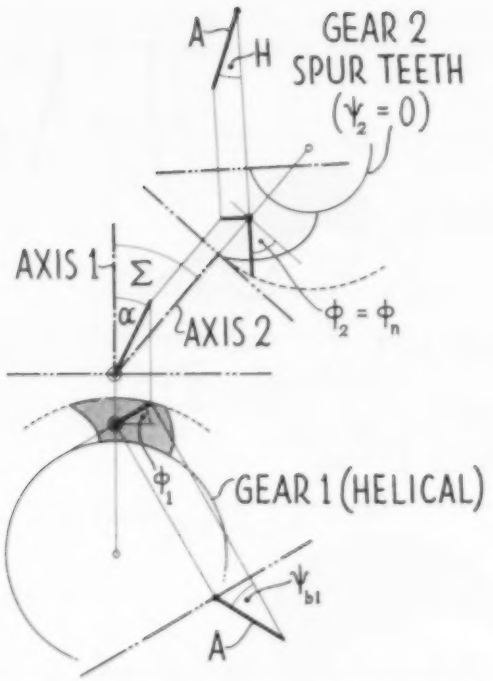

Figure 6. Contact between Helical and Spur Teeth. Establishment of the intersecting angle H of the contacting generatrices of the meshing tooth surfaces.

$$\tan H = \frac{\tan \psi_{b1} \sin \phi_1}{\cos \phi_n (\cos \Sigma + \sin \Sigma \tan \psi_{b1} \cos \phi_1)}$$

$$\tan H = \sin \psi_{b1} \tan \phi_1 \qquad (12)$$

Maximum Compressive Stress and Strain

The formulas, constants, and coefficients are taken from Hertz and later investigators. See References 2, 4, 6, 7 and 9.

It should be noted that K is a constant influenced only by the materials of the gear teeth, while the other constants, δ and Θ depend on the selection of the contact point. See Eqs (13) to (15).

Θ is an auxiliary angle, whose establishment yields the coefficients C_a, C_b and C_d by interpolation from Table I. Additional explanations are given along with the consecutive steps (13) to (19) of the calculation:

$$K = \frac{2}{3}\left(\frac{E_1}{1-\mu_1^2} + \frac{E_2}{1-\mu_2^2}\right) \qquad (13)$$

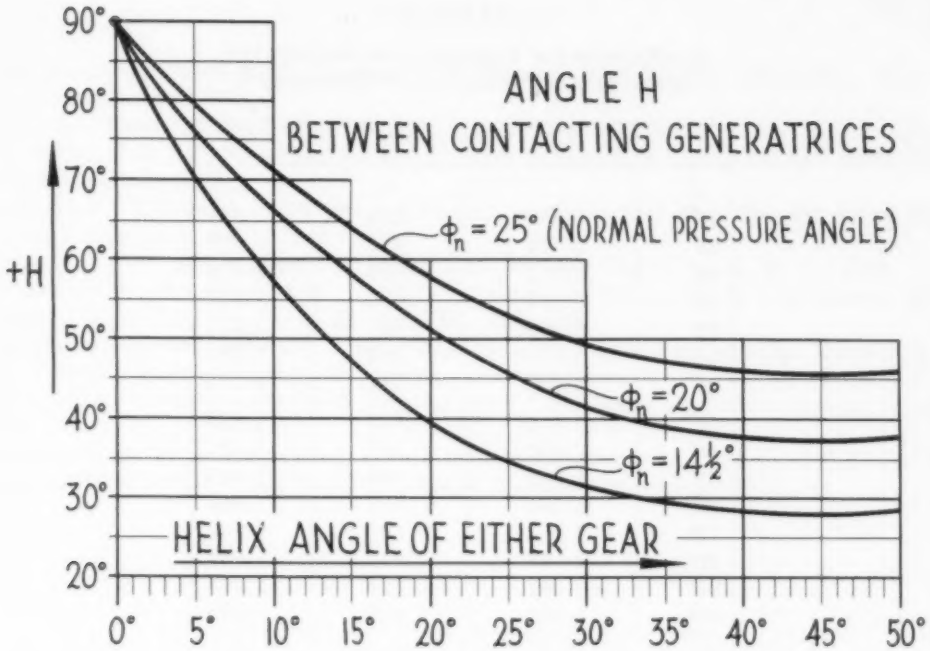

Figure 7. Chart for Right-Angle Involute Spiral Gear Sets. The curves give the intersecting angle H of the contacting generatrices of the meshing helical tooth surfaces. This angle does not change with changing contact positions of the gears.

where E is the modulus of elasticity of the material of either gear and μ is the Poisson's ratio of the material of either gear.

$$\delta = \frac{1}{\frac{1}{\rho_1} + \frac{1}{\rho_2}} \tag{14}$$

$$\cos\theta = \delta\sqrt{\left(\frac{1}{\rho_1}\right)^2 + \left(\frac{1}{\rho_2}\right)^2 + \frac{2\cos 2H}{\rho_1 \rho_2}} \tag{15}$$

where ρ_1 and ρ_2 are the various values ρ_{out} and ρ_{in} taken from either Eqs (3) and (4) or Eqs (5) and (6) or any two ρ_q values belonging to any contact point between these limits.

$$a = C_a \sqrt[3]{\frac{4P\delta}{K}} \tag{16}$$

$$b = C_b \sqrt[3]{\frac{4P\delta}{K}} \tag{17}$$

TABLE I

Coefficients for Equations (16) through (18).
Excerpt from Table XIV of Reference 4.

θ	C_a	C_b	C_d
0°	---	0	---
10°	6.612	.319	.851
20°	3.778	.408	1.220
30°	2.731	.493	1.453
35°	2.397	.530	1.550
40°	2.136	.567	1.637
45°	1.926	.604	1.709
50°	1.754	.641	1.772
55°	1.611	.678	1.828
60°	1.486	.717	1.875
65°	1.378	.759	1.912
70°	1.284	.802	1.944
75°	1.202	.846	1.967
80°	1.128	.893	1.985
85°	1.061	.944	1.996
90°	1.000	1.000	2.000

Where a and b are the respective major and minor semi-axes of the ellipse of contact, and P is the normal tooth load.

$$d = C_d \sqrt[3]{\frac{P^2}{4K^2\delta}} \tag{18}$$

where d equals the total deflection at the point of contact due to surface deformation.

$$S_c = \frac{1.5\,P}{\pi a b} \tag{19}$$

where S_c is the maximum compressive stress.

Thus by using the proper values of H and ρ it can be seen that it is possible to obtain the theoretical stress and deformation in a crossed-axes gear set for any contact position of the gears.

The problem of what is the maximum allowable surface stress can only be answered by tests, but the above equations allow the designer or tester to reduce the loads to a basic stress value. When these basic stress values are considered with the sliding velocity, it should be possible to get a formula for the maximum allowable load.

BIBLIOGRAPHY

1. Buckingham, E. "Analytical Mechanics of Gears," McGraw-Hill Book Co., New York, Toronto and London, 1949.
2. Hertz, H. "Gesammelte Werke," Vol. 1, Leipzig, 1895.
3. McFarland, F.R. "Tooth Deflection and Scuffing in Design of Highly Loaded Gears," Product Engineering, 1947.
4. Roark, R. J. "Formulas for Stress and Strain," McGraw-Hill Book Co., 1st Edit., 6th Impression, New York and London, 1938.
5. Straub, J. C. "Progress Report on PVT Values of Gear Teeth," A. G. M. A., 1950.
6. Thomas, H. R., and Hoersch, V. A. "Stress Due to the Pressure of One Elastic Solid on Another," Eng. Exp. Sta., Univ. Ill. Bull. No. 212, 1930.
7. Timoshenko, S., and Lessells, J. M. "Applied Elasticity," Westinghouse Technical Night School Press, East Pittsburgh, Pa., 1925.
8. Vogel, W. F. "Involutometry and Trigonometry," Michigan Tool Co., Detroit, Michigan, 1945.
9. Whittemore, H. L., and Petrenko, S. N. "Friction and Carrying Capacity of Ball and Roller Bearings," Technical Paper No.201, National Bureau of Standards, 1921.

A GENERAL STEADY-STATE SOLUTION OF THE TWO-MASS TORSION PROBLEM

EARL F. RIOPELLE
Houdaille-Hershey Corporation
Detroit, Michigan

Introduction

The two-mass torsional vibration system is widely used as an example of the application of mathematics to analyze the behavior of machines. Generally, existing articles and texts have analyses which give the natural frequency of the system, and the total relative motion of the two masses when only one mass is driven by an exciting force.

Other factors can be obtained which are useful to the engineer who is concerned about the performance of such a machine that can be idealized as a two-mass vibratory system. These are:

1. Relative amplitude of the masses when they are both excited by harmonic torques at an arbitrary phase angle.
2. The absolute amplitude of the masses.
3. (a) The nodal points of the system at a given forced frequency.
   (b) The nodal point at the resonant frequency.

The mathematics required to derive expressions for the above conditions is elementary, but the results are useful. The derivation, results, and discussion are given in the article.

Discussion

This solution defines the torsional response of idealized driving and driven machines connected by a flexible means. Driving machines are exemplified by electric motors, hydraulic motors, gasoline and diesel engines, etc. Driven machines may be electric generators, fans, hydraulic pumps, air and refrigerator compressors, etc. The flexible connecting means are usually shafting, couplings, chain-gear-and-belt drives, etc.

An analysis such as this is made to determine the loads or stress developed in the coupling medium by the torque fluctuations of the driving or driven machine. The vibratory loads are often neglected in the determination of the size requirements of the connecting medium with results of a seemingly unexplainable failure.

The analysis is made by idealizing the system into two masses of polar moment of inertia equal to those of the driving and driven machines connected by a torsional spring of the same rate as the coupling medium. It is also necessary to know the harmonic content of the torque fluctuation of both the driving and driven members.

The idealized system can be represented schematically by Fig. 1, in which J_1 and J_2 are polar inertias (inch pound second^2), θ_1 and θ_2 are the angular displacements of J_1 and J_2 (radians), K is the torsional spring constant (inch pounds per radian), T_1 and T_2 are maximum torques of the harmonics considered (inch pounds), N and n are harmonic numbers, ω is angular velocity (radians per second), t is time (seconds), and α and β are phase angle relationships of the torques (radians).

The accuracy of the analysis is wholly dependent upon how accurately the above dimensions represent the actual machine.

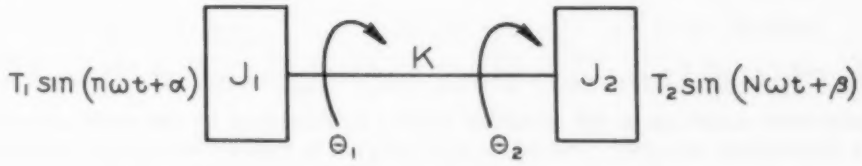

Figure 1

The next step in the analysis is to write the differential equations of motion of the idealized system. This is done by equating the sum of the external forces on each mass to the rate of change of momentum of the mass. Thus,

$$J_1\ddot{\theta}_1 + K(\theta_1-\theta_2) = T_1 \sin(n\omega t+\alpha)$$

$$J_2\ddot{\theta}_2 + K(\theta_2-\theta_1) = T_2 \sin(N\omega t+\beta)$$

$$\ddot{\theta}_1 + \frac{K}{J_1}(\theta_1-\theta_2) = \frac{T_1}{J_1}\sin(n\omega t+\alpha)$$

$$\ddot{\theta}_2 - \frac{K}{J_2}(\theta_1-\theta_2) = \frac{T_2}{J_2}\sin(N\omega t+\beta)$$

Let

$$\frac{K}{J_1} = p_1^2 \qquad \frac{K}{J_2} = p_2^2$$

$$\frac{T_1}{J_1} = Q_1 \qquad \frac{T_2}{J_2} = Q_2$$

$$\ddot{\theta}_1 - \ddot{\theta}_2 + (p_1^2+p_2^2)(\theta_1-\theta_2) = Q_1\sin(n\omega t+\alpha) - Q_2\sin(N\omega t+\beta).$$

The prime concern is of the relative motion of the two masses which can be used to determine the stress or load in the coupling medium. Therefore let

$$\theta_1-\theta_2 = \phi \quad \text{and} \quad \ddot{\theta}_1-\ddot{\theta}_2 = \ddot{\phi}$$

Thus,

$$\ddot{\phi} + (p_1^2+p_2^2)\phi = Q_1\sin(n\omega t+\alpha) - Q_2\sin(N\omega t+\beta).$$

Let:

$$p_1^2+p_2^2 = P^2$$

$$\ddot{\phi} + P^2\phi = Q_1\sin(n\omega t+\alpha) - Q_2\sin(N\omega t+\beta).$$

Expand the sine functions of the sum of two angles with an identity.

$$\ddot{\phi} + P^2\phi = Q_1[\sin n\omega t\cos\alpha + \cos n\omega t\sin\alpha]$$
$$- Q_2[\sin N\omega t\cos\beta + \cos N\omega t\sin\beta].$$

α and β are constants; therefore let

$$\cos\alpha = A \qquad \sin\alpha = B$$

$$\cos\beta = C \qquad \sin\beta = D$$

$$\ddot{\phi} + P^2\phi = Q_1[A\sin n\omega t + B\cos n\omega t] - Q_2[C\sin N\omega t + D\cos N\omega t].$$

The steady-state condition of the resulting motion is described by the particular integral of the above differential equation. The particular integral is easily found by the method given in "Mathematics of Modern Engineering," Doherty and Keller, Vol. 1, pg. 41., equations 90, and 91.

Let $$m = \frac{d\phi}{dt} \qquad m^2 = \frac{d^2\phi}{dt^2}$$

Then

$$[m^2 + P^2]\phi = Q_1 A\sin n\omega t + Q_1 B\cos n\omega t - Q_2 C\sin N\omega t - Q_2 D\cos N\omega t.$$

From the reference text,

$$\frac{1}{F(m^2)}\sin at = \frac{\sin at}{F(-a^2)} \qquad (90)$$

$$\frac{1}{F(m^2)}\cos at = \frac{\cos at}{F(-a^2)} \qquad (91)$$

Therefore, $$F(m^2) = (m^2 + P^2)$$

$$F(-a^2) = (-n^2\omega^2 + P^2)$$

and

$$\phi = \frac{Q_1 A\sin n\omega t}{P^2 - n^2\omega^2} + \frac{Q_1 B\cos n\omega t}{P^2 - n^2\omega^2} - \frac{Q_2 C\sin N\omega t}{P^2 - N^2\omega^2} - \frac{Q_2 D\cos N\omega t}{P^2 - N^2\omega^2}.$$

or

$$\phi = \frac{Q_1}{P^2 - n^2\omega^2}[\sin(n\omega t + \alpha)] - \frac{Q_2}{P^2 - N^2\omega^2}[\sin(N\omega t + \beta)].$$

Recall that $$Q_1 = \frac{T_1}{J_1}, \qquad Q_2 = \frac{T_2}{J_2}$$

$$\phi = \frac{\frac{T_1}{J_1 P^2}\sin(n\omega t + \alpha)}{1 - \left(\frac{n\omega}{P}\right)^2} - \frac{\frac{T_2}{J_2 P^2}\sin(N\omega t + \beta)}{1 - \left(\frac{N\omega}{P}\right)^2}.$$

Recall that $$P^2 = p_1^2 + p_2^2 = \frac{K}{J_1} + \frac{K}{J_2} = \frac{K(J_1+J_2)}{J_1 J_2}$$

Thus, $$\frac{T_1}{J_1 P^2} = \frac{T_1 J_2}{K(J_1+J_2)} \quad \text{and} \quad \frac{T_2}{J_2 P^2} = \frac{T_2 J_1}{K(J_1+J_2)}$$

and $$\phi = \left[\frac{T_1 J_2}{K(J_1+J_2)}\right]\left[\frac{1}{1-\left(\frac{n\omega}{P}\right)^2}\right] \sin(n\omega t+\alpha)$$

$$-\left[\frac{T_2 J_1}{K(J_1+J_2)}\right]\left[\frac{1}{1-\left(\frac{N\omega}{P}\right)^2}\right] \sin(N\omega t+\beta).$$

This is a convenient form for the expression of ϕ.

Notice when P = nw or Nw, the angle ϕ becomes infinite, which would cause failure of the coupling means.

The condition of P = nw is known as resonance or the critical frequency and, when expressed in the expanded form, is

$$P = \sqrt{\frac{K}{J_1} + \frac{K}{J_2}} = \sqrt{\frac{K(J_1+J_2)}{J_1 J_2}} \quad \text{rad./sec.}$$

$$f = \frac{P}{2\pi} = \frac{1}{2\pi}\sqrt{\frac{K(J_1+J_2)}{J_1 J_2}} \quad \text{cycles/sec.}$$

The terms $$\frac{1}{1-\left(\frac{n\omega}{P}\right)^2} \quad \text{and} \quad \frac{1}{1-\left(\frac{N\omega}{P}\right)^2}$$

are known as dynamic magnification factors, and they can be plotted as a general curve (Fig. 2).

Obviously because this analysis describes the twist resulting from the torque fluctuations, the twist resulting from the uniform load must be added.

$$\Phi = \phi_u + \phi$$

Φ = total twist, ϕ_u = uniform twist, and ϕ = fluctuating twist.

Observe that in order to reduce the effect of fluctuating torque, $\frac{nw}{P}$ or $\frac{Nw}{P}$ must be greater than $\sqrt{2}$.

It is customary to design the coupling medium with a torsional (K) low enough to insure a dynamic magnification factor of less than 1 for the principle harmonic of lowest number, thus insuring that all higher harmonics are automatically taken care of.

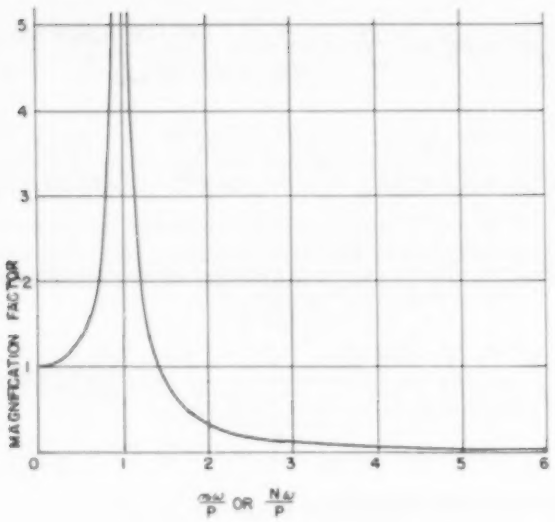

Figure 2.

Thusfar no mention has been made of the effect of phase angles α and β. It is apparent that if sin (nwt + α) and sin (Nwt + β) equal 1 and -1 simultaneously ϕ will be greater than if they do not.

It would be desirable to select α and β so as to minimize ϕ. The surest way of making this selection is to plot separate sine waves of sin (nwt) and sin (Nwt) and plot their sum for a sufficient number of phase relationships between them to establish the minimum.

Although the total twist Φ is of prime concern there are conditions when the amplitudes, θ_1 and θ_2 of the masses J_1 and J_2 are necessary. This would be particularly true if J_1 or J_2 were a reciprocating engine or compressor where the vibratory amplitude of the shaft would contribute greatly to the bearing loads on the unit.

θ_1 and θ_2 can be found from the information already obtained. The computations will be simplified if it is noted that in the expression for ϕ the effect of T_1, T_2, α, and β are independent; hence, they can be treated by the method of superposing their effects. Thus the resultant amplitudes θ_1 and θ_2 as developed by T_1 will be shown; the same can be done for T_2, and the results added to the effect of T_1.

Having

$$\phi = \left[\frac{T_1 J_2}{K(J_1 + J_2)}\right]\left[\frac{1}{1 - \left(\frac{n\omega}{p}\right)^2}\right] \sin n\omega t.$$

$$\theta_1 - \theta_2 = \phi$$

$$\ddot{\theta}_1 + \frac{K}{J_1}(\theta_1 - \theta_2) = \frac{T_1}{J_1} \sin n\omega t$$

$$\ddot{\theta}_2 - \frac{K}{J_2}(\theta_1 - \theta_2) = 0$$

Substituting,

$$\ddot{\theta}_2 - \frac{K}{J_2}\phi = 0$$

$$\ddot{\theta}_2 = \frac{K}{J_2}\phi$$

$$\ddot{\theta}_2 = \frac{K}{J_2}\left[\frac{T_1 J_2}{K(J_1+J_2)}\right]\left[\frac{1}{1-\left(\frac{n\omega}{p}\right)^2}\right]\sin n\omega t.$$

$$\dot{\theta}_2 = -\frac{1}{n\omega}\frac{K}{J_2}\left[\frac{T_1 J_2}{K(J_1+J_2)}\right]\left[\frac{1}{1-\left(\frac{n\omega}{p}\right)^2}\right]\cos n\omega t + C_1 .$$

$$\theta_2 = -\frac{1}{(n\omega)^2}\frac{K}{J_2}\left[\frac{T_1 J_2}{K(J_1+J_2)}\right]\left[\frac{1}{1-\left(\frac{n\omega}{p}\right)^2}\right]\sin n\omega t + C_1 t + C_2$$

Conditions for determining C_1 and C_2:

θ_2 is a harmonic motion and goes to zero, thus, $C_1 = C_2 = 0$.

θ_2 is a maximum when sin nwt = 1; therefore, nwt = $\frac{\pi}{2}, \frac{3\pi}{2}, \frac{5\pi}{2}$, and so forth.

$$\theta_{2\,max.} = -\frac{K}{n^2\omega^2 J_2}\left[\frac{T_1 J_2}{K(J_1+J_2)}\right]\left[\frac{1}{1-\left(\frac{n\omega}{p}\right)^2}\right]$$

$$p^2 = \frac{K}{J_1} + \frac{K}{J_2}$$

$$\theta_{2\,max.} = -\frac{T_1}{n^2\omega^2(J_1+J_2)}\left[\frac{1}{1-\frac{n^2\omega^2}{\frac{K}{J_1}+\frac{K}{J_2}}}\right]$$

$$\theta_{2\,max.} = -\frac{T_1}{n^2\omega^2(J_1+J_2)}\left[\frac{1}{1-\frac{n^2\omega^2 J_1 J_2}{K(J_1+J_2)}}\right]$$

$$\theta_{2\,max.} = -\frac{T_1}{n^2\omega^2(J_1+J_2) - \frac{n^4\omega^4 J_1 J_2}{K}}$$

$$\theta_{2\,max.} = -\frac{T_1}{n^2\omega^2}\left[\frac{K}{K(J_1+J_2) - n^2\omega^2 J_1 J_2}\right]$$

Solve for θ_1 in a like manner.

$$\ddot{\theta}_1 = \frac{T_1}{J_1} \sin nwt - \frac{K}{J_1}\phi$$

$$\ddot{\theta}_1 = \frac{T_1}{J_1} \sin nwt - \frac{K}{J_1}\left[\frac{T_1 J_2}{K(J_1+J_2)}\right]\left[\frac{1}{1-\left(\frac{nw}{p}\right)^2}\right] \sin nwt.$$

$$\ddot{\theta}_1 = \left\{\frac{T_1}{J_1} - \frac{K}{J_1}\left[\frac{T_1 J_2}{K(J_1+J_2)}\right]\left[\frac{1}{1-\left(\frac{nw}{p}\right)^2}\right]\right\} \sin nwt.$$

$$\dot{\theta}_1 = -\frac{1}{nw}\left\{\frac{T_1}{J_1} - \frac{K}{J_1}\left[\frac{T_1 J_2}{K(J_1+J_2)}\right]\left[\frac{1}{1-\left(\frac{nw}{p}\right)^2}\right] \cos nwt + C_3.$$

$$\theta_1 = -\frac{1}{n^2w^2}\left\{\frac{T_1}{J_1} - \frac{K}{J_1}\left[\frac{T_1 J_2}{K(J_1+J_2)}\right]\left[\frac{1}{1-\left(\frac{nw}{p}\right)^2}\right]\right\} \sin nwt + C_3 t + C_4.$$

Conditions for determining C_3 and C_4:

θ_1 is a harmonic motion, thus passes thru zero; therefore, $C_3 = C_4 = 0$

θ_1 is a maximum when sin nwt = 1; therefore, nwt = $\frac{\pi}{2}, \frac{3\pi}{2}, \frac{4\pi}{2}$, and so forth.

$$\theta_{1\,max.} = -\frac{1}{n^2w^2}\left\{\frac{T_1}{J_1} - \frac{K}{J_1}\left[\frac{T_1 J_2}{K(J_1+J_2)}\right]\left[\frac{1}{1-\left(\frac{nw}{p}\right)^2}\right]\right\}.$$

$$\theta_{1\,max.} = -\frac{1}{n^2w^2}\left\{\frac{T_1}{J_1} - \left[\frac{T_1 J_2}{J_1(J_1+J_2)}\right]\left[\frac{1}{1-\dfrac{n^2w^2}{\dfrac{K(J_1+J_2)}{J_1 J_2}}}\right]\right\}.$$

$$\theta_{1\,max.} = -\frac{1}{n^2w^2}\left\{\frac{T_1}{J_1} - \frac{T_1 J_2}{J_1(J_1+J_2) - \dfrac{n^2w^2 J_1^2 J_2}{K}}\right\}$$

$$\theta_{1\,max.} = -\frac{1}{n^2w^2}\left\{\frac{T_1}{J_1} - \frac{K T_1 J_2}{KJ_1(J_1+J_2) - n^2w^2 J_1^2 J_2}\right\}$$

$$\theta_{1\,max.} = -\frac{T_1}{n^2\omega^2 J_1}\left\{1 - \frac{K J_2}{K(J_1+J_2) - n^2\omega^2 J_1 J_2}\right\}.$$

$$\theta_{1\,max.} = -\frac{T_1}{n^2\omega^2 J_1}\left\{\frac{K(J_1+J_2) - n^2\omega^2 J_1 J_2 - K J_2}{K(J_1+J_2 - n^2\omega^2 J_1 J_2}\right\}.$$

$$\theta_{1\,max.} = -\frac{T_1}{n^2\omega^2}\left\{\frac{K - n^2\omega^2 J_2}{K(J_1+J_2) - n^2\omega^2 J_1 J_2}\right\}.$$

It will be noted that the displacements θ_1 and θ_2 are in opposite directions when the exciting frequency is greater than the resonant frequency. This implies that there is a point in the connecting medium where there is no motion or displacement. This point is called the node. It is obvious that if a gear train or chain drive is to be installed on the connecting shaft it would be desirable to locate the drive at the node to eliminate back lash rattle which results in tooth fatigue.

The position of the node can be determined by using the fact that the sum of the torques in the shaft is zero. As

$$-K_2\,\theta_2 = K_1\,\theta_1 = K\,\phi$$

where K_1 is that portion of K from J_1 to the node(in lb./rad.),and K_2 is that portion of K from J_2 to the node(in lb./rad.).

Note that $K = \frac{1}{K_1} + \frac{1}{K_2}$ (Fig. 3).

$$-K_2 = K\frac{\phi}{\theta_2}$$

$$-K_2 = \frac{K\left\{\left[\frac{T_1 J_2}{K(J_1+J_2)}\right]\left[\frac{1}{1-\left(\frac{n\omega}{p}\right)^2}\right]\right\}}{\frac{-T_1}{n^2\omega^2}\left[\frac{K}{K(J_1+J_2)-n^2\omega^2 J_1 J_2}\right]}$$

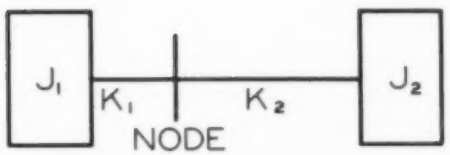

Figure 3

$$-K_2 = \frac{\left[\frac{J_2}{J_1 + J_2}\right]\left[\frac{p^2}{p^2 - n^2\omega^2}\right]}{-\frac{1}{n^2\omega^2}\left[\frac{K}{K(J_1+J_2) - n^2\omega^2 J_1 J_2}\right]}$$

Substitute $$p^2 = \frac{K(J_1 + J_2)}{J_1 J_2}$$

Reduce to lowest terms

$$-K_2 = -J_2 n^2\omega^2 \quad \text{or} \quad n^2\omega^2 = \frac{K_2}{J_2}$$

It is an interesting revelation that if J_1 is excited by a frequency (nw), the node is formed at the position that would form a single-degree-freedom system for J_2 of natural frequency (nw). See Fig. 4.

This makes it very simple to determine the position of the node for any exciting frequency.

The node at the resonant frequency of the system will be as follows:

Note the resonant frequency[2] is $K\left(\frac{J_1 + J_2}{J_1 \quad J_2}\right)$

$$K_2 = J_2\left[\frac{K(J_1+J_2)}{J_1 J_2}\right]$$

$$K_2 = \frac{K(J_1+J_2)}{J_1}$$

Similarly, $$K_1 = \frac{K(J_1+J_2)}{J_2}$$

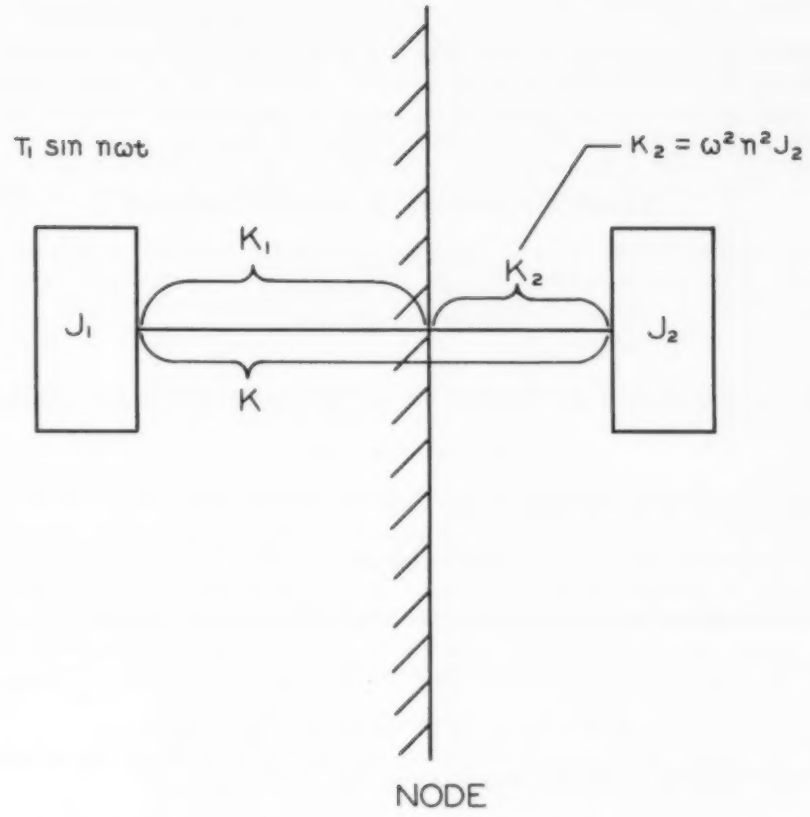

Figure 4

REFERENCES

1. Myklestad, N. O., "Vibration Analysis," McGraw Hill Book Co., Inc., New York, (1944) p. 57.
2. Freberg, C. R., and Kemler, E. N., "Elements of Mechanical Vibration," John Wiley and Sons, Inc., New York (1943) p. 67.
3. DenHartog, J. P., "Mechanical Vibrations," McGraw Hill Book Co., Inc., New York, (1940) p. 38, p. 60.

TRANSIENT MOTIONS IN LINEAR SYSTEMS

J. ORMONDROYD
University of Michigan
Ann Arbor, Michigan

Most readers of this lecture are familiar with simple linear differential equations, such as

$$m\ddot{x} + c\dot{x} + kx = f(t)$$

either in this form or in the old operational form

$$(m D^2 + c D + k) x = f(t)$$

More complicated equations of the same nature exist which can be written

$$Z(D) x = f(t)$$

where $$Z(D) = (\ldots \quad a_2 D^2 + a_1 D + a_0 + \frac{a\text{-}1}{D} + \frac{a\text{-}2}{D^2} \ldots)$$

There are three aspects to the solutions of equations of this type.

(1) Z(D) and f(t) may be given completely and explicitly, the problem being to integrate the differential equation so that X(t) is found as an explicit function of time. This might be called the direct problem.
(2) Z(D) and X(t) may be given, the problem being to infer f(t). This might be called the inverse problem.
(3) X(t) and f(t) may be given, the problem being to find Z(D). This is the problem inherent in Carson's Integral.

Problem 1 is the classic problem of all textbooks and the LaPlace Transform Method is undoubtedly the most acceptable way to carry out the solution for X(t).

Problem 2 is seldom discussed in detail in the textbooks. One common physical problem which leads to problem 2 is the basic problem of all instrumentation in which the mechanical and electrical circuits are all linear. The fundamental problem of all such recording instruments is:

Given the characteristics of the instrument, Z(D), and the record X(t), which might be designated the output of the instrument, what is the correct and accurate value of the disturbing or input function, f(t), the quantity that is being measured?

Problem 3 arises in a calibration of instruments mechanically and electrically so complex that no complete analysis of the characteristics of the instrument exists. This type of problem is practically never discussed in detail, although Carson's Integral is the expression of its formal solution. Carson's Integral holds when f(t) is a step function and X(t) is the response A(t) to the step function.

Problem 1: The Direct Problem

While the LaPlace Transform Method is the best method for the solution of this problem, it is frequently useful to use the older Duhamel Integral Method on some problems. This method is discussed by Timoshenko in Vibration Problems in Engineering, 2nd Edition, pp. 102-109, and by Karman and Biot in Mathematical Methods in Engineering, Chapter X. The emphasis in these treatments is put on systems of one degree of freedom. But the Duhamel's Integral method is even more useful in systems of many degrees of freedom.

If an impulse of short duration is applied at any point in a mechanical system, that point acquires a velocity which is added to the velocity already existing at that point. The added velocity is independent of the configuration of the system at the instant of application of the impulse. The added velocity is

$$V = \frac{1}{m} \int_0^{\Delta t} F dt$$

in which m is the mass of that section of the system in which the impulse $\int_2^{\Delta t} F dt$ is applied. A unit impulse is defined as $\int_0^{\Delta t} F dt = 1$ lb-sec as $F \longrightarrow \infty$ and $\Delta t \longrightarrow o$. The velocity caused by a unit impulse is $V = 1/m$. The response of the system to a unit impulse is designated as $h_{i,t,j,\tau}$ in a lumped system and as $h_{x,t,c,\tau}$ in a lineal distributed system. In words, $h_{i,t,j,\tau}$ is the displacement of body i of the system at time t caused by the application of a unit impulse to body j of the system at time $t = \tau$. For the lineal distributed system, $h_{x,t,c,\tau}$ is the displacement at point x and time t caused by the application of a unit impulse at point $x = c$ and at time $t = \tau$.

To illustrate the use of Duhamel's Integrals, let us take two systems shown in Figure 1 and Figure 2.

Lumped System

The equations of motion for the system shown in Figure 1 are:

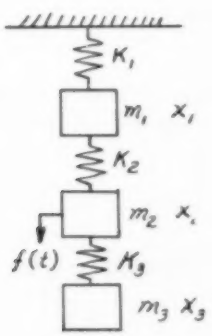

Figure 1

$$m_1\ddot{x}_1 + (k_1 + k_2)x_1 - k_2x_2 = 0$$

$$-k_2x_1 + m_2\ddot{x}_2 + (k_2 + k_3)x_2 - k_3x_3 = f(t)$$

$$-k_3x_2 + m_3\ddot{x}_3 + k_3x_3 = 0$$

To apply Duhamel's Integrals, we solve the easier problem in which $f(t) = O$ for the initial conditions at $t = \tau$ of $x_1 = x_2 = x_3 = O$, $\dot{x}_1 = \dot{x}_3 = O$, and $\dot{x}_2 = 1/m_2$.

These initial conditions will arise if the system has a unit impulse applied to body 2 at times $t = \tau$. The system is otherwise assumed completely quiescent at that time.

Then

$$h_{1,t,2,T} = A \sin p_1(t-T) + B \sin p_2(t-T) + C \sin p_3(t-T)$$

$$h_{2,t,2,T} = \alpha_1 A \sin p_1(t-T) + \alpha_2 B \sin p_2(t-T) + \alpha_3 C \sin p_3(t-T)$$

$$h_{3,t,2,T} = \beta_1 A \sin p_1(t-T) + \beta_2 B \sin p_2(t-T) + \beta_3 C \sin p_3(t-T)$$

where

$$\alpha_n = \frac{p_{11}^2 + p_{21}^2 - p_n^2}{p_{21}^2}$$

$$\beta_n = \frac{p_{33}^2}{p_{21}^2} \frac{p_{11}^2 + p_{21}^2 - p_n^2}{p_{33}^2 - p_n^2}$$

$$p_{ij}^2 = \frac{K_i}{m_j}$$

$$A = \frac{1}{m_2 P_1} \frac{\beta_2 - \beta_3}{\alpha_1(\beta_2 - \beta_3) + \alpha_2(\beta_3 - \beta_1) + \alpha_3(\beta_1 - \beta_2)}$$

$$B = \frac{1}{m_2 P_2} \frac{\beta_3 - \beta_1}{\alpha_1(\beta_2 - \beta_3) + \alpha_2(\beta_3 - \beta_1) + \alpha_3(\beta_1 - \beta_2)}$$

$$C = \frac{1}{m_2 P_3} \frac{\beta_1 - \beta_2}{\alpha_1(\beta_1 - \beta_3) + \alpha_2(\beta_3 - \beta_1) + \alpha_3(\beta_1 - \beta_2)}$$

and the P_n^2 are the three roots of

$$\begin{vmatrix} p_{11}^2 + p_{21}^2 - p^2 & -p_{21}^2 & 0 \\ -p_{22}^2 & p_{22}^2 + p_{32}^2 - p^2 & -p_{32}^2 \\ 0 & -p_{33}^2 & p_{33}^2 - p^2 \end{vmatrix} = 0$$

The differential impulse applied to body 2 is $f(\tau)d\tau$. The actual responses of the bodies in the system to the exciting force f(t) are:

$$X_{1,t} = \int_0^t f(T) h_{1,t,2,T} \, dT$$

$$X_{2,t} = \int_0^t f(T) h_{2,t,2,T} \, dT$$

$$X_{3,t} = \int_0^t f(T) h_{3,t,2,T} \, dT$$

These quadratures give the results of a system initially at rest when the disturbing force f(t) is applied. This case occurs frequently in physical cases of transient motions.

Distributed Lineal System

Considering bending only, the equation of free vibration for a simply supported beam of uniform cross section is

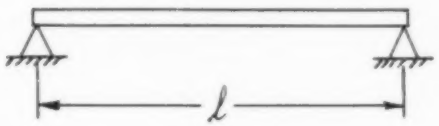

Figure 2

$$\frac{\partial^2 y}{\partial t^2} + a^2 \frac{\partial^4 y}{\partial x^4} = 0$$

where $a^2 = \frac{Eg}{\gamma}\frac{I}{A}$

$y_{x,t}$ = displacement of section at x at time t
E = Young's Modulus of beam material
γ = weight per unit volume of beam material
I = rectangular moment of inertia of beam cross section
A = area of beam cross section
g = acceleration of gravity.

If at time t = O, for all values of x, y = O, then

$$y = \sum_{n=1}^{\infty} b_n \sin\frac{n\pi x}{l} \sin p_n t$$

$$\frac{\partial y}{\partial t} = \sum_{n=1}^{\infty} p_n b_n \sin\frac{n\pi x}{l} \cos p_n t$$

where $p_n = n^2 \frac{\pi^2}{l^2}\sqrt{\frac{Eg}{\gamma}\frac{I}{A}}$

If at time t = O a finite velocity V is applied to small length δ on the beam centered at x = c, this condition can be shown in Figure 3.

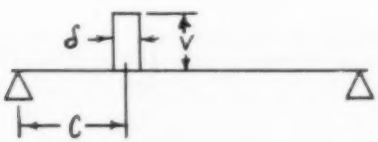

Figure 3

Analytically,

$$\frac{\partial y}{\partial t} = f(x) = \begin{cases} 0 & \text{when } 0 \le x \le c - \delta/2 \\ V & \text{" } \quad c-\delta/2 \le x \le c+\delta/2 \\ 0 & \text{" } \quad c+\delta/2 \le x \le l \end{cases}$$

By the use of the ordinary Fourier Integral,

$$y = \sum_{n=1}^{\infty} \frac{2V\delta}{l p_n} \sin\frac{n\pi c}{l} \sin\frac{n\pi x}{l} \sin p_n t$$

If the initial velocity at x = c was caused by a unit impulse,

$$V = \frac{1}{m} = \frac{g}{A\delta\gamma}$$

and

$$h_{x,t,c,0} = \sum_{n=1}^{\infty} \frac{2}{m p_n} \sin\frac{n\pi c}{\ell} \sin\frac{n\pi x}{\ell} \sin p_n t$$

where m = entire mass of the beam.

For a unit impulse applied at x = c and t = τ,

$$h_{x,t,c,\tau} = \sum_{n=1}^{\infty} \frac{2}{m p_n} \sin\frac{n\pi c}{\ell} \sin\frac{n\pi x}{\ell} \sin p_n (t-\tau)$$

Suppose that a force P = P_0 sin wt is actually acting at x = c. The differential impulse is P_0 sin wτ dτ and

$$y_{x,t} = \int_0^t P_0 \sin w\tau \, h_{x,t,c,\tau} \, d\tau$$

$$y_{x,t} = \int_0^t \sum_{n=1}^{\infty} \frac{2 P_0}{m p_n} \sin\frac{n\pi c}{\ell} \sin\frac{n\pi x}{\ell} \sin p_n (t-\tau) \sin w\tau \, d\tau$$

$$y_{x,t} = 2\frac{P_0}{m\omega^2} \sum_{n=1}^{\infty} \sin\frac{n\pi c}{\ell} \sin\frac{n\pi x}{\ell} \frac{\sin wt - \frac{\omega}{p_n}\sin p_n t}{\frac{p_n^2}{\omega^2} - 1}$$

If the problem concerns the deflection of the side-rod of a locomotive, the inertia load on the side-rod is a function of position and time W = W_0 sin wt lb/in.

where W_0 is the maximum value of the distributed load.

The differential impulse is W_0dc sin wτ dτ. Note that sin nπc/ℓ is the "influence function" for this problem and the variable of integration is c, not x.

$$y_{x,t} = \frac{2w_0}{m} \int_0^t \int_0^{\ell} \sum_{n=1}^{\infty} \frac{1}{p_n} \sin\frac{n\pi x}{\ell} \left(\sin\frac{n\pi c}{\ell} dc \right) \left[\sin w\tau \sin p_n (t-\tau) d\tau \right]$$

$$y_{x,t} = \frac{2}{\pi} \frac{W_0 \ell}{m\omega^2} \sum_{n=1}^{\infty} \frac{1 - \cos n\pi}{n} \sin\frac{n\pi x}{\ell} \frac{\sin wt - \frac{\omega}{p_n}\sin p_n t}{\frac{p_n^2}{\omega^2} - 1}$$

Problem 2: The Inverse Problem

Problem 2 is discussed at some length in the article on "Motion Measurement," Sections 40-43, pp. 375-380, in the Handbook of Experimental Stress Analysis. It can be illustrated by the simple seismic instrument shown in Figure 4.

The equation of motion for this system is

$$m(\ddot{y}+\ddot{x})+c\dot{x}+kx=0$$

or

$$\ddot{x}+2np\dot{x}+p^2x=-\ddot{y}$$

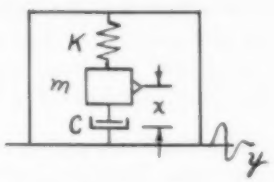

Figure 4

where $y(t)$ = the motion being measured

$x(t)$ = the relative displacement between mass and case

$n \equiv \frac{C}{C_n}$ $\frac{\text{damping constant}}{\text{critical damping constant}}$

$p^2 \equiv \frac{K}{m}$ $\frac{\text{spring constant}}{\text{mass}}$

Seismic instruments respond only to accelerations, and the output is only the relative motion between mass and case. If the relative motion x is magnified mechanically, electrically, or optically and transferred to the record in a linear fashion, the record x is

$$X = \mu x$$

Therefore the record X is related to the input $\ddot{y}$ as follows:

$$\ddot{X}+2np\dot{X}+p^2X=-\mu\ddot{y}$$

or

$$\frac{\ddot{X}}{p^2}+\frac{2n}{p}\dot{X}+X=-\frac{\mu}{p^2}\ddot{y}$$

The record X os accelerometers is usually considered by the users of the instrument to be proportional to the measured acceleration. But the equation above indicates that this is only true if $\ddot{X}$ and $\dot{X}$ are small or P is very large. If none of these conditions exist, the record must be corrected by the addition of the terms $\ddot{x}/p^2$ and $2n/p\,\dot{X}$. These terms call for differentiating the record once and twice, instructions easier to give than to carry through.

The above equation illustrates a common dilemma in all motion-measuring instrumentation. As $p \to \infty$ the record X becomes more and more accurately proportional to $\ddot{y}$, but the sensitivity approaches zero. That is, the record becomes very small. Accuracy and sensitivity are mutually antagonistic goals.

Suppose that the transient motion being measured starts at the beginning of the record so that

$$t = y = \dot{y} = X = \dot{X} = 0$$

Then the record equation can be integrated term by term and

$$X+2np\int X\,dt+p^2\iint X\,dt\,dt=-\mu y$$

The record X is proportional to y only if $\int X dt$, $\iint X dt\, dt$, and p are very small. If none of these conditions exist, the record X must be corrected by the addition of the two terms $2np\int X dt$ and $p^2 \iint X dt\, dt$. These terms call for the integration of the record once and twice, instructions which can be carried out. All displacement meters have small values of p.

Velocity Meter with Low Impedance Output

A seismic instrument widely used is the velocity meter with an induction pickup coil and with recording made by a low resistance electro-magnetic oscillograph. This instrument consists as a whole of two mechanical systems connected by an electrical system. Each mechanical device can be approximated by a single degree of freedom system, and the electrical circuit can be approximated by a single or double mesh circuit. These are shown in Figure 5.

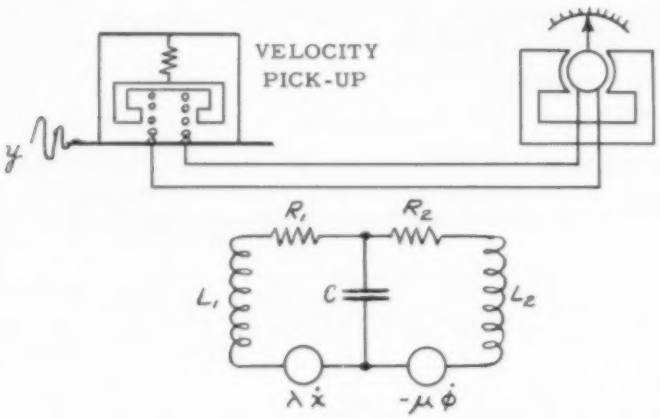

Figure 5

The equations for this system are:

$$1)\quad m\ddot{x} + c\dot{x} + Kx + \xi a_1 = -m\ddot{y}$$

$$2)\quad L_1\dot{a}_1 + R_1 a_1 + \frac{1}{C}\int (a_1 - a_2)\,dt = \lambda\dot{x}$$

$$3)\quad L_2\dot{a}_2 + R_2 a_2 - \frac{1}{C}\int (a_1 - a_2)\,dt + \mu\dot{\phi} = 0$$

$$4)\quad I\ddot{\phi} + \beta\dot{\phi} + \delta\phi = \nu a_2$$

In which y = motion being measured, x = relative motion between mass and case in velocity pickup, Ø = angle of rotation of oscillograph mirror, a_1 = current in mesh that is in the velocity pickup, a_2 = current in mesh that is in the oscillograph, m = mass of suspended weight in the velocity pick up (also a magnet), C = mechanical linear damping constant in velocity pickup, K = linear spring constant of weight suspension in velocity pickup, I = moment of inertia of mirror in oscillograph, β = mechanical torsional damping constant in oscillograph, δ = torsional spring constant of mirror suspension in oscillograph, L_1 = inductance in velocity pickup and half the transmission line, R_1 = resistance in velocity pickup and half the transmission line, L_2 = inductance in oscillograph and half the transmission line, R_2 = resistance in oscillograph and half the transmission line, C = total capacity in velocity pickup, oscillograph and transmission line, ξ = force per unit current reacting on suspended mass of ve-

locity pickup, λ = volts per unit relative velocity generated in velocity pickup coil, μ = back electromotive force per unit angular velocity in oscillograph, and ν = torque per unit current in mirror suspension of oscillograph.

If ρ is the optical lever length in the oscillograph, the record is $\rho\,\phi$. The differential equation relating the record, the constants of the entire system, and the velocity being measured is (provided ϕ and y and all their time derivatives were zero at the time the record starts)

$$\left(D^5+\frac{1}{T_1}D^4+\frac{1}{T_2^2}D^3+\frac{1}{T_3^3}D^2+\frac{1}{T_4^4}D+\frac{1}{T_5^5}+\frac{1}{T_6^6}\frac{1}{D}+\frac{1}{T_7^7}\frac{1}{D^2}+\frac{1}{T_8^8}\frac{1}{D^3}\right)\rho\phi=-\frac{1}{T_0^4}\frac{\rho}{L_1}\dot{y}$$

where $$D^n=\frac{d^n}{dt^n}(\ )$$

and $$\frac{1}{D^m}=\int\cdots\int(\ )\,dt^m$$

and the T_n are characteristic times of the system.

This equation indicates that the record may be a very much distorted picture of the velocity. The user of a velocity meter directly connected to an electromagnetic oscillograph merely hopes that every term on the left hand side is small except $1/T_5^5$. In order to check the accuracy of the instrument, the user is instructed by the differential equation to integrate the record three times and differentiate it five times. He is instructed to know the characteristics of the instruments and the circuits involved in them. The integrations are possible. The differentiations are not. In practice none of these things are done. The operator hopes that the important components of his record will have frequencies lying between the low natural frequency of the velocity pickup and very much higher natural frequency of his oscillograph element. For the rest he trusts to luck.

Problem 3: Experimental Method of Determining the Constants of an Unknown Instrument.

In general, any seismic instrument which contains only linear mechanical and electrical elements has the differential equation

$$\left(\cdots+a_2D^2+a_1D+a_0+\frac{a_{-1}}{D}+\frac{a_{-2}}{D^2}+\cdots\right)X=-\ddot{y}$$

or $$Z(D)X=-\ddot{y}$$

If the analysis of the instrument and its circuits is too difficult to carry out, the values of the a_n can be found by an experiment proposed by Dr. R. D. Specht. This procedure depends on the evaluation of Carson's Integral

$$\frac{1}{DZ(D)}=\int_0^\infty e^{-Dt}A(t)\,dt$$

where A(t) is the response of the instrument (the record) to a unit acceleration, applied to the instrument. If we are satisfied with unit accelerations less the g (the acceleration of gravity), it is easy to imagine and to approximate in construction a setup which will give constant

accelerations. For instance, the instrument might be mounted on a carriage which is accelerated by a falling weight. If the instrument (pickup, amplifier, transmission system, and recorder) has sufficient damping, the response A(t) will settle down to a constant value, Θ, within a finite length of time, T. There are only two possibilities, either $\Theta = 0$, or $\Theta \neq 0$.

Then

$$\frac{1}{DZ(D)} = \int_0^T e^{-Dt} A(t)\,dt + \Theta \int_T^\infty e^{-Dt}\,dt$$

$$\frac{1}{DZ(D)} = \sum_0^\infty D^n \frac{(-1)^n}{n!} \int_0^T t^n A(t)\,dt + \frac{\Theta}{D} \sum_0^\infty \frac{(-1)^n}{n!} D^n T^n$$

$$\frac{1}{DZ(D)} = \frac{\Theta}{D} + \sum_0^\infty \left[A_n + \frac{(-1)^{n+1}}{(n+1)!} \Theta T^{n+1} \right] D^n$$

where

$$A_n = \frac{(-1)^n}{n!} \int_0^T t^n A(t)\,dt$$

If

$$E_n = \frac{(-1)^n}{n!} \int_0^T t^n \left[\Theta - A(t) \right] dt$$

$$E_n = -\frac{(-1)^{n+1}}{(n+1)!} \Theta T^{n+1} - A_n$$

Then $$\int_0^\infty e^{-Dt} A(t)\,dt = \frac{\Theta}{D} - \sum_0^\infty E_n D^n \qquad \text{when } \Theta \neq 0$$

and $$\int_0^\infty e^{-Dt} A(t)\,dt = -\sum_0^\infty E_n D^n = \sum_0^\infty A_n D^n \qquad \text{when } \Theta = 0$$

When $\Theta \neq 0$

$$\frac{1}{DZ(D)} = \frac{\Theta}{D} - \sum_0^\infty E_n D^n$$

and

$$Z(D) = \frac{1}{\Theta - \sum_0^\infty E_n D^{n+1}} = \frac{1}{\Theta} + \frac{E_0}{\Theta^2} D + \frac{E_0^2 + \Theta E_1}{\Theta^3} D^2 + \frac{E_0^3 + 2\Theta E_0 E_1 + \Theta^2 E_2}{\Theta^4} D^3 + \cdots$$

When

$$\theta = 0$$

$$\frac{1}{DZ(D)} = \sum_0^\infty A_n D^n$$

and

$$Z(D) = \frac{1}{\sum_0^\infty A_n D^{n+1}} = \frac{1}{A_0}\frac{1}{D} - \frac{A_1}{A_0^2} + \frac{A_1^2 - A_0 A_2}{A_0^3} D - \frac{A_1^3 - 2A_0A_1A_2 + A_0^2 A_3}{A_0^4} D^2 + \cdots$$

$$A_0 = \int_0^T A(t)\,dt \qquad E_0 = \theta T - A_0$$

$$A_1 = -\int_0^T t\,A(t)\,dt \qquad E_1 = -\frac{1}{2}\theta T^2 + \int_0^T t\,A(t)\,dt$$

$$A_2 = \frac{1}{2}\int_0^T t^2 A(t)\,dt \qquad E_2 = \frac{1}{6}\theta T^3 - \frac{1}{2}\int_0^T t^2 A(t)\,dt$$

$$A_3 = -\frac{1}{6}\int_0^T t^2 A(t)\,dt \qquad E_3 = -\frac{1}{24}\theta T^4 + \frac{1}{6}\int_0^T t^3 A(t)\,dt$$

$$A_n = \frac{(-1)^n}{n!}\int_0^T t^n A(t)\,dt \qquad E_n = -\frac{(-1)^{n+1}}{(n+1)!}\theta T^{n+1} - A_n$$

when $\theta \neq 0$

$$a_{-n} = 0 \quad n = 1, 2, 3 \cdots$$

$$a_0 = \frac{1}{\theta}$$

$$a_1 = \frac{E_0}{\theta^2}$$

$$a_2 = \frac{E_0^2 + \theta E_1}{\theta^3}$$

$$a_3 = \frac{E_0^2 + 2\theta E_0 E_1 + \theta^2 E_2}{\theta^4}$$

when $\theta = 0$

$$a_{-n} = 0 \quad n = 2, 3, 4, \cdots$$

$$a_{-1} = \frac{1}{A_0}$$

$$a_0 = -\frac{A_1}{A_0^2}$$

$$a_1 = \frac{A_1^2 - A_0 A_2}{A_0^3}$$

$$a_2 = -\frac{A_1^3 - 2A_0A_1A_2 + A_0^2 A_3}{A_0^4}$$

It is interesting to note that when $\Theta = 0$ no integral terms exist beyond the first. Referring back to the discussion on the velocity meter, the equation relating the record to the disturbing function for accelerations is

$$\left(D^6 + \frac{D^5}{T_1'} + \frac{D^4}{T_2^2} + \frac{D^3}{T_3^3} + \frac{D^2}{T_4^4} + \frac{D}{T_5^5} + \frac{1}{T_6^6} + \frac{1}{T_7^7}\frac{1}{D} + \frac{1}{T_8^8}\frac{1}{D^2}\right)P\phi = -\frac{1}{T_0^4}\frac{\rho}{L_1}y''$$

Now, a velocity meter subjected to a step acceleration is so constructed that $\Theta = 0$. Here we seem to have a contradiction between Z(D) calculated by detailed analysis and Z(D) got from Carson's Integral operating on a record taken with a step acceleration excitation. But if the detailed analysis is carried out on the velocity meter, it will be found that

$$\frac{1}{T_9'} = \frac{K}{m}\cdot\frac{\sigma}{I}\cdot\frac{1}{CL_1}\cdot\frac{1}{CL_2} - \frac{K}{m}\cdot\frac{\sigma}{I}\cdot\frac{1}{CL_1}\cdot\frac{1}{CL_2} = 0$$

so that there is no contradiction between the two developments.

SOME COMPUTING PROBLEMS IN THE AUTOMOTIVE INDUSTRY

PAUL T. NIMS
Chrysler Corporation
Detroit, Michigan

This first meeting of the Association for Computing Machinery in the Detroit area affords a welcome opportunity for some of us in local manufacturing industries to learn what is being done in the computing field and what kinds of machines may become available in the future. It also gives us a forum in which to discuss industrial mathematics and its computing problems.

I have been asked this morning to introduce some typical problems of the automotive segment of Detroit industry. The term "automotive industry" is rather a broad one and means many things to many people; not only the vehicles that you and I drive on Sunday afternoons but trucks of all sizes, tractors, tanks and self-propelled guns, railroad equipment, internal-combustion engines for aircraft service, and perhaps even certain heating, air conditioning, and refrigerating equipment. No one man can be acquainted with all aspects of such a diverse collection of automotive products, to say nothing of the other things made in Detroit. Hence, this morning I shall mention only those matters that I have heard about and those few with which I have had some direct experience.

This is an opportune time to talk about computation in the automotive industry for a number of reasons. There is the matter of the balance between experimental investigation and computational investigation. Where the physics of the problem is well enough understood to permit calculation of the strength and performance of the device with reasonable confidence, then the decision as to whether to calculate these matters for a range of designs or whether to test a series of designs is largely an economic one. As the cost of experimental procedures and of experimental parts is growing daily, there is a growing realization of the advantages to be gained in time and money by substituting the computational approach for a large part of the usual experimental testing.

There is also a special reason for talking about this kind of thing in the automotive industry instead of, let us say, the building industry. In an activity where it is traditional to make extensive changes in the product annually and where in the lifetime of one individual several sets of drastic changes are likely to occur, the burden of engineering work in connection with these changes becomes very heavy. For example, the introduction of a completely new automotive engine together with a new transmission, suspension, and braking system represents a whole collection of new engineering problems that must be solved rapidly and repeatedly until an optimum design of each of the components and of their interaction is found.

There is still another reason why computation is important in the automotive industry today, and that is the flood of military contracts which we are beginning to face. While most of these devices will have rotating and reciprocating mechanical parts, the similarity to the peace time design problem ends at this point as these military devices are subjected to quite different stresses, weight limitations, and performance requirements. They also are often much larger. This means the design of completely new and often quite unfamiliar devices.

For these reasons, therefore, I think the computing problems of the automotive industry are of special interest at this time and will mention a few of them both by physical kind and

mathematical kind in the hope that you will find the time to look into them further and perhaps devise equipment and methods which can be of general use in the industry.

Kinds of Problems

A. Substitution in Formulae

Probably the most common recurrent problem is that of putting numbers into formulae. These formulae may relate to the performance of the vehicle, to the stresses in various parts of the structure, or to the necessary size of some parts. A man designing the differential gear train in the rear axle may cover pages with numbers relating to the shape of the teeth and the setting of the various knobs and dials on the machinery necessary to cut these teeth. The formulae abound in sines, cosines, arc tangents, and various products and quotients. The calculations for a single formate hypoid gear require the evaluation of about 670 items of which roughly one-third are trigonometric functions. The data are calculated to six figures. This calculation, with a desk machine, requires the full attention of a man for six days and is usually checked by a duplicate calculation by another man. While the programming of this problem will be difficult, the time saved should be considerable.

The gear designer is also interested in smaller jobs of calculation. After a gear is designed, it is often necessary to check the design for involute interference and for involute undercutting. In addition, some special dimensions are required for the inspection of the gear after it is cut, a typical calculation being the diameter over inspection rolls. You may find a portion of the formulae which are used in gear design in a book entitled "Involutometry" by Professor Vogel at Wayne University.

The design of the cams which open the valves in a modern automotive engine is an exercise in the juggling of acceleration forces and has been attacked with many quite complicated formulae. The designer is given the required lift, duration of opening, and permissible acceleration and must produce a table showing the lift to the nearest one hundred-thousandth of an inch for each degree of camshaft rotation. This table is then copied on the drawing as a guide to the machine shop in the production of a master cam, and the copy must be rechecked for errors. A cam design method mentioned by Professor Winston Dudley in the January, 1948, SAE Transactions uses polynomials to represent the cam contour. This type of formula has been evaluated on punched card machines by several groups of people and in at least one case involved summing terms up to the twentieth power.

Another very common calculation is that for finding the loads on the bearings of the crankshaft. In this case, one must consider the magnitude of the force of the expanding hot gases as the engine goes through its thermodynamic cycle, the inertia of the piston and other reciprocating parts, the inertia of the rotating balance weights on the crankshaft, the angularity of the connecting rod (which gives a nonsinusoidal motion to the piston), and may even have to consider the deflections of the crankshaft. Such calculations must be made for an assortment of crankshaft angles covering two full engine revolutions, and all the forces must of course be summed with proper regard for their vector properties. This sort of thing can be done, and is being done, with an adequate supply of blank paper and a slide rule, but in view of the fact that it would be desirable to study these bearing loads at a variety of engine speeds and throttle openings, the computing problem assumes large proportions and these tools become inadequate.

Some portions of the design of hydrodynamic torque converters are extended exercises in analytic geometry. A part of the specifications on the drawing is a table of the coordinates of the points of intersection of the ruled surfaces of the blades with the parabolic cone surface of the hub. The repetitive arithmetic of this calculation should be well suited to an automatically sequenced calculator.

B. Sequential and Iterative Calculations

For some kinds of calculations we are not so fortunate as to have explicit formulae for the quantities desired and find it necessary to calculate through a set of formulae several times in order to find a satisfactory set of values for the unknown quantities. The design of an ordinary round wire spring is a simple example of this sort of thing, as it is necessary to make compromises between allowable stress, space occupied by the spring, the rate of the spring, its solid height, and the size of the wire used in its manufacture. Presumably the criteria for the compromise could be inserted in a set of instructions and the formulae evaluated repeatedly until a satisfactory solution is found, i. e., until all of the quantities desired are smaller than pre-assigned upper limits or until the machine stops and reports that no such spring can be built in the space available.

The gear designer again seems to get the palm for complication when he attempts to modify gear tooth forms to obtain an optimum balance of tooth life between the gear and the pinion in a train. Present practice is to deal with the transcendental equations involved by various graphical methods which are quite time consuming. Programming of this calculation for an iterative solution method will be difficult, but easy computation may permit a more economical use of the alloy steels required for gears.

C. Table Look-Up

As a part of substituting numbers in formulae, one encounters over and over again tabulated functions of one sort or another. Trigonometric functions are quite common in any problem involving geometrical concepts, such as those just mentioned, and logarithmic functions appear frequently in the study of thermodynamic cycles. In brake drum analysis, thermal transients can best be described in terms of the error function so that tables of this and of the exponential are sometimes of interest. Now, of course, looking up numbers in tables is not exactly heavy manual labor, but it is possible for the volume of the work to build up so that the dangers of errors of transcription are great. These operations of consulting a table occur generally in the midst of the evaluation of formulae so that they are unusually awkward for machine calculation.

D. Data Reduction and Automatic Data Taking

Another class of substitution in formulae arises from the experimental side of the industry. When testing engines, for example, it is customary to record the torque, speed, number of seconds to burn a pound of fuel, and the temperature and barometric conditions. From these data can be calculated the corrected horsepower and the corrected brake specific fuel consumption together with other similar data. The amount of this kind of work varies with the kind of engine testing program which is under way and seems to be at a maximum with large aircraft engines. It is possible that some consideration should be given to the automatic recording of these data directly from the motions of the various indicating instruments and in such a form that the calculations can also be carried through automatically. This problem is complicated by the fact that a typical installation may have fifty different test cells in operation, and it would be desirable to record and calculate these data for any or all of the test cells without the use of separate, duplicate equipment in each room.

E. Sorting

Some of the problems of the automotive industry are quite similar to those encountered by chemists. For example, keeping a cross index of the system of internal reports by which the work of the engineering laboratories is recorded and keeping bibliographies generally is related to the problem of hunting through infrared spectrograms in an attempt to find spectral peaks corresponding to those of an unknown compound. This is primarily a sorting problem, although the application of the principles of logical truth calculators might make for much more intelligent selection of the bibliographical items to be given detailed study.

F. Sets of Algebraic Equations

Automotive structures are generally indeterminate. That is, a V8 crankshaft is supported on five main bearings, and a modern steel body structure, while it bears some resemblance to a bridge truss, is very definitely not pin connected but typically has additional bracing at all corners. Study of the stresses and deflections of structures of this kind leads to sets of simultaneous algebraic equations. Similarly, spectroscopic analysis of the components of an antifreeze solution yields a simultaneous set of algebraic equations, and rapid methods of solving these sets are convenient in speeding up the production of useful answers.

G. Integration

Thus far, the mathematical procedures I have mentioned are not beyond the attainments of a college freshman. This was deliberate. While occasionally it is necessary to make investigations of the greatest mathematical sophistication, the burden of computation is largely that of lifting numbers and putting them into cubby holes, that is, of substituting in formulae. However, such matters as centrifugal stresses in rotating discs may require step-by-step integration for discs of arbitrary cross section, and test records of acceleration versus time may require similar treatment to find the velocities. The ordinary differential equation can appear in a study of the motion of an automobile and its passengers on a rough road. In fact, very complex sets of nonlinear differential equations will be required to discuss adequately the effects of shock absorbers, friction between the leaves of springs, and the special kind of spring rates which are sometimes used in suspensions.

Extensive studies of the torsional vibrations of crankshafts and similar structures are made by some companies, and one of the members of the Industrial Mathematics Society reports that most of his professional activity is concerned with the repeated solution of the problem of two flywheels connected by a flexible shaft. Similar sets of ordinary differential equations may be obtained in the study of the transients in automotive ignition equipment.

The partial differential equation turns up from time to time, mostly in the study of heat flow problems, such as the thermal conditions around a spark plug, which lead to a three-dimensional diffusion equation. There are also some possibilities of this kind in the study of aerodynamics of grilles and radiator ornaments.

I think it may be seen from this partial list that the problems of interest in Detroit are somewhat different from those which inspired the first flowering of machine computation in this country. That is, we have relatively few occasions to solve a simple set of differential equations for a very large number of initial conditions. However, the problems are more complicated than that of computing payrolls so that we see here an intermediate computing problem between those already so well provided for in existing machinery.

Machines

It would be profitless to tell this group how to design computing machinery, but it seems worthwhile to mention some of the desirable properties of machines for industrial computation. The differential equations of interest usually represent the oscillations of some mechanical system with many degrees of freedom, and the result desired is usually an estimate of the amplitudes and periods of the motion. This kind of problem is well suited to the capabilities of analogue machines like the Differential Analyzer at Wayne University and the various electronic differential analyzers which are commercially available.

The remaining problems seldom involve the repeated evaluation of small steps along a curve but rather the evaluation of a few more complicated formulae. This kind of work can be done very comfortably without the blinding speed of some of the newer computers. Much more important than speed is ease of application, that is, simple programming and rapid changes

from one problem set up to another. For the optimum use of machine computation by automotive engineers, the machines ought to be directly accessible to the man who has the problem, and it should not be necessary for him to have long, specialized training in tricks of programming. This probably means that a large number of subroutines should be available by a simple code, not only to extract square roots, but to solve right triangles, interpolate in tables, sum series, and perhaps do often repeated groups of operations used in a particular problem.

Rather than burden the computing machine itself with these many special program orders, it may be desirable to build a translating machine, that is, one into which a formula for evaluation may be entered symbolically and in which the various parts of the formula are divided into arithmetic steps and the appropriate holes punched in a program tape for subsequent use in the computer. If we think of each mathematical symbol in a formula as a logical proposition, it is entirely possible that chains of relays can be wired to select appropriate groups of program steps from a tape or card storage unit. These groups could be combined by the coding machine in the order dictated by the formula.

Convenient operation will probably also require floating decimal operation and storage capacity (for a hundred 12-digit numbers and their signs) which can be readily changed to storage of two hundred 6-digit numbers with sign. An additional convenience would be some method of typing the name of a quantity on the answer sheet alongside the magnitude of the quantity, as often the answers do not come out as columns of pairs of values of x and y coordinates.

Conclusion

I have indicated some of the computing problems of the automotive industry and some desirable properties of machines for their solution. It should be emphasized again that the computations are probably too diverse to allow the use of special-purpose machines and that ease of application is quite important. Finally, if such equipment can be made available at less than the price of a new car, it should be of wide interest.

A SURVEY OF INDUSTRIAL SUBSIDY OF THE STUDY OF APPLIED MATHEMATICS

THOMAS H. SOUTHARD
Wayne University
Detroit, Michigan

In the spring of 1950, the Education Committee of the Industrial Mathematics Society wrote to twenty-four organizations representing various industries (automobiles, steel, oil, electrical manufacturing, utilities, chemicals, business machines, aircraft, railroads, radio manufacturing, etc.) in an attempt to obtain information of use in the Society's campaign to promote the use and point up the relative efficiency of the analytical approach to many of the problems of production, research and development and related industrial fields. Twenty replies were received.

The twenty replies included four from the automotive industry, three each from oil companies and utilities, two each from electrical manufacturers, business machine companies, distillers and one each from the steel, chemical, aviation, and radio manufacturing industries.

Our attempt to secure information included the following two specific questions:

(1) What courses in "applied mathematics" (beyond the calculus, but including review calculus as well as such courses as hydrodynamics, elasticity, etc., not normally called mathematics) are you offering for your employees on your own premises or elsewhere?

(2) What subsidy, in the form of time off, money, or other forms of encouragement, do you give your employees while attending courses sponsored by your organization or offered by nearby universities?

Seventeen of the twenty replies indicated some kind of subsidy of the study of applied mathematics. These seventeen affirmative answers indicate essentially two types of programs which can be characterized either as "regular" or "occasional".

Seven of the seventeen affirmative respondents are companies which sponsor "regular" (i. e. regularly scheduled) programs including work in applied mathematics. Four of the seven regular programs are degree programs, three are non-degree.

The typical degree program leads, on completion, to a full-fledged college or university degree in engineering, mathematics, or physics. In one case an employee can work for the bachelor's degree, in another the master's, and two companies sponsor programs leading to the Ph. D. Most of these degree programs are staffed partly by university personnel, partly by company personnel. The typical program is in operation during the evening; some courses are taught on company premises, others at the cooperating university.

Universities co-sponsoring these degree programs include Illinois Institute of Technology, University of Pittsburgh, Indiana University, New York University, Polytechnical Institute of Brooklyn, Stevens Institute of Technology, University of Pennsylvania, Cornell University, and John Hopkins University. Employees in some instances pay only part tuition, with premiums for good grades in some cases: in other instances they enjoy free or reduced tuition for courses taken under an Industrial Lecturer (company employee on the teaching staff) but pay full tuition for courses taken under the resident university staff.

In addition to the four companies with regular programs leading to a degree, three other companies have regularly scheduled non-degree programs. These are usually staffed by company personnel and are taught during the day on company time at no student expense. These programs are in general more likely to be aimed at training company personnel in techniques of special use to employees in their work, but they do include some applied mathematics.

Besides the regular programs, there are occasional courses sponsored by fourteen of the twenty respondents (this number includes four companies which also have regular programs). There are three typical kinds of subsidy involved:

(1) A course on the premises, for employees, taught by employees or nearby university personnel, during working hours.

(2) A course on the premises, for employees, taught by employees or nearby university personnel, after working hours.

(3) Regular university courses, chiefly evening.

For the first category the only subsidy is time-off (and the instructor's salary when an outsider is involved). In the second case, the only subsidy is the instructor's salary, if any. In the third case, the typical subsidy is part of the tuition, although in some instances even more is subsidized. This part tuition varies from 1/3 to 2/3 and in some cases the greater subsidy is made only for A or B grades. The courses must be approved by the company and must be rather directly related to work the employee is doing or will be doing, unless they are part of a degree program which satisfies this requirement.

One company allows its employees up to five hours per week of time off to attend approved daytime courses at nearby universities. Another company occasionally sends one of its research men to summer school for more work in applied mathematics.

As to specific courses mentioned by the several companies, the most popular appear to be Mathematics (or Calculus) Review, Ordinary Differential Equations, Advanced Engineering Mathematics, and Probability and Statistics. Not far behind are Advanced Calculus, Theory of Complex Variable, Vector Analysis, and Operational Mathematics.

Most of the companies replying to the questionnaire are enthusiastic about the results of their efforts in this area of their over-all training program. They feel that the subsidy pays for itself both directly and indirectly.

Those who have gone furthest with their programs are inclined to be the most enthusiastic about the results to be attained. One letter ends as follows: "I ... believe that the program upon which your Society has embarked is well worth the time and effort expended."

THERMAL DESIGN OF EVAPORATIVE CONDENSERS

HUGH J. SCULLEN
Consulting Engineer
Detroit, Michigan

The purpose of this paper is to show how fairly elaborate methods of analysis and synthesis may very profitably be applied to test data of a relatively low degree of accuracy when the object is a comprehensive rather than a precise picture of the character of a heat transfer device.

The particular kind of device used as an example is what is known as an "Evaporative Condenser". This is essentially a forced-draft, air-cooled condenser provided with means for maintaining a layer of water on the air side of its heat transfer surface so that heat will be removed from it by evaporation as well as by convection.

The specific apparatus used to obtain the test data used in this paper is shown in Figure 1. Details of the condenser are given in Table 1 and the actual test data are shown in Table 2. The tests were run as part of a preliminary study and, consequently, were run with the emphasis on speed with moderate accuracy rather than extreme precision. For this reason as well as because the data is used here simply to demonstrate a method of handling a heat transfer problem, no detailed description of the test set-up or procedure will be given.

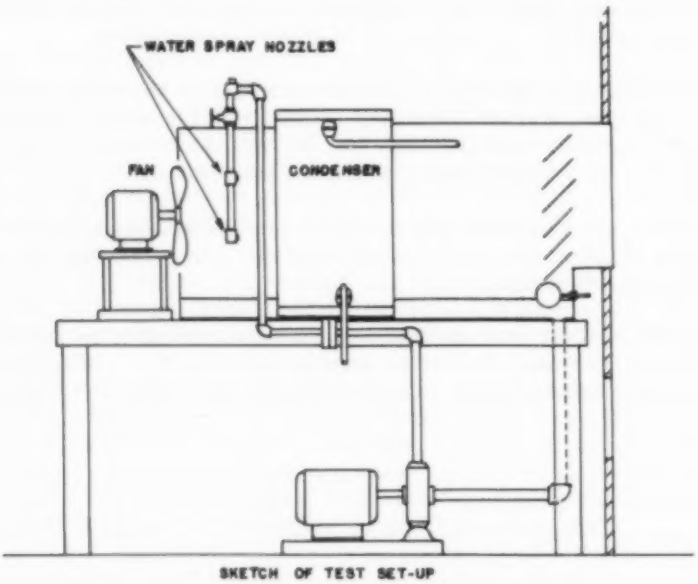

Figure 1

The discussion will be limited to a study of the design factors of heat transfer only. No mention will be made of such other very important factors as the air fan or water pump and their accessories.

The heat dissipated by an ordinary dry-surface, air-cooled condenser can be computed by the well-known equation

$$q = U\,A\,\frac{\Delta t_1 - \Delta t_2}{\ln\frac{\Delta t_1}{\Delta t_2}} \tag{1}$$

where the factor U, called the "Overall Coefficient of Heat Transfer", is a function of air velocity and, to a small degree, temperature and rate of condensation.

It is common practice to show the results of air-cooled condenser tests by plotting this coefficient U against the air velocity V, neglecting the effect of temperature and rate of condensation. A much more useful way of summarizing test data is to give equations or charts for the values of the individual film coefficients which combine to form the overall coefficient. The relation between the coefficients is

$$\frac{1}{U} = \frac{1}{h_g} + \frac{1}{Rh_L} \tag{2}$$

As shown in detail in Appendix 1, the heat dissipated by a wetted-surface, air-cooled condenser can be computed in an analogous way by using the equation

$$q = U'\,A\,\frac{\Delta i_1 - \Delta i_2}{\ln\frac{\Delta i_1}{\Delta i_2}} \tag{3}$$

where the factor U', which may be called the "Overall Coefficient", is again a function of the air velocity and, this time to an appreciable degree, the rate and temperature of condensation. An additional quantity which might affect the value of U' is the rate of circulation of water over the external surface, since this will determine the thickness, distribution and turbulence of the layer of water on the external surface and, in addition, may have a noticeable effect on the turbulence of the air stream.

Thus, the results of tests on wetted-surface condensers can be shown by plotting curves for the coefficient U' against the air velocity V for a number of constant values of the other independent variables or, exactly as in the case of dry-surface condensers, by giving equations or curves for the individual coefficients which this time can be combined to form U' by the equation

$$\frac{1}{U'} = \frac{s}{h_g} + \frac{s + \alpha r}{Rh_L} \tag{4}$$

where s and r are constants; α is a known function of the condensing temperature and rate; and h_g and h_L are individual film coefficients of the same sort as occur in the equation for the overall coefficient for dry-surface condensers. For the sort of work with which this paper is concerned, these individual coefficients may be accurately enough represented by equations of the type

$$h_g = C\,V^{0.8} \tag{5}$$

$$h_L = D \tag{6}$$

In these equations the factors C and D will be constants, as in the case of dry-surface apparatus, unless the effect of changing the water rate is found to be important. In this case C and D should be expressed as functions of the rate of water circulation, thus including that variable in the equation for U'.

Because there are so many independent variables it is not very practical to plot curves for U' directly from the test data or even to show the test results in this form. However, if the tests are separated into groups run at constant water rates (so as to avoid immediate consideration of this variable), it is fairly easy to determine the values of the individual coefficients by any of a number of methods.

In the present case, the test points (Table II) were not preselected for the application of the theory so that it was necessary to develop a method of analysis that did not require selected test points. The method is described in detail in Appendix 2 of this paper. Briefly, it consisted in assuming values for the individual film coefficient constants C and D and then using these assumed values to calculate values of the overall coefficient U' for each of the test operating conditions by using Eq (4). In general these values were not equal to the values computed directly from the test data by using Eq (3) in the form

$$\frac{1}{U'} = \frac{A}{q} \frac{\Delta i_1 - \Delta i_2}{\ln \frac{\Delta i_1}{\Delta i_2}} \tag{7}$$

The differences between the values of U' computed by these two methods were said to be due to errors in the assumed values of the constants C and D. The amounts of these errors were then computed by the methods given in Appendix 2, and their average values were added to the originally assumed values of C and D to get new values for these constants, which procedure caused the equations to fit the test data to a satisfactory degree of precision. The originally assumed values of the constants were those which previous tests had yielded for dry-surface condensers. By referring to the discussion of the theory in Appendix 1, it will be seen that the values of the individual coefficients h_g and h_L should be about the same for wet- as for dry-surface condensers.

In the present case, the application of these methods of analysis reduced the test data to the equations

$$h_g = 0.212\, V^{0.6} \tag{8}$$

$$h_L = 200 \tag{9}$$

By inserting these specific values in the general equations, it is easy to synthesize a usably accurate description of the thermal performance of any proposed evaporative condenser.

How well such a description fits the experimental condenser is shown in Figure 2 where values of heat dissipated computed by the above method are compared with the observed test values.

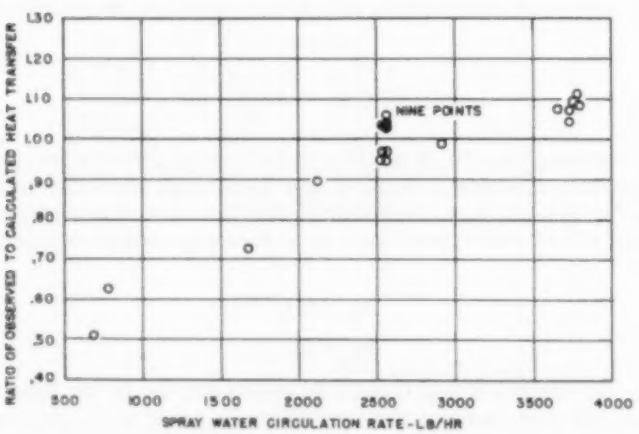

Figure 2

When a number of designs are under consideration or when complete performance curves are to be made, a great deal of time and effort can be saved by plotting the equations with their test-determined constants in the form of nomographs or alignment charts. One such set

of charts based on the data of this paper is shown on Figures 3, 4 and 5. As an example of their use, suppose we have given q = 305,000 btu per hr, A = 410 sq ft, RA = 147 sq ft, t_r = 111.6 F, and V = 5,000 cfm, and it is desired to find what inlet air wet bulb temperature will be required.

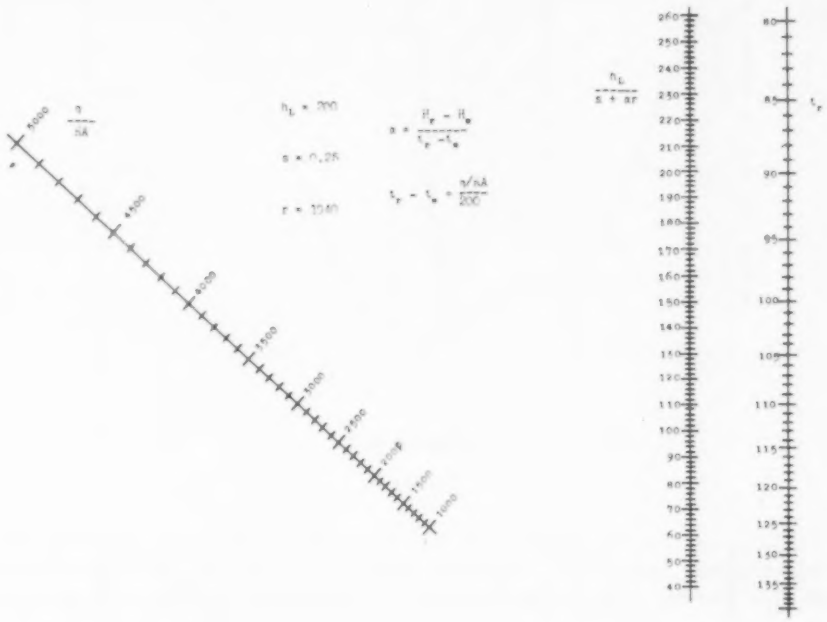

Figure 3

On Figure 3 draw a straight line from the given value, q/RA = 2070, on the left-hand scale to the given value, t_r = 111.6, on the right-hand scale. At the intersection of this straight line with the middle scale read $h_L/(s + ar)$ = 100.

Multiply this by R, the given ratio of internal to external surface, and then on Figure 4 draw a straight line from $Rh_L/(s + ar)$ = 35.8 on the right hand scale to the given quantity V = 400 on the left hand scale. At the intersection of this straight line with the middle scale read U' = 16.55.

Next, on Figure 5 draw a straight line from U' = 16.55 on the left-hand scale to the given quotient W/A = 12.2 on the right-hand scale. At the intersection of this line with the middle scale read $q/(\Delta i_1 W)$ = 1.17.

Δi is equal to the quotient of the given q/W divided by this quantity, 1.17, and the value of i , the inlet air enthalpy, can be obtained by subtracting this quotient, Δi_1 = 52.1, from 88.1 the enthalpy of saturated air at the refrigerant temperature. Having thus determined that i_1 = 36.0, the corresponding wet bulb temperature of the inlet air, t_1 = 80 F, can be read from any psychrometric chart or table.

In case the only interest is in exploring design possibilities, the labor can be greatly decreased by using constant values for the refrigerant condensing temperature and inlet air wet bulb temperature. This, in effect, sets a general design standard for the temperature difference. When this is done the remaining variables can all be shown on a single nomograph so that all the relations between the major variables for a complete design can be determined simply by drawing one straight line.

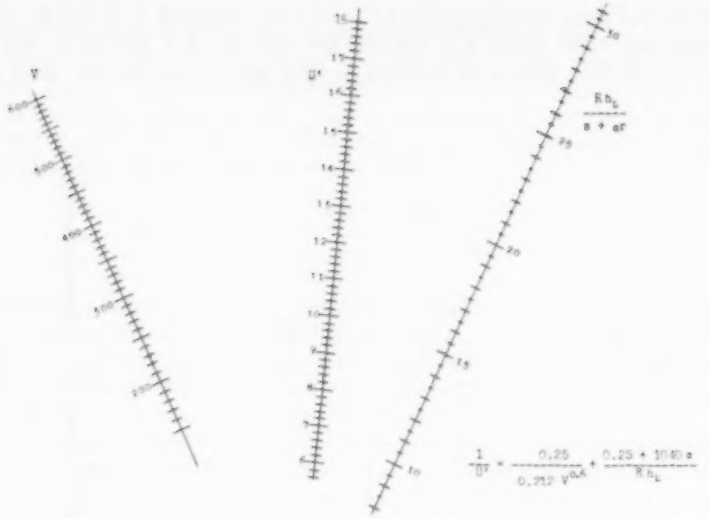

Figure 4

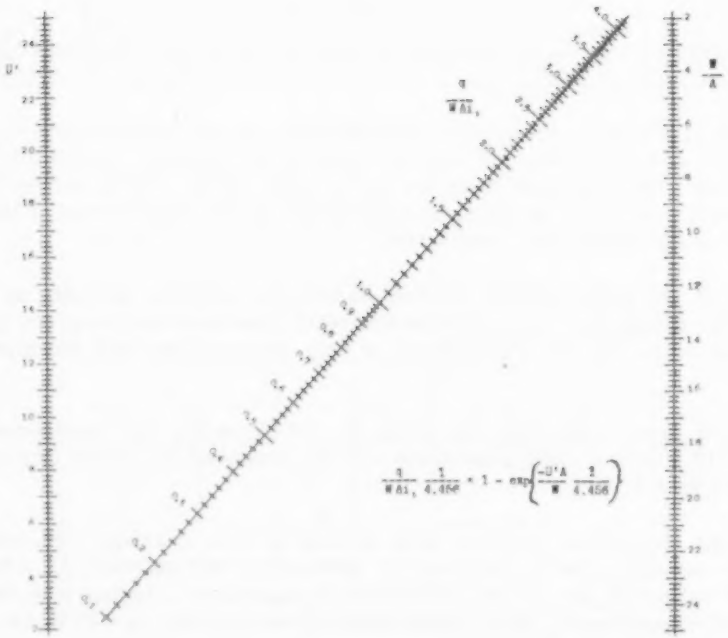

Figure 5

Such a nomograph, based on the data of the present tests, is shown in Figure 6. This nomograph shows the relation between heat dissipated, External Surface, Internal Surface, Air Volume, and Air Velocity for fixed values of Inlet Air Wet-Bulb Temperature and Refrigerant Temperature.

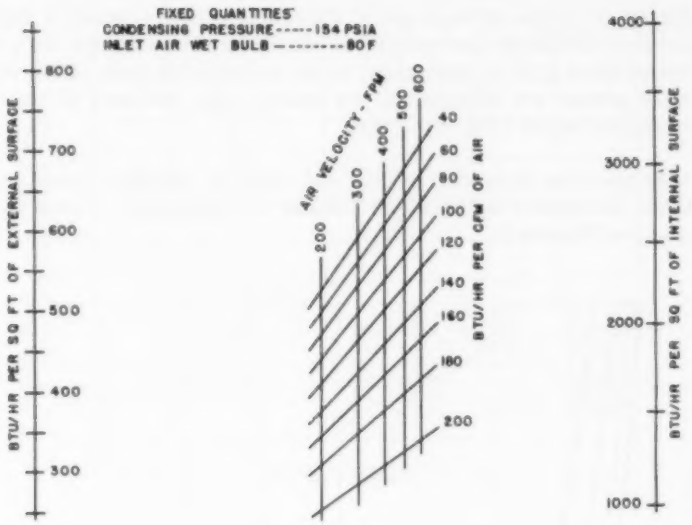

Figure 6

A typical design study is shown on Figures 7 to 11. These exhibit the possibilities in the design of an evaporative condenser for a twenty-ton unit. The design performance was set at 153,000 btu/hr at a condensing temperature of 111.6 F and an inlet air wet-bulb temperature of 80 F.

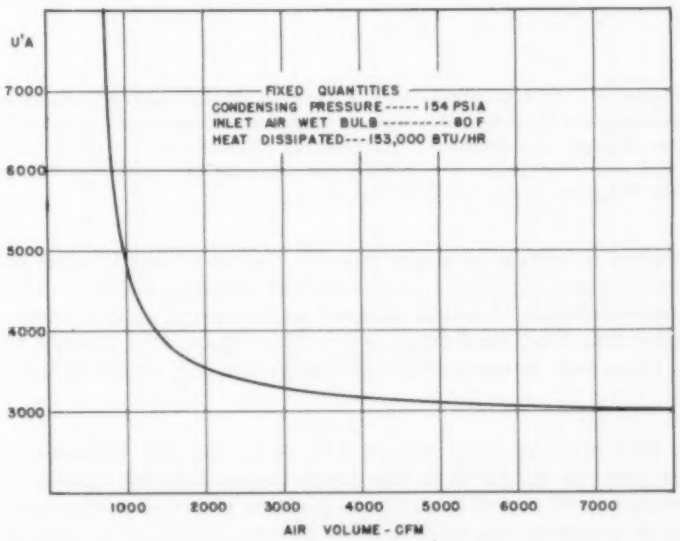

Figure 7. Design Study of a Freon-12 Evaporative Condenser Showing the Balance Between Surface and Air Volume for the Design Conditions Condensing Pressure . . 154 psia; Inlet Air Wet-bulb . . . 80F; Heat Dissipated . 153,000 btu/hr.

Figure 7 was plotted from the nomograph of Figure 5. From a study of this figure it is easy to make a preliminary choice of the quantity of air to be used through the condenser, because an increase in the product U' A is equivalent to an increase in cost. With this in mind, it will be apparent that the proper air volume will be located near the knee of the curve. A reasonable preliminary choice would be 2,500 CFM.

Figure 8 shows the relation between internal and external surface areas for a number of air velocities, all at the previously selected air volume of 2,500 CFM. These curves were plotted from the nomograph of Figure 6.

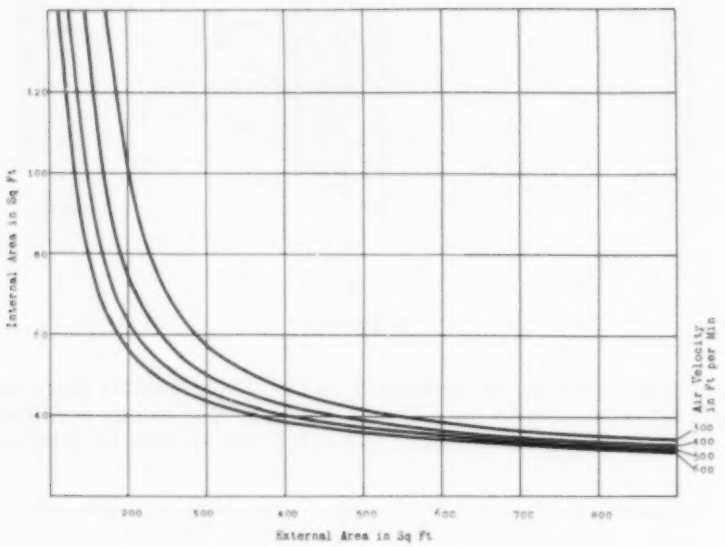

Figure 8. Design Study of a Freon-12 Evaporative Condenser Showing the Balance Between Internal and External Surface for the Design Conditions: Condensing Pressure · · 154 psia; Inlet Air Wet-bulb · · · 80F; Heat Dissipated · 153,000 btu/hr; Air Volume · · · · · 2,500 cfm.

By making a tentative selection of materials for the tubes and fins the curves of Figure 8 can easily be converted into curves of weight against external surface. The results of such a conversion are shown in Figure 9, which is based on the use of copper tubes of 0.035-inch wall thickness and copper fins 0.022 inch thick. From this figure, it is at once evident that for any given air velocity there will be one particular design that will result in the most effective use of material.

Figure 10 was plotted directly from Figure 9 to show how the minimum weights vary with air velocity. Each point on the curve of this figure represents the lightest condenser, built of the specified materials, that can be designed to give the required performance at the indicated air supply. While no minimum appears on these curves, it should be bourne in mind that the cost of fan and motor for supplying the air increases as the air velocity is increased so that if the weights were converted to costs and added to the cost of fan and motor the resulting curve of cost against air velocity would certainly show a minimum.

Figure 11 shows how the various physical dimensions of the condenser of minimum weight vary as the air velocity is changed, all at an air supply of 2500 CFM.

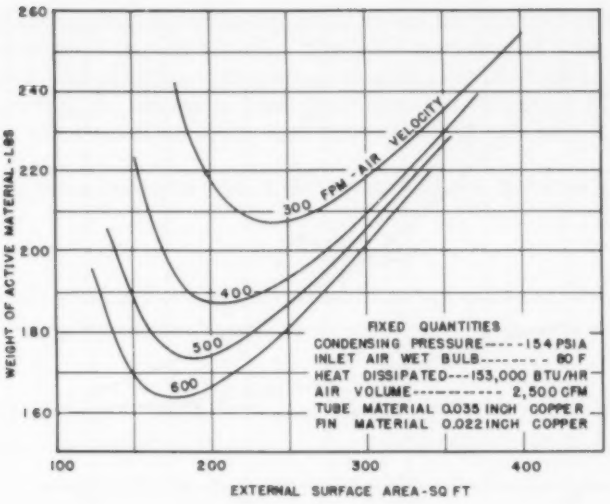

Figure 9. Design Study of a Freon-12 Evaporative Condenser Showing the Balance Between Surface, Air Velocity and Weight of Active Material for the Design Conditions: Condensing pressure · · 154 psia; Inlet Air Wet-bulb · · · 80F; Heat Dissipated · 153,000 btu/hr; Air Volume · · · · · 2,500 cfm; Tube Material 0.035 inch Copper; Fin Material 0.022 inch Copper.

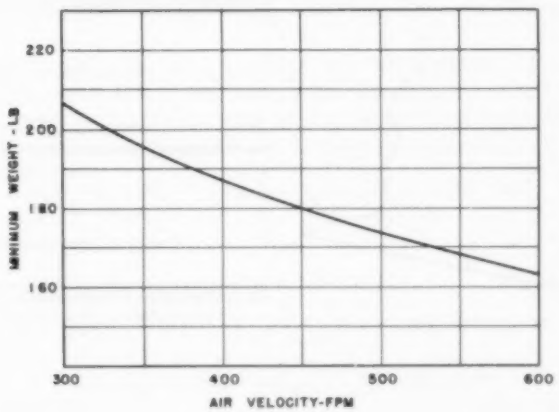

Figure 10

APPENDIX 1

Derivation of the Equations for Heat Flow

Consider the simple wetted-surface heat transfer apparatus shown in Figure 12. It consists of a rectangular, insulated duct of constant width y and length x divided lengthwise by a thin metal wall. The space below this wall is kept full of a pure saturated vapor which is condensing on the wall, while the portion of the duct above the dividing wall serves as a channel

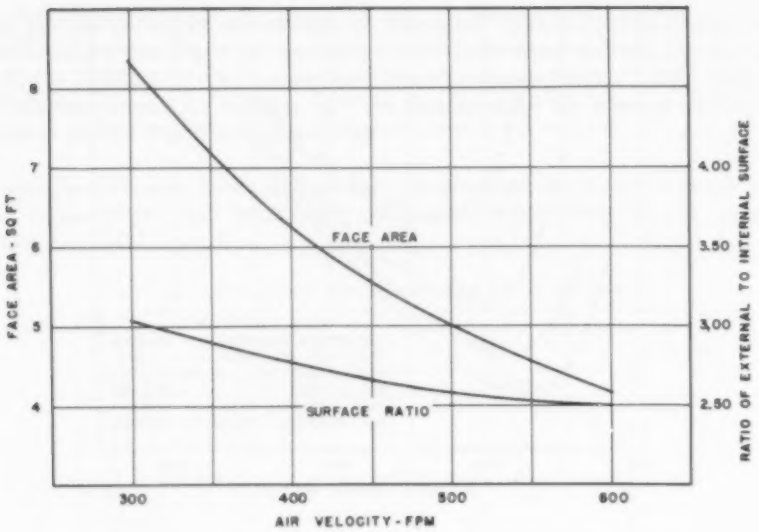

Figure 11

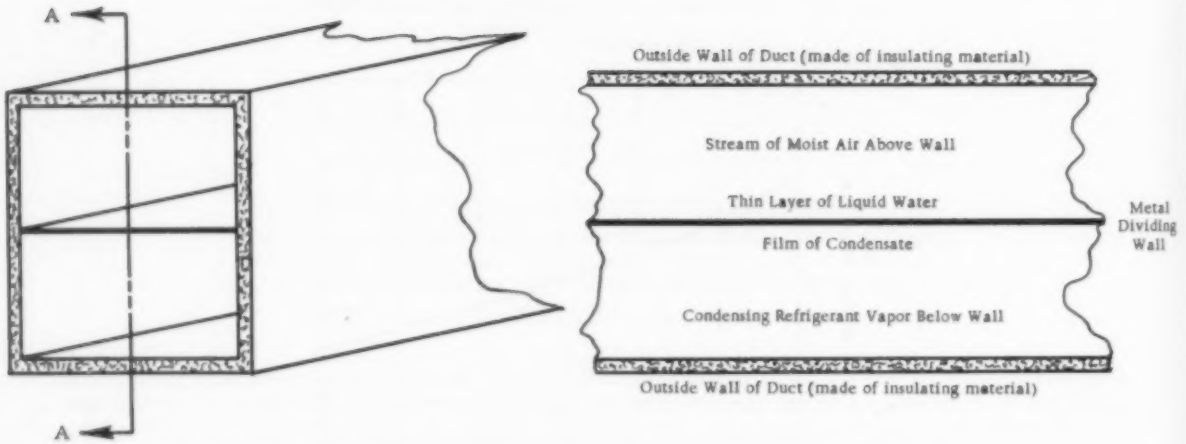
A
A
Outside Wall of Duct (made of insulating material)
Stream of Moist Air Above Wall
Thin Layer of Liquid Water
Film of Condensate
Metal Dividing Wall
Condensing Refrigerant Vapor Below Wall
Outside Wall of Duct (made of insulating material)

Isometric End View of Duct

Section A-A

Figure 12. Simplified Wetted-surface Condenser Used in Developing the Theory of Heat Flow.

for a stream of moist air. The air-side of the dividing wall is kept covered with a thin film of liquid water. The refrigerant or vapor side evidently will be covered by a film of condensate from the saturated vapor.

When the moist air is at or near normal atmospheric pressure and the temperature of the dividing wall is less than 212 F, it is obvious that the hydraulic pressure exerted on the water film by the air will prevent the formation of vapor bubbles in the water, so that all evaporation must take place at the surface of the water film. Therefore, all the heat released at the surface of the condensate film by the condensation of the refrigerant must pass through the condensate film, dividing wall and water film, in series, to the surface of the liquid water. Here, part of

the heat will be used to vaporize the water while the remainder passes on through the "stagnant air film" to the main body of the air stream. The relative rates of flow of heat and diffusion of water vapor through this air film will determine what part of the heat is used to evaporate the water, thus increasing the moisture content or humidity of the air stream, and what part passes through to the air stream directly, thus increasing its temperature.

The rate at which any small element ydx of the surface of the water is gaining heat from the refrigerant is

$$dq = (t_r - t_w)h_L y dx \tag{1-1}$$

in which the condensate film, metal wall and water film are considered a composite wall, that is,

$$\frac{1}{h_L} = \frac{1}{h_C} + \frac{\delta_D}{k_D} + \frac{\delta_w}{k_w} \tag{1-2}$$

The rate at which this element of surface is losing heat to the air stream directly is

$$dq_1 = (t_w - t)h_g y dx \tag{1-3}$$

while the rate at which water vapor is diffusing from the water surface through the air film to the main air stream is

$$dw_w = (H_w - H)K y dx \tag{1-4}$$

The heat absorbed by the evaporation of this quantity of water is

$$dq_2 = r dw_w \tag{1-5}$$

so that the rate at which the element of surface of the water is losing heat by evaporation is

$$dq_2 = r(H_w - H)K y dx \tag{1-6}$$

In the steady state, when conditions at all points are independent of the time, it is obvious that heat cannot be stored anywhere in the apparatus. Hence, the rate at which the element of water surface is losing heat to the air stream by conduction and evaporation must be equal to the rate at which it is gaining heat from the condensing refrigerant so that

$$dq = dq_1 + dq_2 = \left[(t_w - t)h_g + r(H_w - H)K\right] y dx \tag{1-7}$$

As a matter of convenience write

$$K = h_g / \beta \tag{1-8}$$

Then after substituting this value in Eq (1-7) and rearranging terms we have

$$dq = \frac{h_g}{\beta}\left[(\beta t_w + r H_w) - (\beta t + r H)\right] y dx \tag{1-9}$$

But from Eq (1-1)

$$t_w = t_r - \frac{dq}{h_L y dx} \tag{1-10}$$

and if we write

$$\alpha = \frac{H_r - H_w}{t_r - t_w} \tag{1-11}$$

then

$$H_w = H_r - \frac{\alpha\, dq}{h_L y dx} \tag{1-12}$$

So that after using Eqs (1-10) and (1-12) to eliminate the conditions at the water surface from Eq (1-9), we obtain after grouping terms

$$dq = U' P y dx \tag{1-13}$$

where as a matter of convenience we have written

$$\frac{1}{U'} = \frac{\beta}{h_g} + \frac{\beta + \alpha r}{h_L} \tag{1-14}$$

and

$$P = (\beta t_r + r H_r) - (\beta t + r H) \tag{1-15}$$

Integrating Eq (1-13) between the limits yx = 0 and yx = A and using the Mean Value Theorem, we obtain

$$q = \int_0^a U' P y dx = U'_{mean} \int_0^a P y dx = U'_{mean} A P_{mean} \tag{1-16}$$

In the case of air and water vapor mixtures β is very nearly equal to s so that, for work of this sort, Δi can be substituted for P. Also, experience has shown that the logarithmic mean is a convenient and practically useful approximation to P_{mean}. When these approximations are used, it is easy to compute corresponding values of U'_{mean} directly from the test data by the equation

$$U'_{mean} = \frac{q/A}{\dfrac{\Delta i_2 - \Delta i_1}{\ln \dfrac{\Delta i_2}{\Delta i_1}}} \tag{1-17}$$

and U' can be broken down into individual coefficients by the equation

$$\frac{1}{U'} = \frac{s}{h_g} + \frac{s + \alpha r}{R h_L} \tag{1-18}$$

where α is to be evaluated at the mean value

$$t_r - t_w = \frac{q}{R h_L} \tag{1-19}$$

The constant R has been introduced as a multiplier of h_L in Eqs (1-18) and (1-19) to permit expressing this coefficient per unit area of refrigerant side surface when dealing with finned tubing. In this case the areas of the air side and refrigerant side of the wall would not be equal, as they were assumed to be in the preceding discussion.

An estimate of the error involved in the use of the logarithmic mean can be obtained in the following manner.

By equating the heat absorbed by the air in passing over an element of the surface to the heat transfered to it from the surface we obtain

$$G \frac{di}{dP} dP = U' P dx \tag{1-20}$$

so that, taking di/dP = 1,

$$P = P_1 \exp \int_0^X \frac{U'}{G} dx \tag{1-21}$$

Let

$$P' = P \exp \int_0^X \frac{U'}{G} dx \tag{1-22}$$

The logarithmic mean is

$$\text{log mean } P = \frac{P_2 - P_1}{\ln \frac{P_2}{P_1}} = \frac{1}{A} \int_0^a P_1 \exp \left(\frac{x}{A} \ln \frac{P_2}{P_1} \right) dx \tag{1-23}$$

But by integration of Eq (1-21),

$$\ln \frac{P_2}{P_1} = \int_0^a \frac{U'}{G}\, dx = \frac{U'_{mean} A}{G} \tag{1-24}$$

Therefore

$$\text{log mean } P = \frac{1}{A} \int_0^a P_1 \exp \left(\frac{x}{A} \int_0^a \frac{U'}{G}\, dx \right) dx \tag{1-25}$$

$$P_{mean} = \frac{1}{A} \int_0^a P_1 \exp \left(\int_0^a \frac{U'}{G}\, dx \right) dx \tag{1-26}$$

and

$$P'_{mean} = \frac{1}{A} \int_0^a P_1 \exp \left(\int_0^x \frac{U'}{G}\, dx \right) dx \tag{1-27}$$

From which since U' continuously increases as x increases, it is obvious that

$$P'_{mean} < P_{mean} < \text{log mean } P \tag{1-28}$$

so that the error incurred by using the logarithmic mean will be less than that given by the equation

$$P_{mean} = (1 - E) \text{ log mean } P \tag{1-29}$$

where

$$E < 1 - \frac{\left(\frac{P_2}{P_1}\right)^Y - 1}{Y \left(\frac{P_2}{P_1} - 1 \right)} \tag{1-30}$$

with

$$Y = \frac{U'_1}{U'_{mean}} \tag{1-30}$$

APPENDIX 2

Evaluation of the Individual Coefficients

Assume values for C and D in Eqs (5) and (6). Then Eq (4) can be written

$$\left[\frac{1}{U'}\right]_0 = \frac{s}{V^{0.8}} \left[\frac{1}{C}\right]_0 + \left[\frac{1}{Rh_L}\right]_0 + r(\alpha)_0 \left[\frac{1}{Rh_L}\right]_0 \tag{2-1}$$

where the subscripts $_0$ are used to denote assumed values of C and h_L and the corresponding calculated value of U' as distinguished from the test value of U' computed from the test data by means of Eq (7). The difference between the calculated value and the test value of U' for each test can be regarded as due to errors ΔC and Δh_L in the assumed values of these constants. That is

$$\Delta \frac{1}{U'} = \frac{1}{U'} - \left[\frac{1}{U'}\right]_0 = \frac{s}{V^{0.8}} \Delta \frac{1}{C} + (s + \alpha r)_0 \Delta \frac{1}{Rh_L} + r \left[\frac{1}{Rh_L}\right]_0 \Delta\alpha \tag{2-2}$$

For any constant value of t_r and over a small range of values of $t_r - t_w$ we may write as a close approximation

$$\Delta\alpha = a\Delta(t_r - t_w) \tag{2-3}$$

where a is a constant. This is equivalent to using a quadratic equation, $H = a_1 + a_2 t + a_3 t^2$, to fit a short section of the t-H curve. The constant a_3 in the quadratic equation would then be equal to the constant a in Eq (2-3).

Since

$$t_r - t_w = \frac{q/A}{Rh_L} \tag{2-4}$$

and since q/A will have a fixed value for each test, we can write,

$$\Delta\alpha = a(q/A)\Delta\frac{1}{Rh_L} \tag{2-5}$$

With this substitution Eq (2-2) becomes

$$\Delta\frac{1}{U'} = \frac{s}{V^{0.8}}\Delta\frac{1}{C} + \left[(s+\alpha r)_0 + ar\left[\frac{q/A}{Rh_L}\right]_0\right]\Delta\frac{1}{Rh_L} \tag{2-6}$$

so that each test point supplies an equation for the variables $/(1\Delta C)$ and $\Delta(1/Rh_L)$ of the form

$$A_1\Delta\frac{1}{C} + A_2\Delta\frac{1}{Rh_L} = A_3 \tag{2-7}$$

Where the constants A_1, A_2 and A_3 will have different values for the various test points. Their values can be computed from the test data by means of the equations,

$$A_1 = \frac{s}{V^{0.8}} \tag{2-8}$$

$$A_2 = (s+\alpha r)_0 + ar\left[\frac{q/A}{Rh_L}\right]_0 \tag{2-9}$$

$$A_3 = \Delta\frac{1}{U'} = \frac{1}{U'} - \left[\frac{1}{U'}\right]_0 \tag{2-10}$$

Thus, any two tests will furnish a pair of simultaneous equations from which the values of $\Delta(1/Rh_L)$ and $\Delta(1/C)$ can be calculated. The results of more than two tests can be averaged by the method of least squares. In this case the pair of simultaneous equations, called the "Normal Equations", are

$$\Delta\frac{1}{C}\Sigma A_1^2 + \Delta\frac{1}{Rh_L}\Sigma A_1A_2 = \Sigma A_1A_3 \tag{2-11}$$

$$\Delta\frac{1}{C}\Sigma A_1A_2 + \Delta\frac{1}{Rh_L}\Sigma A_2^2 = \Sigma A_2A_3 \tag{2-12}$$

in which each term of the summation includes data from only one test.

If it is desired to assign different weights, W_1, W_2 etc., to the various tests, this can be done by adding the data from each test W times in making the summations, that is, the summation terms will be ΣWA_1^2, ΣWA_2A_1 etc., instead of ΣA_1^2, ΣA_2A_1 etc. For example, in the case of the tests at 2500 - 2600 lbs per hr water rate, 10 of the 13 tests were run at an air velocity of about 300 fpm. In order to avoid overemphasizing the 300 fpm velocity, each of the 10 tests at this velocity was assigned a weight of unity, while each of the remaining tests, at other air velocities, was given a weight of 10.

The assumed values of C and D used in applying this method of analysis to the data of Table 2

were based on the results of previous tests on dehumidifiers and dry-surface condensere. The values were

$$(C)_0 = 0.178 \text{ and } (D)_0 = 200 \tag{2-13}$$

that is

$$(h_g)_0 = 0.178\ V^{0.8} \text{ and } (h_L)_0 = 200 \tag{2-14}$$

The results of the analysis of the data of Table 2 are as follows:

Test Group I - Water rate 3700 - 3800 lb per hr

All tests given equal weight,

$$h_g = 0.237\ V^{0.8} \text{ and } h_L = 212 \tag{2-15}$$

Test Group II - Water rate 2500 - 2600 lb per hr

A - All tests given equal weight,

$$h_g = 0.251\ V^{0.8} \text{ and } h_L = 178 \tag{2-16}$$

B - Each of the 10 tests at 300 fpm air velocity given a weight equal to 0.1 that of each of the three tests at other air velocities. As previously mentioned, the purpose of this was to avoid overemphasizing the 300 fpm velocity.

$$h_g = 0.212\ V^{0.8} \text{ and } h_L = 190 \tag{2-17}$$

After considering these results of the analysis it was concluded that over the range 2500-3800 lb per hr the effect of a change in the water rate could be neglected and the test data could be represented by the equations

$$h_g = 0.212\ V^{0.8} \text{ and } h_L = 200 \tag{2-18}$$

Figure 2 compares the values of U' calculated from these coefficients with the values obtained directly from the test data.

APPENDIX 3

List of Symbols

A = Total area of heat transfer surface exposed to air - sq ft
A_1, A_2 and A_3 = Constants defined by Eqs (2-8), (2-9) and (2-10)
a = Proportionality factor defined by Eq (2-3)
C = Constant defined by Eq (5)
D = Constant defined by Eq (6)
G = Mass rate of flow of dry air over heat transfer surface-lb of dry air per hr
H = Average humidity of moist air over cross-section of stream at x - lb of water vapor per lb of dry air.
H_r = Humidity of saturated air at condensing temperature "t_r"
H_w = Humidity of saturated air at temperature "t_w"
H_1 and H_2 = Humidity of air entering and leaving heat transfer apparatus
h_c = Coefficient of heat transfer from condensing refrigerant vapor to heat transfer surface - btu/(hr) (sq ft) (F)
h_g = Coefficient of heat transfer from heat transfer surface to air - btu/(hr) (sq ft) (F)
h_L = Coefficient of heat transfer from condensing vapor to air side surface of water film - btu/(hr) (sq ft of vapor side surface) (F)
i = Average enthalpy of moist air over cross-section of stream at x - btu per lb of dry air
i_r = Enthalpy of saturated air at condensing temperature "t_r"
i_1 and i_2 = Average enthalpy of air entering and leaving heat transfer apparatus

K = Coefficient of diffusion of water vapor from water surface to air - (lb of water)/(hr) (sq ft) (unit humidity difference between saturated air at temperature of water surface and air)

k_D = Thermal conductivity of dividing wall - btu/(hr) (sq ft) (F/ft)

k_W = Thermal conductivity of liquid water

q = Rate of flow of heat from condensing refrigerant vapor to air stream - btu per hr.

R = Ratio of area of heat transfer surface exposed to refrigerant to area of heat transfer surface exposed to air

r = Latent heat of evaporation of water - btu per lb

s = Humid heat of moist air (i.e.,the specific heat per lb of dry air) - btu/(F)(lb of dry air)

t = Average temperature of moist air over cross-section of stream at x - F

t_r = Temperature of condensing saturated refrigerant vapor - F

t_w = Temperature of water surface in contact with air - F

t_1 and t_2 = Average temperature of air entering and leaving heat transfer apparatus

U = Overall coefficient of heat transfer for dry-surface air-cooled condensers - btu/ (hr) (sq ft of air side surface) (F)

U' = Overall coefficient for wetted-surface air-cooled condensers - lb/(hr)(sq ft of air side surface)

V = Average linear velocity of air stream - ft per minute

w_w = Mass rate of diffusion of water vapor from water surface to air - lb per hr

α = Proportionality factor defined by Eq (1-11)

δ_D = Thickness of dividing wall - ft

δ_w = Thickness of water film - ft

$\Delta i_1 = i_r - i_1$

$\Delta i_2 = i_r - i_2$

$\Delta t_1 = t_r - t_1$

$\Delta t_2 = t_r - t_2$

TABLE 1

Details of Test Condenser

Core Size		Tube Details	
Height	2.14 ft.	Material	Copper (tinned)
Width	1.00 ft.	Outside diameter	0.500 in.
Depth	1.21 ft.	Wall thickness	0.028 in.
Face Area	2.14 sq. ft.	No. of rows	9
		No. per row	16
		Spacing	1.56 in.x 1.56 in.
Surface Area		**Fin Details**	
Tubes (External)	18.8 sq. ft.	Material	Copper (tinned)
Fins	65.3 sq. ft.	Height	2.14 ft.
Total External	84.1 sq. ft.	Width	1.21 ft.
Internal	16.7 sq. ft.	Thickness	0.022 in..
Ratio	1 to 5.04	Spacing	0.75 in.

Does not include return bends.

Table II - Test Data

Test No.	Air					Water		Cond. Pr. Lb/sq. in. Absolute	Heat Released B.t.u./hr.		
	Velocity fpm "V"	Temperatures - °F				Temp. at Spray Nozzle °F	Rate of Circulation Lb/Hr		Note 1 Calculated from Refr. Data	Calculated from Air Data	% Differ.
		Inlet		Outlet							
		Dry Bulb	Wet Bulb	Dry Bulb	Wet Bulb						
3	303	100.0	80.2	99.1	94.9	97.0	2570	162.9	50000	52800	5.6
4	305	90.0	80.1	96.3	94.5	96.2	2570	160.4	49600	51450	3.7
6	305	110.0	94.0	108.0	103.0	106.3	2570	180.4	46500	42500	-8.5
7	303	90.0	73.5	93.5	90.5	92.3	2570	154.4	49300	53400	8.2
8	305	90.0	83.3	97.2	96.6	98.2	2570	164.4	48400	51050	3.7
9	305	100.0	92.2	103.5	102.9	104.1	2570	174.9	46950	49550	5.7
10	305	100.0	86.0	100.5	98.8	100.2	2570	167.9	48100	52100	8.3
11	307	110.0	80.2	100.8	94.9	96.6	2570	162.0	49100	53600	9.1
12	306	100.0	75.4	95.7	91.7	94.1	2570	155.9	49000	54150	10.6
1A	317	97.0	76.7	96.6	92.5	94.6	2570	156.9	49450	55550	12.3
2A	309	97.0	76.4	106.8	94.2	98.3	780	196.9	45900	61500	34.0
4A	305	97.0	76.8	94.5	91.5	95.2	3800	153.5	50150	49450	-1.5
1C	319	100.0	80.9	97.0	95.0	98.0	3780	158.0	49450	54450	10.0
2C	319	100.0	80.9	97.3	95.0	98.4	2920	162.5	48700	54450	11.7
3C	319	100.0	80.9	102.6	97.0	102.4	1680	182.5	44450	63800	43.6
6C	315	100.0	83.2	100.6	96.8	100.8	2125	171.5	47500	53500	12.8
7C	319	100.0	80.5	108.1	94.5	105.2	692	215.5	41800	53450	28.0
1D	319	100.0	80.0	96.0	93.2	96.5	3770	157.0	48750	49150	1.0
2D	131	100.0	80.0	105.9	105.0	107.1	3780	178.5	45950	44700	-2.7
3D	194	100.0	80.0	101.8	100.0	102.6	3770	169.6	46000	48600	5.9
4D	466	100.0	80.4	95.4	90.0	93.9	3660	151.0	50400	49300	-2.1
1E	128	100.0	79.7	106.8	105.9	108.8	2570	187.0	44800	46500	3.8
2E	322	100.0	79.7	98.8	93.8	98.0	2535	163.0	48700	52900	8.4
3E	481	100.0	80.0	96.8	90.8	94.9	2525	156.6	49300	58500	18.8

Note 1 - The values of Q used in the analysis were taken from this column.

SCHEDULE OF PAPERS FOR 1950-51

October 13, 1950 — General Meeting

Samuel R. Williams, "Applications of Elementary Mathematics to Problems in Magnetism" (originally entitled "Elementary Mathematics as a Scientific Tool") (Published in this issue of INDUSTRIAL MATHEMATICS)

November 10, 1950 — Orientation Lecture

J. Ormondroyd, "Prediction of Transient Motion in Linear Systems of One or Many Degrees of Freedom" (Published in this issue of INDUSTRIAL MATHEMATICS)

December 5, 1950 — Members' Papers Meeting

Leonard S. Lustick, "An Application of Liebman's Iteration Method to Viscous Flow" (Published in this issue of INDUSTRIAL MATHEMATICS)

Paul T. Nims, "Some Punched Card Techniques in Engineering Computation"

Douglas G. Anderson, "A Method for Design of High Efficiency Cantilever Springs" (Published in this issue of INDUSTRIAL MATHEMATICS)

Arvid E. Roach and Howard H. Kehrl, "Performance of Centrifugal Pumps from Affinity Laws at Non-Corresponding Operating Points" (Published in this issue of INDUSTRIAL MATHEMATICS)

Douglas Hughson, "An Analytical Method for Deriving Gear-Tooth 'X' Factors" (Published in this issue of INDUSTRIAL MATHEMATICS)

Earl F. Riopelle, "A General Steady-State Solution of the Two-Mass Torsion Problem" (Published in this issue of INDUSTRIAL MATHEMATICS)

January 17, 1951 — Orientation Lecture

Ben Dushnik, "Applications of Infinite Series"

January 26, 1951 — General Meeting

John H. Curtiss, "Applied Mathematical Statistics as a Branch of Industrial Mathematics"

March 24, 1951 — Joint Meeting of Michigan Academy of Science, Arts and Letters and Mathematical Association of America (1)

Thomas H. Southard, "A Survey of Industrial Subsidy of the Study of Applied Mathematics" (Published in this issue of INDUSTRIAL MATHEMATICS)

Leonard G. Johnson, "An Inverse Two-Dimensional Problem in Elasticity"

Gerald Harrison, "The Solving of Systems of Linear Equations in College Algebra"

March 27, 1951 — Joint Meeting of Association for Computing Machinery, Industrial Mathematics Society, and Advisory Committee for Wayne University Computation Laboratory (1)

Paul T. E. Nims, "Some Computing Problems in the Automotive Industry" (Published in this issue of INDUSTRIAL MATHEMATICS)

April 20, 1951 — Orientation Lecture

L. S. Johnston, "Constructing Nomographic Charts"

May 24, 1951 — Annual Meeting

Calvin Hall, "Undercutting Spur Gear Teeth"

Albert F. Beam, "Relative Motion of Crossed-Axes Gearing"

Victor Francis, "Surface Stress and Strain of Spiral Involute Gears" (Published in this issue of INDUSTRIAL MATHEMATICS)

Keith Symon, "Design and Coding of a Simple Digital Computer"

Note 1. Only those papers presented under IMS sponsorship are listed.

OFFICERS, COMMITTEES, AND STUDY GROUPS

OFFICERS

President: Robert Schilling, General Motors Corporation
Past President: Arvid W. Jacobson, Wayne University
Vice-President: Paul T. Nims, Chrysler Corporation
Secretary: Arvid E. Roach, General Motors Corporation
Treasurer: L. S. Johnston, University of Detroit

COMMITTEES

Program Committee: Clayton R. Lewis, Chairman
Group Activities Committee: Earl F. Riopelle, Chairman
    Orientation Lectures Subcommittee: Clayton J. Pajot, Chairman
    Study Groups Subcommittee: Robert A. Roggenbuck, Chairman
Education Committee: Thomas H. Southard, Chairman
Editorial Board: Paul T. Nims, Editor-in-Chief
Planning Committee: Nevin C. Fisk, Chairman
Membership Committee: Roderick Craves, Chairman
Publicity Committee: George V. Constantakis, Chairman

STUDY GROUPS

Gear Design Study Group: Douglas Hughson, Group Leader
    W. F. Vogel, Advisor

Computing Machines Study Group: Robert A. Roggenbuck, Group Leader
Arvid W. Jacobson, Advisor
Servemechanisms Study Group: Jorma O. Sarto, Group Leader
W. H. Bixby, Advisor
Electric Circuit Theory Study Group: P. J. Willson, Group Leader
K. R. Symon, Advisor
Stress Analysis Study Group: Egon Benesi, Group Leader and Advisor

LITHOPRINTED IN THE UNITED STATES OF
CUSHING - MALLOY, INC. ANN ARBOR, MICH.